VOLUME 2

MIT Quantum Science and Engineering Consortium

QSEC Quarterly

Fall 2021

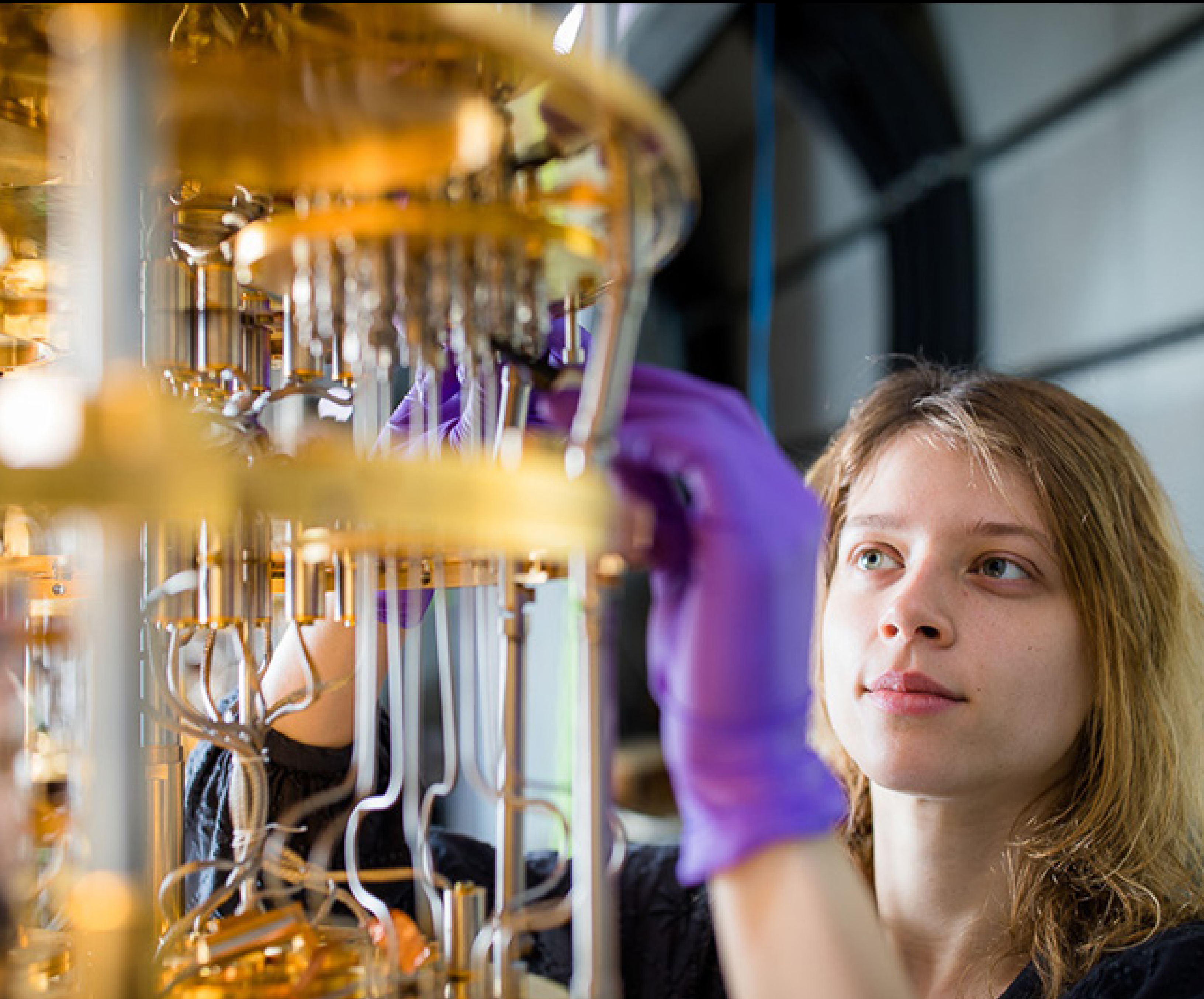

Contents

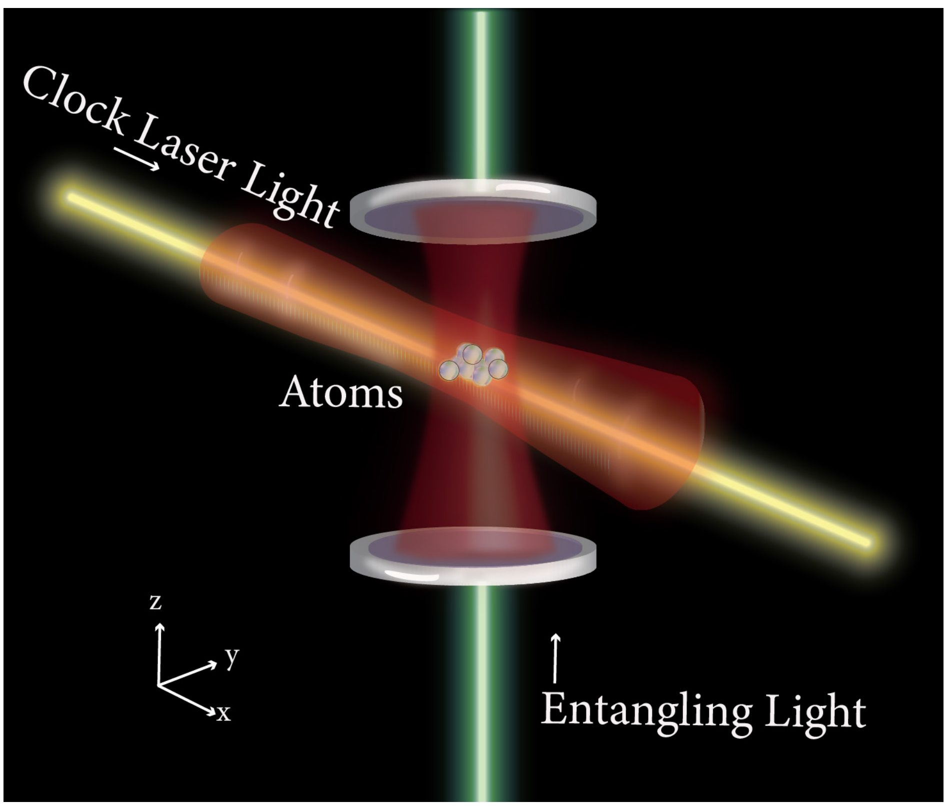

Now out in Physics@MIT Journal: MIT Prof. Vladan Vuletic and the Vuletic Group have built an atomic clock that measures not a cloud of randomly oscillating atoms, as state-of-the-art designs measure now, but instead atoms that have been quantumly entangled. The atoms are correlated in a way that is impossible according to the laws of classical physics, and that allows the scientists to measure the atoms' vibrations more accurately.

MIT-CQE Mission

MIT's Center for Quantum Engineering is dedicated to the academic pursuit and practice of science and engineering to accelerate the practical application of quantum technologies for the betterment of humankind.

FROM THE DIRECTOR

It is our pleasure to present the Fall 2021 edition of the Quantum Science and Engineering Consortium (QSEC) newsletter.

The fall term is well underway at MIT, and it is exciting to have students back on campus and to be teaching again "in person."

The fall term also brought with it several membership activities. One is the continuing iQuISE-CQE weekly seminar series, which features leading researchers worldwide and is organized by MIT's iQuISE graduate student group. We also hosted our member recruiting fair on September 30th. Please reach out to Paula Jorgensen to learn more about taking advantage of these activities developed for our QSEC members.

QuARC February 6th & 7th, 2022.

Hold the dates! We are pleased to announce the dates for our annual QSEC member meeting, the QSEC Annual Research Conference (QuARC). The **QuARC** will be held in-person on campus in Cambridge, Massachusetts and features the work of our students, faculty, and guest speakers. Activities include:

- a social gathering for industry members and students on Sunday evening February 6th
- a full day of speakers and poster sessions on Monday, February 7th, 2022

This is a unique opportunity to engage directly with students and experience the latest quantum research happening across the Institute.

DIRECTOR
MIT Center for Quantum Engineering (CQE)

PROFESSOR
of Electrical Engineering and Computer Science and of Physics

LINCOLN LABORATORY FELLOW

We hope you will join us!

William D. Oliver

William D. Oliver
william.oliver@mit.edu

CQE PI FEATURE

You want to turn those photons into classical signals that you can read, that you can measure

KEVIN O'BRIEN
Assistant professor of Electrical Engineering and Computer Science

From an early age, **Kevin O'Brien** has been very curious about how things work. Now an assistant professor of Electrical Engineering and Computer Science, O'Brien says he was engrossed in the "science of everyday life" as a child, whether that meant exploring the biological processes going on in the pond at his childhood home in Indiana or studying radios and televisions by disassembling them.

"My parents always give me a hard time because when I was in grade school, I would take things apart, but only after a few more years could I put them back together," O'Brien says. "We had all sorts of disassembled TVs and radios for a while there."

In the years after O'Brien reassembled his family's electrical appliances, he decided that studying physics best satisfied his boundless curiosity.

"With physics, you can understand things at their most basic level and build up from there," he says. "In reality the lines between disciplines aren't really as sharp as we expect. Chemistry involves a huge amount of physics, and biology involves a huge amount of physics and chemistry. But I think when I was younger, I wanted to study physics just because it sort of forms the basis of how we understand the world."

O'Brien earned his PhD at the University of California, Berkeley, in nanoscale optics and nanomaterials, engineering artificial nanostructures to get new optical properties. One such property is negative refractive index, in which light moving through a material propagates backward toward its source. The research group O'Brien worked with at Berkeley, which was led by Xiang Zhang, an international renowned expert on metamaterial engineering, exploited negative indices of refraction to create the much-heralded "invisibility cloak."

It was in 2016 at a Mexican restaurant in Berkeley that O'Brien, his housemate who was in a different research group and another graduate student happened onto the idea of using metamaterials to create better quantum-limited amplifiers.

“They were telling me about the issues they were having with these parametric amplifiers,” O’Brien says. “We realized that metamaterial concepts could solve the issues, were a viable solution to this problem. I certainly didn’t understand all of it and had to do the math and equations, but yeah, that was it.”

O’Brien then turned his attention toward quantum computing and helped realize an amplifier that is now standard, the Josephson Traveling Wave Parametric Amplifier, which is commonly used to read quantum bits.

“It was through that collaboration that I realized, wow, quantum computers are really close, they’re actually viable,” says O’Brien. “I guess that was the moment that I realized this is a really exciting field and something I want to contribute to and start a group to aid in this effort.”

O’Brien joined MIT’s Research Laboratory of Electronics in 2018 and leads the Quantum Coherent Electronics research group. The stated aim of the group is to “advance the state of the art in superconducting quantum computing, microwave quantum optics and quantum metamaterials.”

Controlling how photons behave in a quantum computer is the fundamental benefit represented to the quantum computing field by metamaterials, O’Brien says. The photons are very weak, he says, with a very small amplitude. Their behavior is very much quantum mechanical.

“But you want to talk to your quantum computer. You want to turn those photons into classical signals that you can read, that you can measure,” O’Brien says. Low-noise or quantum-limited amplifiers “improve the quantum efficiency, making sure you don’t lose any of those precious photons that you want to amplify.”

Although O’Brien allows that most of us will never use the amplifiers in everyday life, because they have to be cooled to near absolute zero to work, he feels satisfied that they have so much scientific potential.

“I also love working on things that have applications where it can actually change something for the better,” he says.

Not only are the amplifiers used in many quantum computing experiments, even at companies like Google and IBM, O’Brien says, they are also being investigated for use as dark matter detectors.

“Amplifying very weak electromagnetic signals without adding much noise is something that is probably applicable to a lot of different areas of research,” he says.

O’Brien ponders the possibilities, even as he bicycles around Boston or is home cooking exotic meals. Rather than having a particular time or place when he does his best thinking, O’Brien says some of his research questions simply run in the background while he is engaged in his everyday activities.

"Real physics and engineering, it's not just abstractly thinking about things. It's also doing the work, doing the coding and experiments," he says. "But I think there's some quote by Feynman that you want to have the problems that are important to you in the back of your mind. Periodically, you'll get insights."

As a teacher and a mentor, O'Brien encourages the same kind of curiosity and questioning that he has enjoyed. He tells his students to speak up and participate without concern for any kind of hierarchical structure and meets with the students in his research group every week individually and as a group.

"I try to make it very clear that they should always speak their mind, always ask questions," O'Brien says. "If they think something is wrong or if they think we're not taking the right path on something, then I tell them, please talk about it."

He says he has found that kind of collaboration throughout his experience at MIT.

"You hear rumors that MIT is like a really hardcore place. But, you know, when I interviewed and when I got here, I was blown away by how collaborative and friendly everyone is. We all want to work hard and do the best work we can, but it really is quite collaborative."

When O'Brien's students are feeling stumped by a problem, he passes on advice he was given by one of his postdoc mentors—advice that probably resonates with his lifelong devotion to learning how things work. "You might spend a lot of time and work very hard on this," he tells his students, "but eventually it's going to make sense. In the end, science works. And we might not understand it right now, but we will figure it out."

CQE STUDENT FEATURE

Quantum Coherent Electronics Group: Jennifer Wang

Research group name: Quantum Coherent Electronics

Research Advisor: Dr. Kevin P. O'Brien, MIT Assistant Professor of EECS; Principle Investigator of MIT RLE Quantum Coherent Electronics Group; Member of the MIT Center for Quantum Engineering

Hometown, Country: Houston, TX, USA

Academic History Prior to coming to MIT: B.A. in Physics and minor in Computer Science, Wellesley College

What brought you to MIT? During undergrad, I worked primarily with quantum materials, including NV centers in diamond and topological phononic metamaterials. I had always been curious about how the quantum properties I was observing could be used in a complex system, so I interned at MIT Lincoln Laboratory to work on the Quantum Network Testbed. My mentor, Dr. Catherine Lee ('17), was incredibly supportive and introduced me to MIT's vibrant research community.

What interests you the most about your research? I'm most fascinated by how we can actively take advantage of quantum mechanics to design extraordinarily efficient, secure, and scalable devices. My research involves Josephson travelling wave parametric amplifiers (JTWPAs), which are chip-based amplifiers widely used in superconducting quantum systems. In particular, due to a macroscopic quantum phenomenon called the Josephson effect, we can introduce nonlinear elements that enable the JTWPA to achieve high signal gain over a broad bandwidth, which is essential for qubit readout and multiplexing. At each step of the design process, our work involves combining and translating between the fields of quantum optics and classical circuitry. I enjoy the interdisciplinary nature of this work, and I plan to investigate how we can use these devices not only for quantum computing, but also for axion and particle detection at high frequencies.

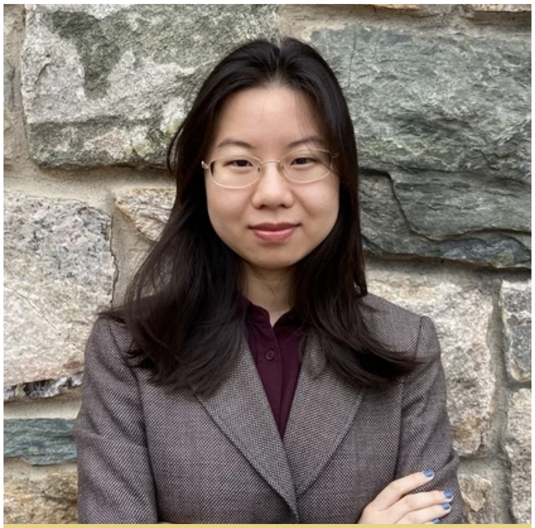

JENNIFER WANG
CQE-LPS Doc Bedard Fellow. This three-year graduate fellowship is awarded through the MIT Center for Quantum Engineering. It is funded by the Laboratory of Physical Sciences and recognizes the achievements and technical leadership of Dr. Fernand (Doc) Bedard, a pioneer of cryogenic computing.

What are your future plans? Since I am interested in research and technology transfer, I would like to work at a small to mid-sized quantum computing hardware startup. I also deeply enjoy making physics and engineering accessible to all, and hope to incorporate grassroots outreach efforts in every stage of my career.

AROUND THE INSTITUTE

Meet our MIT-CQE Principal Investigators

RAYMOND ASHOORI
Physics

MARC BALDO
EECS

JOHN BARRY
Lincoln Laboratory

KARL BERGGREN
EECS

RAFAEL GOMEZ-BOMBARELLI
DMSE

DON BORONSON
Lincoln Laboratory

DANIELLE BRAJE
Lincoln Laboratory

COLIN BRUZEWICZ
Lincoln Laboratory

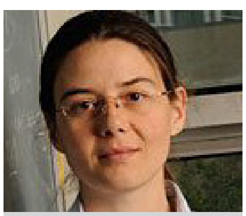

PAOLA CAPPELLARO
NSE

JOSEPH CHECKELSKY
Physics

JOHN CHIAVERINI
Lincoln Laboratory

ISAAC CHUANG
EECS, Physics

MICHAEL CUSUMANO,
Sloan School

RICCARDO COMIN
Physics

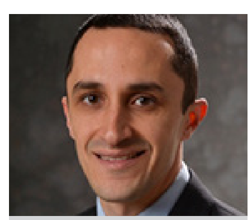

ERIC DAULER
Lincoln Laboratory

BENJAMIN DIXON
Lincoln Laboratory

MIT Center for QuantumEngineering

MIT Quantum Science and Engineering Consortium

AROUND THE INSTITUTE

Meet our MIT-CQE Principal Investigators

DIRK ENGLUND
EECS

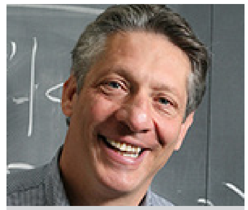

EDWARD FARHI
Physics

RICHARD FLETCHER,
Physics

JOSEPH A. FORMAGGIO
Physics

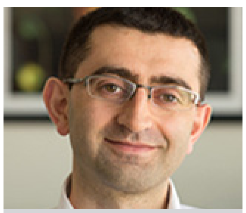

NUH GEDIK
Physics

MARK GOUKER
Lincoln Laboratory

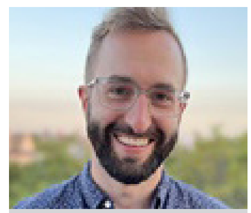

JEFF GROVER,
RLE

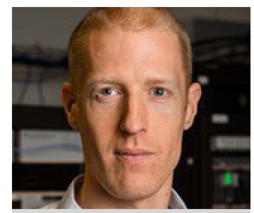

SIMON GUSTAVSSON,
RLE

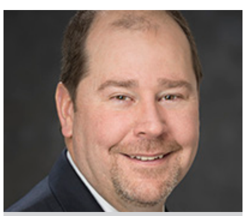

SCOTT HAMILTON,
Lincoln Laboratory

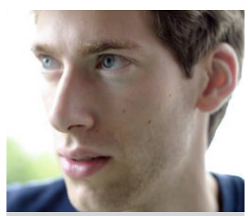

ARAM W. HARROW,
Physics

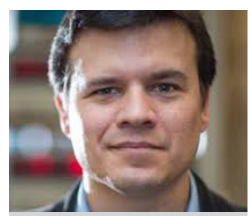

PABLO JARILLO-HERRERO,
Physics

LONG JU,
Physics

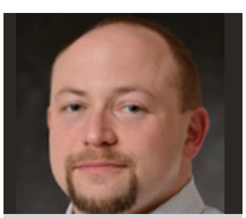

ANDREW J. KERMAN,
Lincoln Laboratory

WOLFGANG KETTERLE,
Physics

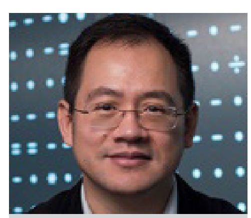

JU LI,
NSE MSE

MINGDA LI,
NSE

Meet our MIT-CQE Principal Investigators

LUQIAO LIU,
EECS

SETH LLOYD,
ME, ES, Physics

ROBERT McCONNELL,
Lincoln Laboratory

ANAND NATARAJAN,
EECS

KEVIN OBENLAND,
Lincoln Laboratory

KEVIN P. O'BRIEN,
EECS

WILLIAM D. OLIVER,
EECS, Physics, Lincoln Laboratory

TERRY ORLANDO,
EECS

LINH PHAM,
Lincoln Laboratory

RAJEEV RAM,
EECS

DANNA ROSENBERG,
Lincoln Laboratory

MOLLIE SCHWARTZ,
Lincoln Laboratory

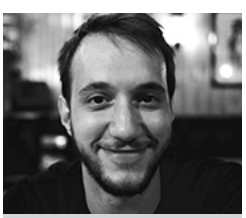

KYLE SERNIAK,
Lincoln Laboratory

JEFFREY H. SHAPIRO,
EECS

PETER SHOR,
Mathematics

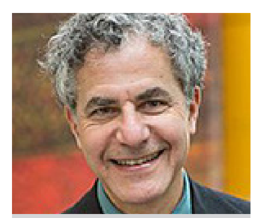

MICHAEL SIPSER,
Mathematics

MIT Center for Quantum Engineering
MIT Quantum Science and Engineering Consortium

AROUND THE INSTITUTE

Meet our MIT-CQE Principal Investigators

VIVISHEK SUDHIR, *ME*

TROY VAN VOORHIS, *Chemistry*

VLADAN VULETIC, *Physics*

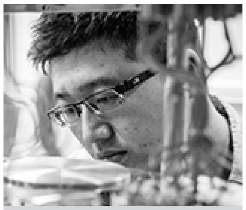

JOEL I-JAN WANG, *RLE*

LINDLEY WINSLOW, *Physics*

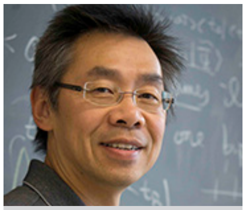

FRANCO N. C. WONG, *RLE*

WAYNE WOODS, *Lincoln Laboratory*

BILGE YILDIZ, *NSE MSE*

JONILYN YODER, *Lincoln Laboratory*

MARTIN ZWIERLEIN, *Physics*

RAYMOND ASHOORI, *Physics*

“Strong interlayer charge transfer due to exciton condensation in an electrically isolated GaAs quantum well bilayer”
J. Jang, H.-M. Yoo, L.N. Pfeiffer, K.W. West, K.W. Baldwin, R.C. Ashoori
Applied Physics Letters (2021)

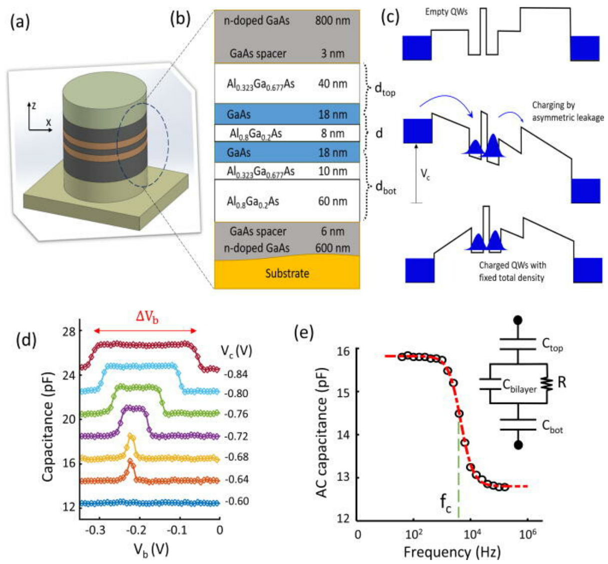

Sample design and means for controlling total and differential density. (a) Schematic of a cylindrically etched device. (b) The wafer growth profile used in this work. The GaAs QWs of 18 nm width are tunneling-coupled to each other and form a QW bilayer. (c) Sequence of charging the bilayer system. An initially empty bilayer is charged by first inducing leakage current over the structure and capturing the charges in the bilayer. (d) Capacitance measured at 13 Hz as a function of V_bVb at various values of V_cVc used in the charging sequence of (c). Evidenced by the range of the high capacitance (red arrow), the amount of the total charge in the system grows with the increasing magnitude of V_cVc. Curves are shifted for clarity. (e) A frequency dependent capacitance measurement shows a roll-off behavior with the frequency ($f_c=1/2\pi RC_{bilayer}$fc=1/2πRCbilayer) proportional to the strength of interlayer charge transfer conductance ($S_{in}=1/R$Sin=1/R). The red dotted line is a fit to the frequency response function of the effective circuit in the inset.

MARC BALDO, *EECS*

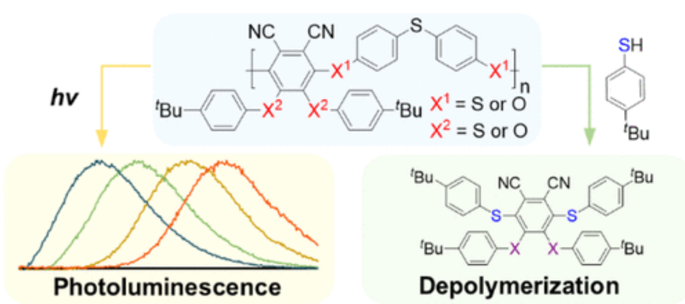

“Polymerization and Depolymerization of Photo-luminescent Polyarylene Chalcogenides”
Zachary Nelson, Nathan A. Romero, Jan Tiepelt, Marc Baldo, Timothy M. Swager
Macromolecules (2021)

“Interfacial trap-assisted triplet generation in lead halide perovskite sensitized solid-state upconversion”
Lili Wang, Jason J. Yoo, Ting-An Lin, Collin F. Perkinson, Yongli Lu, Marc A. Baldo, and Moungi G. Bawendi
Adv. Mater. 2100854 (2021)

KARL K. BERGGREN, *EECS*

"Impedance-matched differential superconducting nanowire detectors"
M. Colangelo, B. Korzh, J. P. Allmaras, A. D. Beyer, A. S. Mueller, R. M. Briggs, B. Bumble, M. Runyan, M. J. Stevens, A. N. McCaughan, D. Zhu, S. Smith, W. Becker, L. Narváez, J. C. Bienfang, S. Frasca, A. E. Velasco, C. H. Peña, E. E. Ramirez, A. B. Walter, E. Schmidt, E. E. Wollman, M. Spiropulu, R. Mirin, S. W. Nam, K. K. Berggren, M. D. Shaw
arXiv:2108.07962 (2021)

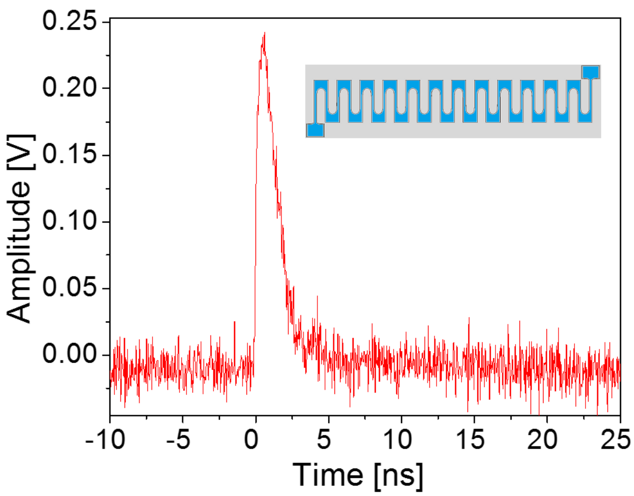

"Physical properties of amorphous molybdenum silicide films for single photon detectors"
Xiaofu Zhang, Ilya Charaev, Huanlong Liu, Tony X. Zhou, Dong Zhu, Karl K. Berggren, Andreas Schilling
Superconductor Science and Technology 34, 9 (2021)
arXiv (2021)

"Precise, Subnanosecond, and High-Voltage Switching Enabled by Gallium Nitride Electronics Integrated into Complex Loads"
John Simonaitis, Benjamin Slayton, Yugu Yang-Keathley, Phillip Keathley, Karl K. Berggren
Reviews of Scientific Instruments 92 (2021) arXiv (2021)

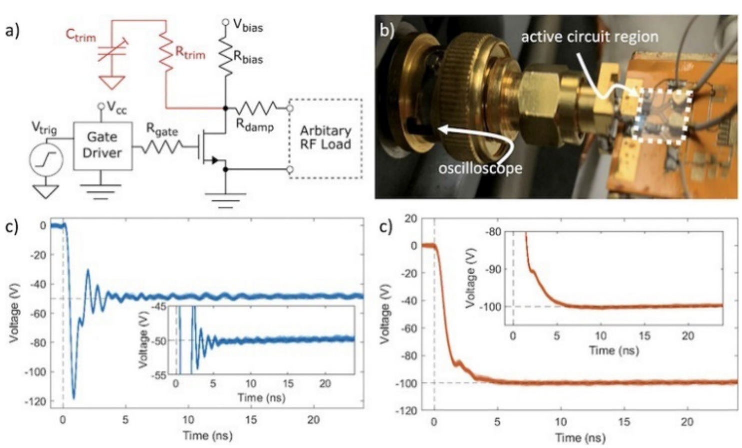

FIG. 1. Test-bed for GaN pulsing. (a) The circuit schematic, where the gate driver is LMG1020 and GaNFET is EPC2012C. R_{gate} damps the gate turn on loop, R_{damp} damps the load loop, and R_{bias} sets the power usage and load recovery time. The optional trimming circuit in red allows for fine tuning of the load damping that the course-valued resistors used could not achieve, though this was not used in the results shown. (b) The physical layout of the circuit mounted on a Kapton on copper substrate. The highlighted white region shows the active portion of the circuit, which is less than 0.25 cm2. The circuit is directly coupled into a LeCroy

KARL K. BERGGREN, *EECS*

6200A oscilloscope with ~20 pF of input capacitance through a 2.2 pF capacitor. (c) The undamped response, showing significant long-term ringing. The inset shows a zoomed in version of this ringing. The full transition is ~540 ps, while the 10%–90% transition is in 230 ps. (d) The same pulse edge, but damped through a 200 Ω resistor. It achieves a 10%–90% transition in 1.5 ns, 0%–90% accuracy in 1.9 ns, and 0%–99% accuracy in 5.1 ns. Note that all traces are multiplied by a factor of ~10 to account for the voltage division caused by the 2.2 pF coupling capacitor in order to match the final voltage to the biasing applied.

"Long term field emission current stability characterization of planar field emitter devices"
Ranajoy Bhattacharya, Marco Turchetti, P. Donald Keathley, Karl K. Berggren, and Jim Browning
Journal of Vacuum Science & Technology B 39 (2021)

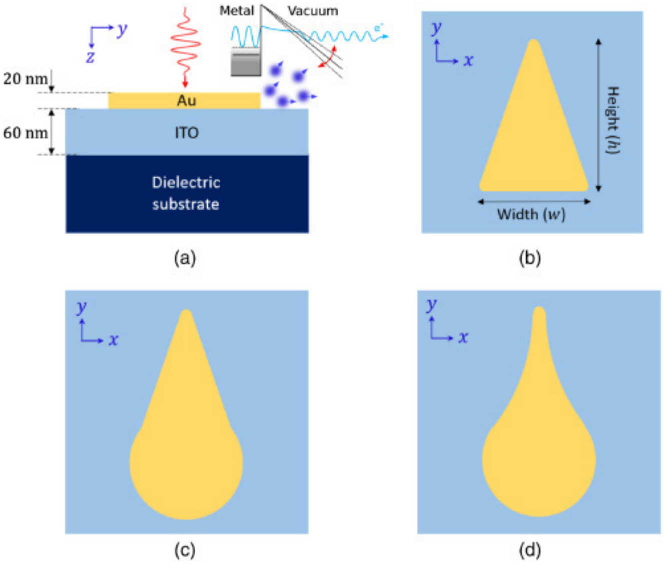

"Nanoantenna design for enhanced carrier–envelope-phase sensitivity"
Drew Buckley, Yujia Yang, Yugu Yang-Keathley, Karl K. Berggren, and Phillip D. Keathley
JOSA B 38, 9 (2021)
arXiv (2021)

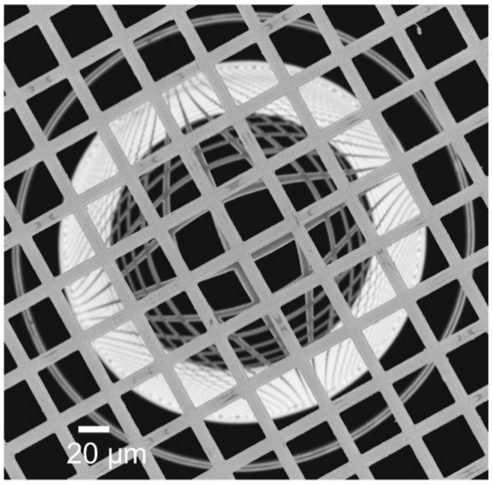

"Electrostatic electron mirror in SEM for simultaneous imaging of top and bottom surfaces of a sample"
Navid Abedzadeh, M. A. R. Krielaart, Chung-Soo Kim, John Simonaitis, Richard Hobbs, Pieter Kruit, Karl K. Berggren
Ultramicroscopy 226 (2021) arXiv (2020)

KARL K. BERGGREN, *EECS*

"Single-photon detection in the mid-infrared up to 10 μm wavelength using tungsten silicide superconducting nanowire detectors"
V. B. Verma, B. Korzh, A. B. Walter, A. E. Lita, R. M. Briggs, M. Colangelo, Y. Zhai, E. E. Wollman, A. D. Beyer, J. P. Allmaras, H. Vora, D. Zhu, E. Schmidt, A. G. Kozorezov, K. K. Berggren, R. P. Mirin, S. W. Nam, and M. D. Shaw
APL Photonics 6 (2021) arXiv (2020)

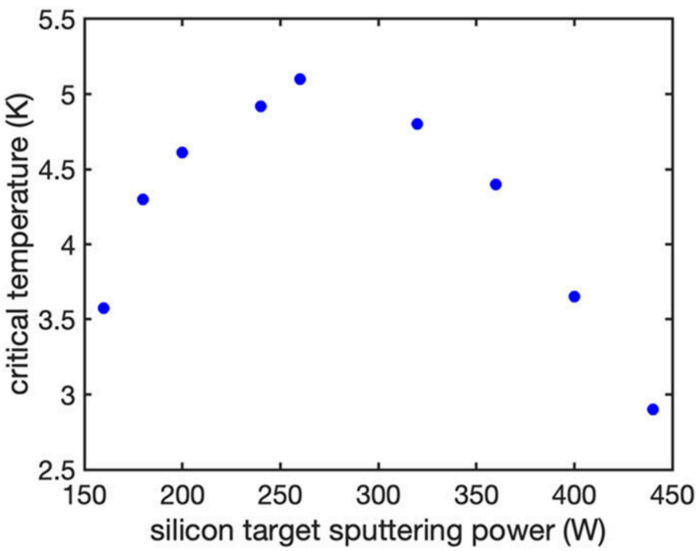

Superconducting transition temperature (Tc) as a function of sputtering power on the silicon target during co-sputtering of the WSi film. The W sputtering power is fixed at 100 W. Measurements were performed on bulk films with thickness greater than or equal to 50 nm.

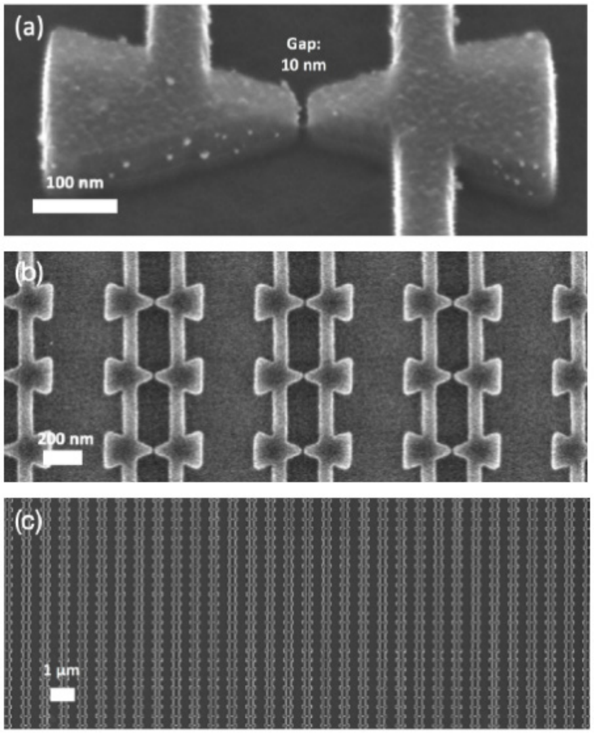

"Nanoscale refractory doped titanium nitride field emitters"
Alberto Nardi, Marco Turchetti, Wesley A. Britton, Yuyao Chen, Yujia Yang, Luca Dal Negro, Karl K. Berggren, Phillip D. Keathley
Nanotechnology (2021) arXiv (2020)

KARL K. BERGGREN, *EECS*

“On-chip sampling of optical fields with attosecond resolution”
Mina R. Bionta, Felix Ritzkowsky, Marco Turchetti, Yujia Yang, Dario Cattozzo Mor, William P. Putnam, Franz X. Kärtner, Karl K. Berggren, Phillip D. Keathley
Nature Photonics 15 (2021) arXiv (2020)

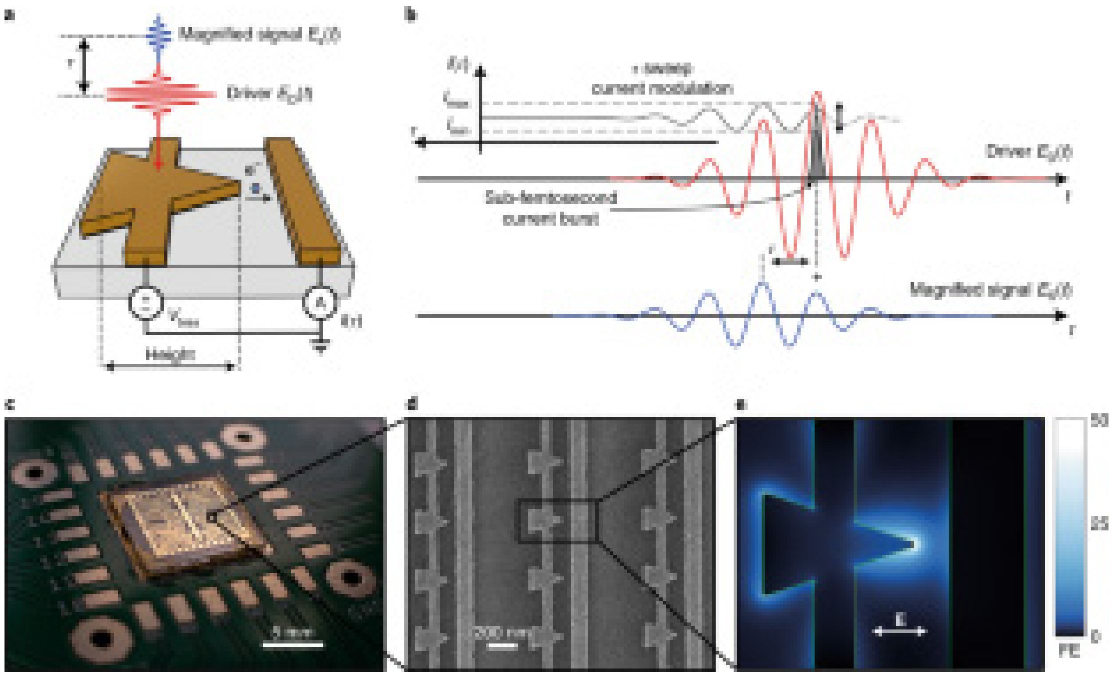

Device Overview

“Image-Histogram-based Secondary Electron Counting to Evaluate Detection Quantum Efficiency in SEM”
Akshay Agarwal, John Simonaitis, Karl K. Berggren
Ultramicroscopy 224 (2021) arXiv (2020)

“Impact of DC bias on Weak Optical-Field-Driven Electron Emission in Nano-Vacuum-Gap Detectors”
Marco Turchetti, Mina R. Bionta, Yujia Yang, Felix Ritzkowsky, Denis Ricardo Candido, Michael Flatté, Karl K. Berggren, Phillip D. Keathley
JOSA B 38, 3 (2021) arXiv (2020)

RAFAEL GOMEZ-BOMBARELLI, *DMSE*

"Differentiable sampling of molecular geometries with uncertainty-based adversarial attacks"
Daniel Schwalbe-Koda, Aik Rui Tan & Rafael Gómez-Bombarelli
Nature Communications (2021)

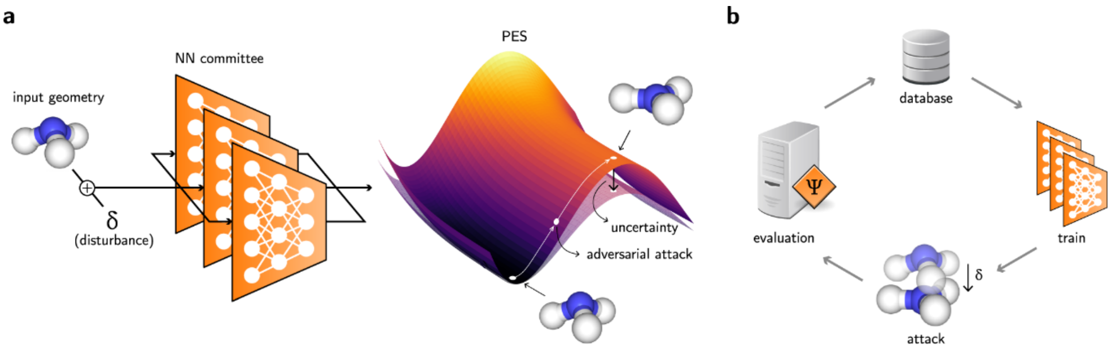

(a) Nuclear coordinates of an input molecule are slightly displaced by δ. Then, a potential energy surface (PES) and its associated uncertainty are calculated with an NN potential committee. By backpropagating an adversarial loss through the NN committee, the displacement δ can be updated using gradient ascent techniques until the adversarial loss is maximized, thus converging to states that compromise high uncertainty with low energy. (b) Schematic diagram of the active learning loop used to train the NN potential committee. The evaluation can be performed with classical force fields or electronic structure methods.

"Excited state, non-adiabatic dynamics of large photoswitchable molecules using a chemically transferable machine learning potential"
Simon Axelrod, Eugene Shakhnovich, Rafael Gómez-Bombarelli
arXiv:2108.04879

Sampling Lattices in Semi-Grand Canonical Ensemble with Autoregressive Machine Learning
James Damewood, Daniel Schwalbe-Koda, Rafael Gomez-Bombarelli
arXiv:2107.05109

PAOLA CAPPELLARO, *NSE*

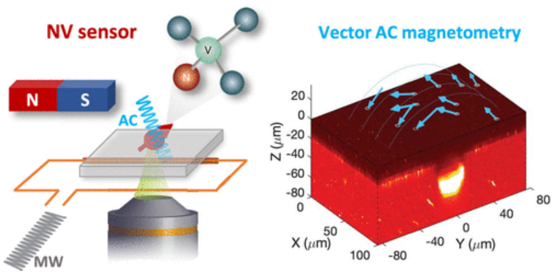

[“Nanoscale Vector AC Magnetometry with a Single Nitrogen-Vacancy Center in Diamond”]
Guoqing Wang, Yi-Xiang Liu. Yuan Zhu, Paola Cappellaro
Nano Lett. 2021, 21, 12, 5143–5150

“Non-thermal energy fluctuations of a diamond spin qutrit with feedback-controlled dissipative dynamics”
S. Hernández-Gómez, S. Gherardini, N. Staudenmaier, F. Poggiali, M. Campisi, A. Trombettoni, F. S. Cataliotti, P. Cappellaro, N. Fabbri
arXiv:2105.14011 (2021)

“Observation of symmetry-protected selection rules in periodically driven quantum systems”
Guoqing Wang, Changhao Li, Paola Cappellaro
arXiv:2105.12209 (2021)

JOSEPH CHECKELSKY, *Physics*

“A flat band-induced correlated kagome metal”
L. Ye, S. Fang, M. Kang, J. Kaufmann, Y. Lee, J. Denlinger, C. Jozwiak, A. Bostwick, E.Rotenberg, E. Kaxiras, D. C. Bell, O. Janson, **R. Comin, J. G. Checkelsky**
arXiv:2106.10824 (2021)

JOHN CHIAVERINI, *Lincoln Laboratory*

"Heating of a Trapped Ion Induced by Dielectric Materials"
Markus Teller, Dario A. Fioretto, Philip C. Holz, Philipp Schindler, Viktor Messerer, Klemens Schüppert, Yueyang Zou, Rainer Blatt, John Chiaverini, Jeremy Sage, and Tracy E. Northup
Phys. Rev. Lett. 126, 230505 (2021)

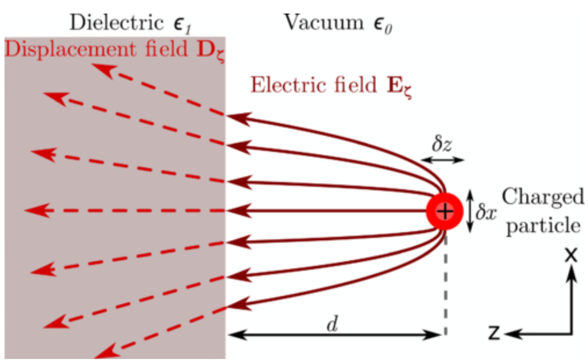

A charged particle is placed a distance d from a dielectric material with permittivity $\varepsilon 1$. The particle oscillates in vacuum (permittivity $\varepsilon 0$) with amplitude $\delta\zeta \ll d$, with $\delta\zeta \in \{\delta x, \delta z\}$. The charge generates an electric field $E\zeta$ outside the dielectric and a displacement field $D\zeta$ inside.

"omg Blueprint for trapped ion quantum computing with metastable states"
D. T. C. Allcock, W. C. Campbell, **J. Chiaverini**, **I. L. Chuang**, E. R. Hudson, I. D. Moore, A. Ransford, C. Roman, J. M. Sage, D. J. Wineland
arxiv.org/abs/2109.01272

ISAAC CHUANG, *EECS, Physics*

"Quantum advantage for noisy channel discrimination"
Zane M. Rossi, Jeffery Yu, Isaac L. Chuang, Sho Sugiura
arXiv:2105.08707 **(2021)**

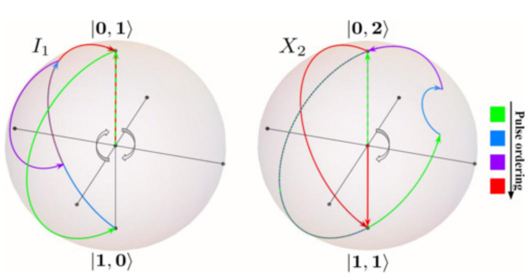

"Constructing Qudits from Infinite Dimensional Oscillators by Coupling to Qubits"
Yuan Liu, Jasmine Sinanan-Singh, Matthew T. Kearney, Gabriel Mintzer, Isaac L. Chuang
Phys. Rev. A 104, 032605 (2021)

A pulse sequence for $n=2$ to realize $I_1 \oplus X_2$ in the first two sQM subspaces. Each Bloch sphere represents an sQM subspace spanned by the states at the north and south poles. The initial Bloch vector in dashed green (pointing toward the north pole) is rotated to the final Bloch vector in solid red with the four-pulse sequence from Eq.

AROUND THE INSTITUTE

ISAAC CHUANG, *EECS, Physics*

“A Grand Unification of Quantum Algorithms”

John M. Martyn, Zane M. Rossi, Andrew K. Tan, Isaac L. Chuang
arxiv.org/abs/2105.02859v3 (2021)

RICCARDO COMIN, *Physics*

Also featured on Joe Checkelsky research and Nuh Gedik research

“Local electronic structure of rutile RuO2”

C. A. Occhialini, V. Bisogni, H. You, A. Barbour, I. Jarrige, J. F. Mitchell, R. Comin, J. Pelliciari
Physical Review Research 3, 033214 (2021)

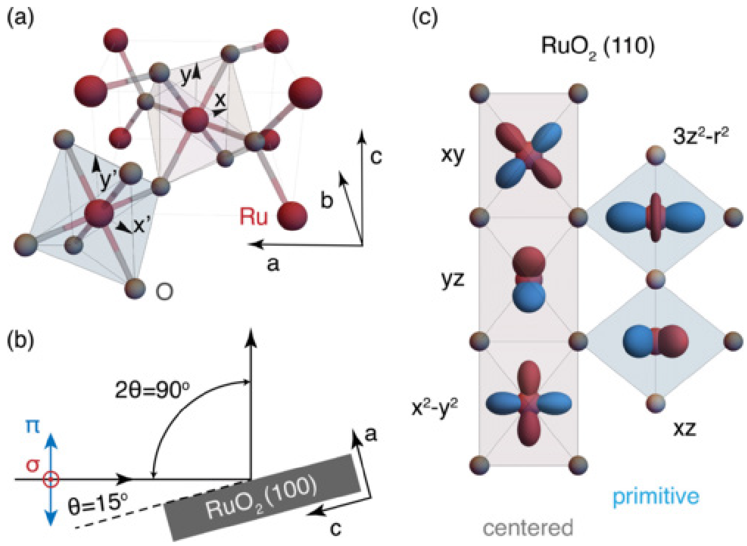

(a) The rutile crystal structure of RuO_2, denoting the local Ru site axes, xy and x′y′, used for orbital definitions at the two Ru lattice sites, and (b) the scattering geometry used for all experiments. (c) A depiction of the 4d orbitals at the centered and primitive Ru lattice sites as viewed in the RuO_2 (110) plane, where the xy and $3z^2-r^2$ orbitals belong to the e_g set and the xz/yz/x^2-y^2 to the t_{2g} set.

RICCARDO COMIN, *Physics*

Structure and Fermi surface of FeSe bulk and FeSe/SrTiO3 (STO)

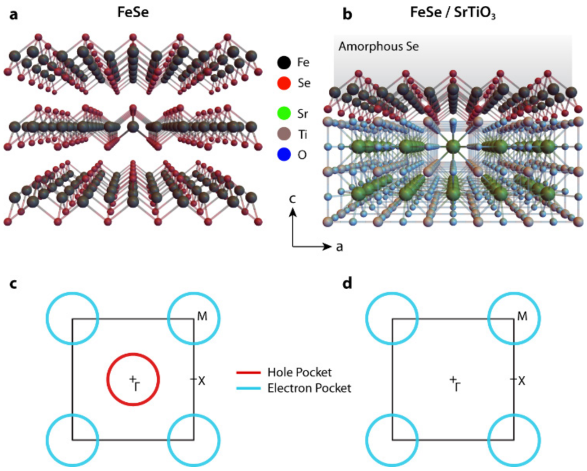

["Evolution of spin excitations from bulk to monolayer FeSe"]
J. Pelliciari, S. Karakuzu, Q. Song, R. Arpaia, A. Nag, M. Rossi, J. Li, T. Yu, X. Chen, R. Peng, M. García-Fernández, A. C. Walters, Q. Wang, J. Zhao, G. Ghiringhelli, D. Feng, T. A. Maier, K.-J. Zhou, S. Johnston, R. Comin
Nature Communications 12, 3122 (2021)

"Sudden Collapse of Magnetic Order in Oxygen-Deficient Nickelate Films"
J. Li, R. J. Green, Z. Zhang, R. Sutarto, J. T. Sadowski, Z. Zhu, G. Zhang, D. Zhou, Y. Sun, F. He, S. Ramanathan, R. Comin
Physical Review Letters 126, 187602 (2021)

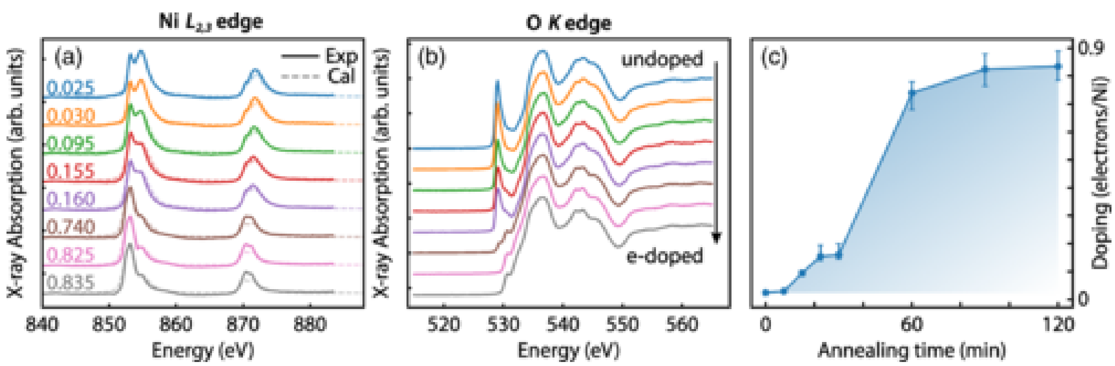

(a) Measured (solid) and simulated (dashed) x-ray absorption spectra across the Ni $L_{2,3}$ edges for $SmNiO_{3-x}$ with different electron-doping levels, obtained by annealing stoichiometric films in an oxygen deficient atmosphere. The doping level (number of doped electrons per Ni) is specified for each simulated spectrum. Spectra are vertically offset for clarity. (b) x-ray absorption spectra across the O K edges for the same SmNiO3−x samples. The same color legend is used as the data series in Fig. 1. (c) The doping levels vs annealing time for each sample, as extracted from the comparison between experimental and theoretical spectra. Vertical error bars reflect the uncertainty in the doping level for each sample.

"Synthesis, engineering, and theory of 2D van der Waals magnets"
M. Blei, J. L. Lado, Q. Song, D. Dey, O. Erten, V. Pardo, R. Comin, S. Tongay, A. S. Botana
Applied Physics Reviews 8, 021301 (2021)

DIRK ENGLUND, *EECS*

“Thermally-Polarized Solid-State Spin Sensor”
Reginald Wilcox, Erik Eisenach, John Barry, Matthew Steinecker, Michael O’Keeffe, Dirk Englund, Danielle Braje
scirate.com/arxiv/2109.01576 (2021)

“Ultrastrong magnetic light-matter interaction with cavity mode engineering”
Hyeongrak, Choi and Dirk Englund
scirate.com/arxiv/2108.13266 (2021)

“Universal linear optics by programmable multimode interference”
Hugo Larocque, Dirk Englund
scirate.com/arxiv/2107.06107 (2021)

“Accurate Self-Configuration of Rectangular Multiport Interferometers”
Ryan Hamerly, Saumil Bandyopadhyay, Dirk Englund
arxiv.org/abs/2106.03249 (2021)

“Stability of Self-Configuring Large Multiport Interferometers”
Ryan Hamerly, Saumil Bandyopadhyay, Dirk Englund
scirate.com/arxiv/2106.04363 (2021)

“Ultrasensitive Calorimetric Measurements of the Electronic Heat Capacity of Graphene”
Mohammed Ali Aamir, John N. Moore, Xiaobo Lu, Paul Seifert, Dirk Englund, Kin-Chung Fong, Dmitri K. Efetov
Nano Lett. 2021, 21, 12, 5330–5337 (2021)

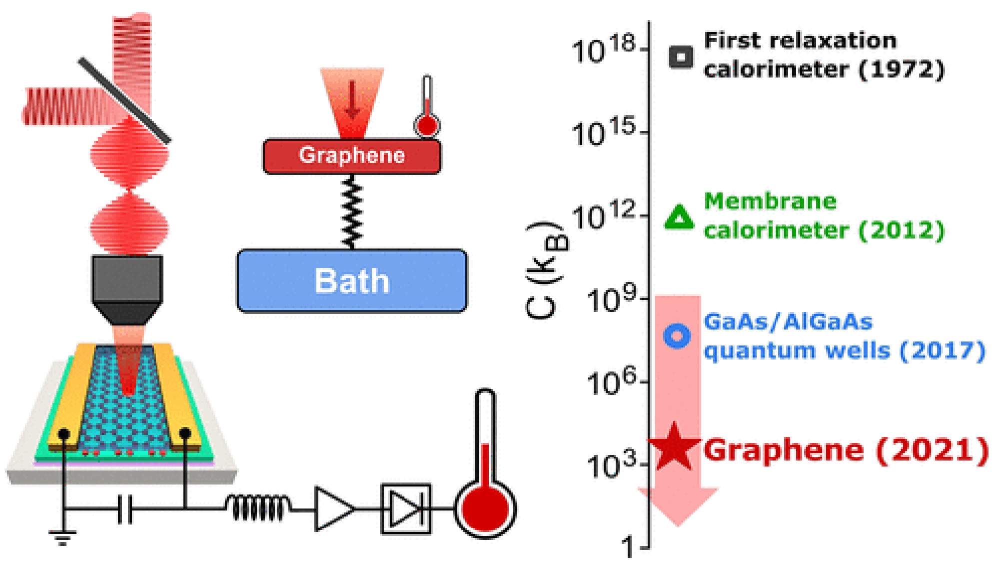

DIRK ENGLUND, *EECS*

"A phononic interface between a superconducting quantum processor and quantum networked spin memories"

Tomas Neuman, Matt Eichenfield, Matthew Trusheim, Lisa Hackett, Prineha Narang, Dirk Englund
npj quantum information (2021)

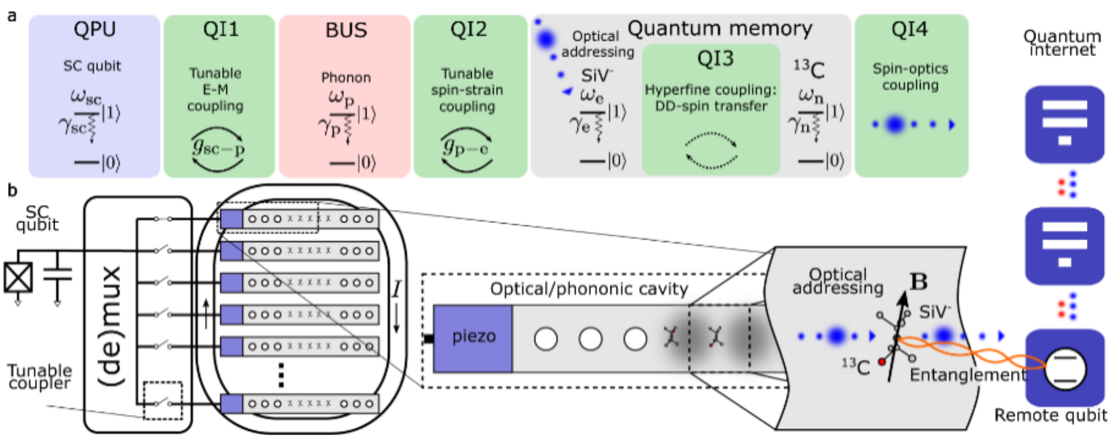

(a) An SC quantum processing unit (QPU) is connected via piezoelectric `quantum interface 1› (QI1) to a phononic BUS. The phonon couples to electronic spin-orbit states of an AA, forming quantum interface 2 (QI2). The AA's fine-structure states can further couple to nuclear-spin to realize a QM via quantum interface 3 (QI3) or they connect to photons in quantum interface 4 (QI4), which finally connects to the quantum internet (blue dots: photonic interconnects). (b) A physical realization of the scheme outlined in (a). A superconducting qubit is connected via a phononic or microwave multiplexer (mux) to a series of phononic or microwave waveguides that are each interfaced with a mechanical cavity hosting one or many AAs whose electronic fine-structure (spin-orbit) states serve as qubits. The spin-orbit states of each AA interacts with the spin states of a nearby ^{13}C nucleus via the hyperfine interaction, providing ancillae qubits with long coherence times. The AA optical transitions provide an optical interface to quantum networks, for example by multiple attempts of photon-based electron spin entanglement to provide an on-demand entanglement resource. Underlying these capabilities is a transduction scheme that exploits: tunable electro-mechanical (E-M) coupling between the SC qubit and the mechanical mode, tunable spin-strain coupling between the mechanical mode and the electron spin, optical addressing of the electron spin, and hyperfine coupling to connect the electron spin to the nuclear QM.

"Quantum control of the tin-vacancy spin qubit in diamond"

Romain Debroux, Cathryn P. Michaels, Carola M. Purser, Noel Wan, Matthew E. Trusheim, Jesús Arjona Martínez, Ryan A. Parker, Alexander M. Stramma, Kevin C. Chen, Lorenzo de Santis, Evgeny M. Alexeev, Andrea C. Ferrari, Dirk Englund, Dorian A. Gangloff, Mete Atatüre
scirate.com/arxiv/2106.00723 (2021)

"High-speed programmable photonic circuits in a cryogenically compatible, visible-NIR 200 mm CMOS architecture"

Mark Dong, Genevieve Clark, Andrew J. Leenheer, Matthew Zimmermann, Daniel Dominguez, Adrian J. Menssen, David Heim, Gerald Gilbert, Dirk Englund, Matt Eichenfield
scirate.com/arxiv/2105.12531 (2021)

DIRK ENGLUND, *EECS*

“A Vertically Loaded Diamond Microdisk Resonator (VLDMoRt) for Quantum Networks”

Yuqin Duan, Kevin C. Chen, Dirk R. Englund, Matthew E. Trusheim
arxiv.org/abs/2105.05695 (2021)

“Quantum networks based on color centers in diamond”

Maximilian Ruf, Noel H. Wan, Hyeongrak Choi, Dirk Englund, Ronald Hanson
Journal of Applied Physics (2021)

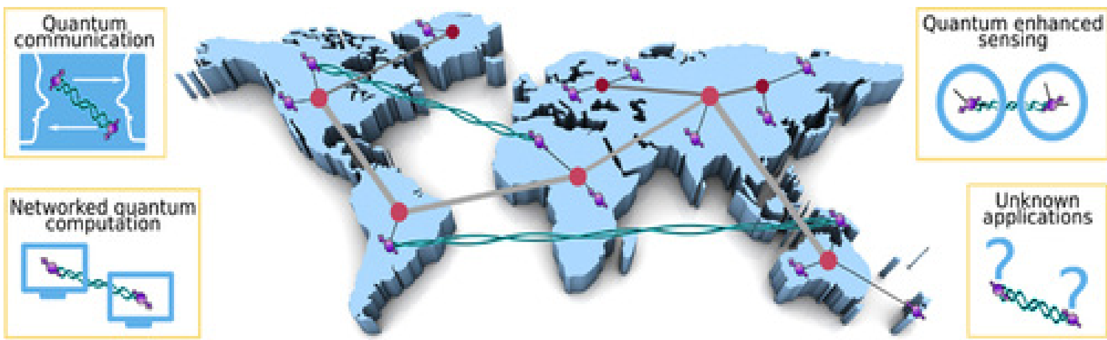

Schematic overview of a future large-scale quantum network, consisting of nodes containing optically interfaced qubits (purple) with long coherence times. Photons routed via optical fibers or free-space channels serve as mediators to create entanglement (blue wiggled lines). Local area and trunk backbone quantum repeaters (dark and light red circles, respectively) are used to enable a high entanglement generation rate over large distances, overcoming photon transmission loss. The entanglement generation is heralded, meaning that detection of certain photon statistics signals the successful generation of an entangled state that is available to a network user for further processing and applications such as networked quantum computation, quantum secured communication, quantum enhanced sensing, and potential not yet discovered tasks.

“Scalable and High-Fidelity Quantum Random Access Memory in Spin-Photon Networks”

Kevin C. Chen, Wenhan Dai, Carlos Errando-Herranz, Seth Lloyd, Dirk Englund
PRX Quantum (2021)

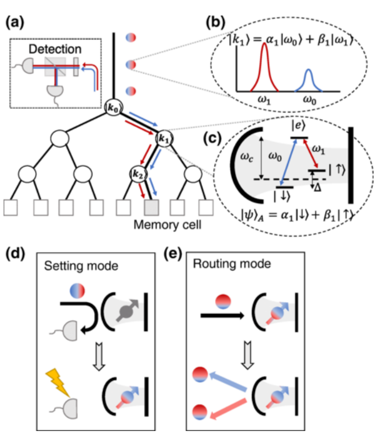

An illustrative bucket-brigade model with a cavity-coupled Λ-level atom at each tree node. (a) The address $|j\rangle$ consisting of the register qubits $|k0\rangle|k1\rangle|k2\rangle$ arrives at the three-level binary tree containing $N=2^3$ memory cells. (b) Each register is a frequency-encoded photonic qubit in the $\{\omega 0,\omega 1\}$ basis. (c) For our implementation, each tree node is a Λ-atom coupled to a single-sided nanocavity, the resonant frequency ωc of which is tuned to the average of the two atomic transition frequencies, $\omega 0$ and $\omega 1$, which are separated by a Zeeman splitting Δ. For layer 1, the register $|k1\rangle$ sets the internal state of the node to $|\psi A\rangle=\alpha 1|\downarrow\rangle+\beta 1|\uparrow\rangle$ that routes the successive register $|k2\rangle$. Two essential operations are (d) the setting mode via cavity reflection and (e) the routing mode.

DIRK ENGLUND, *EECS*

“Optically-Heralded Entanglement of Superconducting Systems in Quantum Networks”

Stefan Krastanov, Hamza Raniwala, Jeffrey Holzgrafe, Kurt Jacobs, Marko Lončar, Matthew J. Reagor, and Dirk R. Englund
Phys. Rev. Lett (2021)

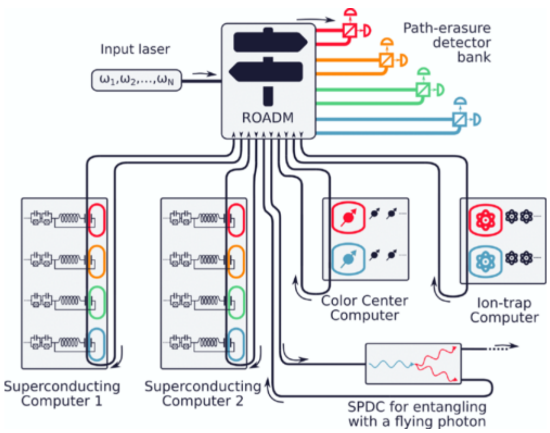

Future outlook for interfridge connectivity. Replacing the single path-erasure detection with a reconfigurable optical add-drop multiplexer (ROADM) will allow us to route a frequency comb pump laser to qubits in several quantum nodes. By connecting the ROADM to a bank of path-erasure detectors for each frequency channel, this design will enable multiplexed heralded entanglement generation between multiple fridges of different quantum modalities.

“Intrinsic Donor-Bound Excitons in Ultraclean Monolayer Semiconductors”

Pasqual Rivera, Minhao He, Bumho Kim, Song Liu, Carmen Rubio-Verdú, Hyowon Moon, Lukas Mennel, Daniel A. Rhodes, Hongyi Yu, Takashi Taniguchi, Kenji Watanabe, Jiaqiang Yan, David G. Mandrus, Hanan Dery, A bhay Pasupathy, Dirk Englund, James Hone, Wang Yao, Xiaodong Xu
Nature Communications (2021)

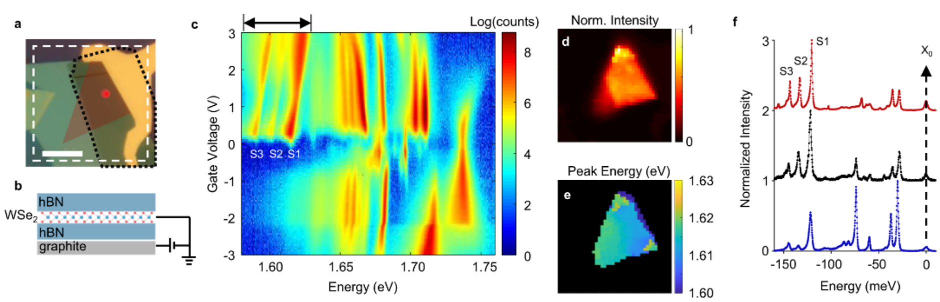

(a) Optical image of electrostatic gating device composed of exfoliated monolayer WSe_2 (red area) encapsulated in hBN with graphite backgate (outlined in black). Scale bar is 10 μm. (b) Schematic of sample side view. (c) Photoluminescence as a function of back gate voltage with the laser spot indicated by the red dot in (a). Three satellites peaks near 1.60 eV appear when the sample is n-doped. (d) Spatial map of the integrated PL from the satellite peaks at $V_b = 0.5$ V. Integration spectral region shown by arrows on top of (c), and spatial region outlined by dashed white lines in (a). (e) Spatial map of the peak energy of the highest-energy satellite at $V_b = 0.5$ V. (f) Waterfall plot of PL spectra from three different samples, showing homogeneous satellite binding energies and robust three peak spectral features. The energy axis is scaled relative to the free neutral exciton (X0 at ~1.735 eV).

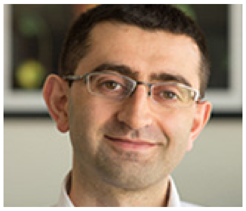

JOSEPH A.FORMAGGIO, *Physics*

"Precision measurement of the electron energy-loss function in tritium and deuterium gas for the KATRIN experiment"

Aker, M., Beglarian, A., Behrens, J...., Formaggio, J.A.... et al.
Eur. Phys. J. C 81, 579 (2021)

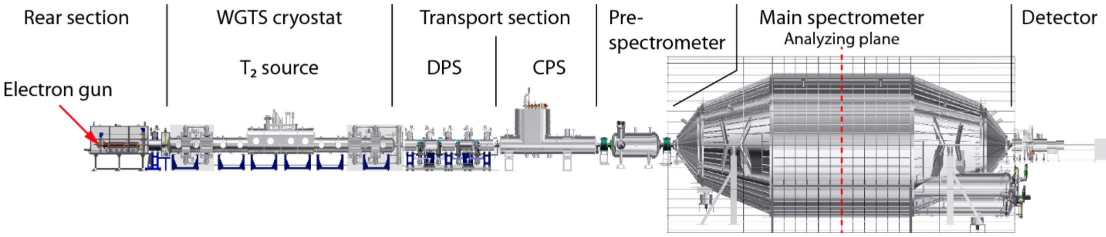

Overview of the KATRIN experiment. The main components are from left to right: The rear section containing calibration and monitoring systems as well as the electron gun (see Fig. 2) used in this work; the 10-m-long windowless gaseous tritium source (WGTS) with differential pumps on both sides; the transport section consisting of a differential (DPS) and cryogenic pumping section (CPS); the spectrometer and detector section with the pre- and main spectrometer, and the silicon detector. The overall length of the experimental setup is more than 70 m

NUH GEDIK, *Physics*

"Unconventional hysteretic transition in a charge density wave"

B. Q. Lv, Alfred Zong, D. Wu, A.V. Rozhkov, Boris V. Fine, Su-Di Chen, Makoto Hashimoto, Dong-Hui Lu, M. Li, Y.-B. Huang, Jacob P. C. Ruff, Donald A. Walko, Z. H. Chen, Inhui Hwang, Yifan Su, Xiaozhe Shen, Xirui Wang, Fei Han, Hoi Chun Po, Yao Wang, Pablo Jarillo-Herrero, Xijie Wang, Hua Zhou, Cheng-Jun Sun, Haidan Wen, Zhi-Xun Shen, N. L. Wang, Nuh Gedik
arxiv.org/abs/2106.09774 (2021)

"Experimental realization of a single-layer multiferroic"

Qian Song, Connor A. Occhialini, Emre Ergeçen, Batyr Ilyas, Kenji Watanabe, Takashi Taniguchi, Nuh Gedik, Riccardo Comin
arxiv.org/abs/2106.07661 (2021)

NUH GEDIK, *Physics*

“Trimeron-phonon coupling in magnetite”

Przemysław Piekarz, Dominik Legut, Edoardo Baldini, Carina A. Belvin, Tomasz Kołodziej, Wojciech Tabiś, Andrzej Kozłowski, Zbigniew Kakol, Zbigniew Tarnawski, José Lorenzana, Nuh Gedik, Andrzej M. Oleś, Jürgen M. Honig, and Krzysztof Parlinski
Phys. Rev. B 103, 104303 (2021) arXiv:2010.11564 (2020)

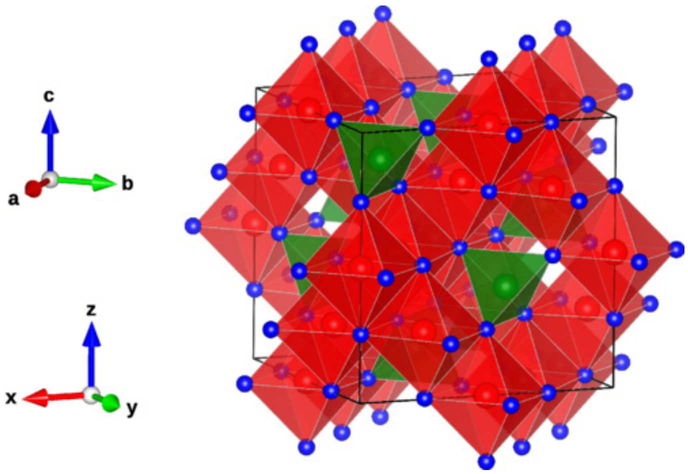

The unit cell of the cubic $Fd\bar{3}m$ *structure of magnetite. Green, red, and blue spheres represent* Fe_A, Fe_B, *and O atoms, respectively. The* Fe_AO_4 *tetrahedra and* Fe_BO_6 *octahedra are presented in green and red colors, respectively. The main crystallographic directions of the cubic* (x,y,z) *and monoclinic* (a,b,c) *unit cells are included. The image was rendered using VESTA software.*

“Unconventional light-induced states visualized by ultrafast electron diffraction and microscopy”

Alfred Zong, Anshul Kogar, & Nuh Gedik
arxiv.org/abs/2104.10373 (2021)

Crystal structure and optical properties of NiPS3.

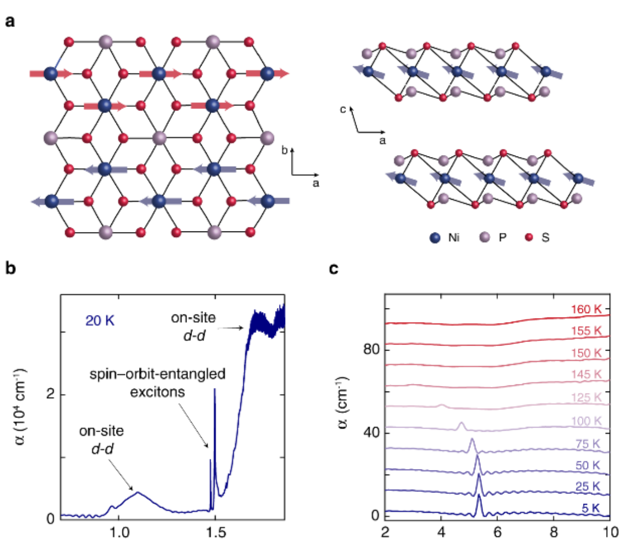

“Exciton-driven antiferromagnetic metal in a correlated van der Waals insulator”

Carina A. Belvin, Edoardo Baldini, Ilkem Ozge Ozel, Dan Mao, Hoi Chun Po, Clifford J. Allington, Suhan Son, Beom Hyun Kim, Jonghyeon Kim, Inho Hwang, Jae Hoon Kim, Je-Geun Park, T. Senthil, Nuh Gedik
Nature Communications 12, 4837 (2021)

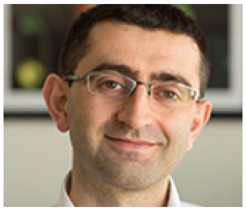

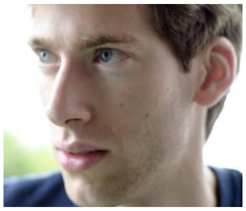

NUH GEDIK, *Physics*

"Phonoritons as Hybridized Exciton-Photon-Phonon Excitations in a Monolayer h-BN Optical Cavity"

Simone Latini, Umberto De Giovannini, Edbert J. Sie, Nuh Gedik, Hannes Hübener, Angel Rubio
Phys. Rev Lett. 126, 227401 (2021) arXiv:2102.09472 (2021)

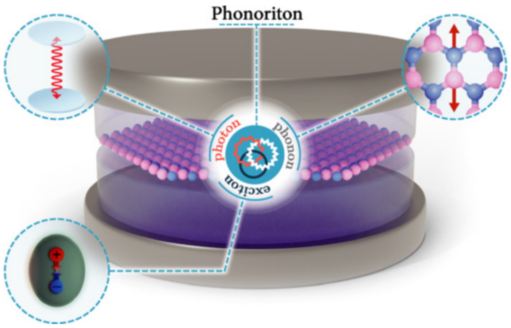

The phonoriton is a hybridization between excitons, phonons, and photons that can be realized by embedding a crystal in an optical cavity.

ARAM W. HARROW, *Physics*

"Separation of Out-Of-Time-Ordered Correlation and Entanglement"

Aram W. Harrow, Linghang Kong, Zi-Wen Liu, Saeed Mehraban, and Peter W. Shor
PRX Quantum 2, 020339 (2021) https://arxiv.org/abs/1906.02219 (2019)

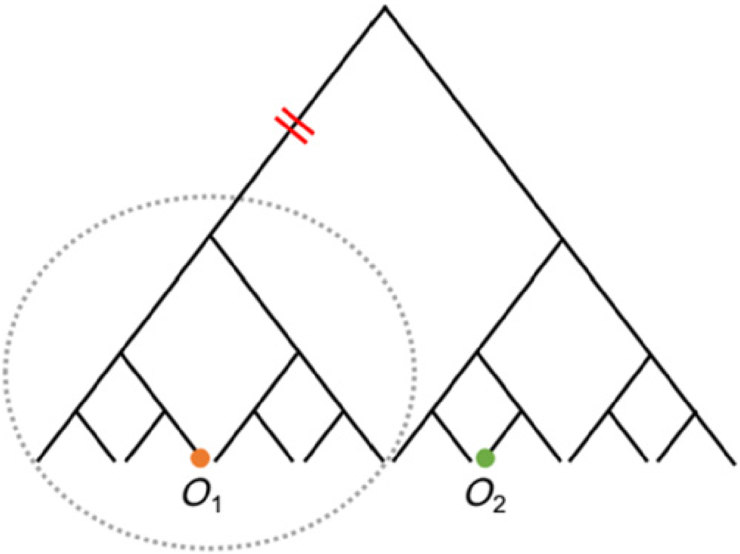

Illustration of the binary-tree model of depth 4. We consider OTOC between local operators originally acting on two farthest vertices (a leaf of the left and right subtrees, respectively, for example, O_1 and O_2 in the diagram), and entanglement between the left subtree (dashed circle) and the rest of the graph (the cut shown by the red double line).

MIT Center for Quantum Engineering · MIT · MIT Quantum Science and Engineering Consortium

PABLO JARILLO-HERRERO, *Physics*

“Fractional Chern insulators in magic-angle twisted bilayer graphene”
Yonglong Xie, Andrew T. Pierce, Jeong Min Park, Daniel E. Parker, Eslam Khalaf, Patrick Ledwith, Yuan Cao, Seung Hwan Lee, Shaowen Chen, Patrick R. Forrester, Kenji Watanabe, Takashi Taniguchi, Ashvin Vishwanath, Pablo Jarillo-Herrero, Amir Yacoby
arXiv:2107.10854 (2021)

“Cyclotron resonance overtones and near-field magnetoabsorption via terahertz Bernstein modes in graphene”
D. A. Bandurin, E. Mönch, K. Kapralov, I. Y. Phinney, K. Lindner, S. Liu, J. H. Edgar, I. A. Dmitriev, P. Jarillo-Herrero, D. Svintsov, S. D. Ganichev
arXiv:2106.02117 (2021)

“Pauli-limit violation and re-entrant superconductivity in moiré graphene”
Yuan Cao*, Jeong Min Park*, Kenji Watanabe, Takashi Taniguchi, Pablo Jarillo-Herrero
Nature 595, 526-531 (2021) arXiv:2103.12083 (2021)
featured on MIT news (2021)

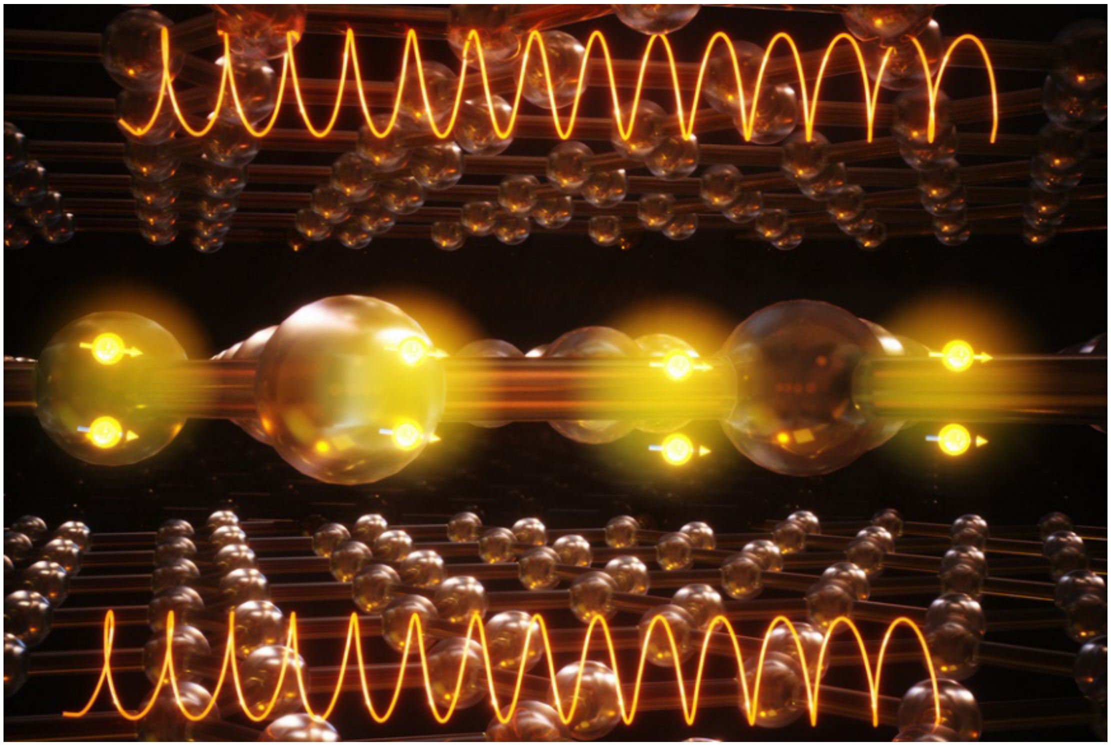

MIT Physicists have observed signs of a rare type of superconductivity in a material called “magic-angle” twisted trilayer graphene.

PABLO JARILLO-HERRERO, *Physics*

“Strong interminivalley scattering in twisted bilayer graphene revealed by high-temperature magnetooscillations”

I. Y. Phinney, D. A. Bandurin+, C. Collignon, I. A. Dmitriev, T. Taniguchi, K. Watanabe, P. Jarillo-Herrero
Phys. Rev. Lett. 127, 056802 (2021) Editor’s suggestion (2021)
arXiv:2106.02088 (2021)

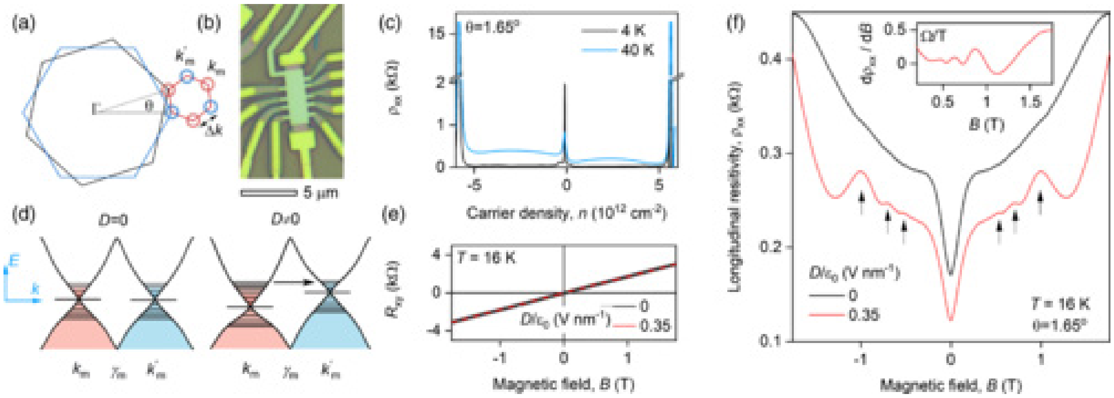

Interminivalley magneto-oscillations in small-angle twisted bilayer graphene. (a) Schematic illustration of the mini-BZ of the SA TBG superlattice. Red and blue circles represent Fermi surfaces in different minivalleys, labeled k_m *and* k'_m*. (b) Optical photograph of an encapsulated SA TBG device. Yellow, gold contacts; dull green, top gate; light brown, Hall bar mesa. (c)* ρ_{xx} *as a function of n for the 1.65° device at 4 K (black) and 40 K (blue).* $B=0$, $D=0$. *(d) Calculated single-particle band structure for the 1.65° SA TBG. At low energies two Dirac cones are formed in the vicinity of the* k_m *and* k'_m *points. The horizontal black lines represent unevenly spaced LLs that form in the presence of a perpendicular magnetic field. When* $D\neq0$*, the cones are shifted with respect to each other. When LLs from different minivalleys get aligned inside the thermal window around the Fermi level, interminivalley scattering (arrow) is enhanced resulting in excess resistivity. (e) Hall resistance* R_{xy} *as a function of B for two characteristics* $D=0$ *and* $D/\epsilon_0=0.35$ V/nm *yielding* $n\approx0.7\times10^{12}$ cm^{-2} *measured at* $T=16$ K. *(f)* ρ_{xx} *(symmetrized) as a function of* B *for the same* D, n, *and* T *as in (e). Inset: derivative of the* $\rho_{xx}(B)$ *dependence for the case of* $D/\epsilon_0=0.35$ V/nm.

“Fizeau drag in graphene plasmonics”

Y. Dong, L. Xiong, I. Y. Phinney, Z. Sun, R. Jing, A. S. McLeod, S. Zhang, S. Liu, F. L. Ruta, H. Gao, Z. Dong, R. Pan, J. H. Edgar, P. Jarillo-Herrero, L. S. Levitov, A. J. Millis, M. M. Fogler, D. A. Bandurin & D. N. Basov
Nature 594, 513–516 (2021) arXiv:2103.10831 (2021)
Nature News and Views (2021)

“Stacking-engineered ferroelectricity in bilayer boron nitride”

Kenji Yasuda, Xirui Wang, Kenji Watanabe, Takashi Taniguchi, Pablo Jarillo-Herrero
Science 372, 1458-1462 (2021) arXiv:2010.06600 (2021)

MIT Center for Quantum Engineering
MIT Quantum Science and Engineering Consortium

PABLO JARILLO-HERRERO, *Physics*

"Highly Tunable Junctions and Nonlocal Josephson Effect in Magic Angle Graphene Tunneling Devices"
Daniel Rodan-Legrain*, Yuan Cao*, Jeong Min Park*, Sergio C. de la Barrera, Mallika T. Randeria, Kenji Watanabe, Takashi Taniguchi, Pablo Jarillo-Herrero
Nature Nanotechnology (2021) arXiv:2011.02500 (2021)
Nature Nanotechnology News and Views (2021)
featured on Science "Latest News" (2021) Featured on MIT News (2021)

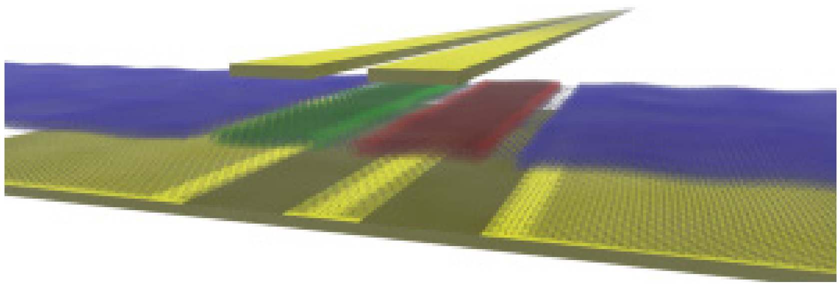

Schematic of a device made in magic-angle twisted bilayer graphene

ANDREW J. KERMAN, *Lincoln Laboratory*

"Superconducting Circuit Realization of Combinatorial Gauge Symmetry"
Claudio Chamon, Dmitry Green, and Andrew J. Kerman
PRX Quantum 2, 030341 (2021) arXiv:2006.10060 (2021)

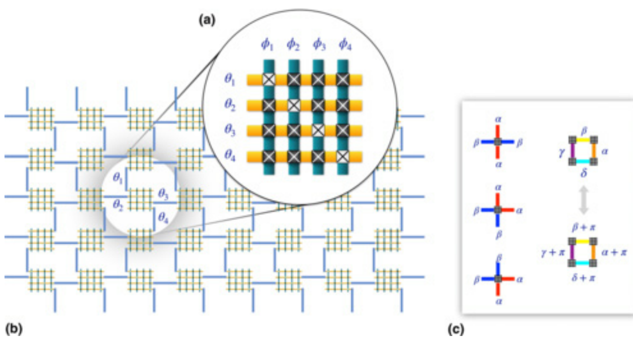

(a) An array of intersecting superconducting wires which form a single "waffle" site in the lattice. Vertical (green) wires are "matter" degrees of freedom with phase ϕ_n and charge q_n. Horizontal (yellow) wires are "gauge" degrees of freedom with phase θ_i and charge Q_i. Wires are coupled by Josephson junctions depicted as black or white crosses depending on the sign of the coupling. This array mirrors the interaction matrix W and implements combinatorial gauge symmetry. (b) The full lattice with links (blue) connecting the gauge degrees of freedom. One site is highlighted to illustrate how sites are connected; links that it shares with neighboring sites are labeled by their gauge phases θ_i. The matter wires with phases ϕ_n are connected only to gauge wires. (c) This geometry leads to exact $\mathbb{Z}_2$ topological order, as illustrated by the allowed configurations of the gauge phases θ emanating from each waffle site. We show the limit in which the capacitances are large (i.e., classical limit), where the gauge phases are good quantum numbers. Gauge phases must be equal pairwise α (red) and β (blue) at each site, where both phases are defined modulo π. In the context of lattice models, such vertices are related to loop models. Additionally, plaquettes may be flipped back and forth by shifting all gauge phases around the plaquette $(\alpha,\beta,\gamma,\delta)$ by π.

WOLFGANG KETTERLE, *Physics*

"Rotational Coherence Times of Polar Molecules in Optical Tweezers"
S. Burchesky, L. Anderegg, Y. Bao, S.S. Yu, E. Chae, W. Ketterle, K.K. Ni, and J.M. Doyle
Phys. Rev. Lett., arxiv.org/abs/2105.15199

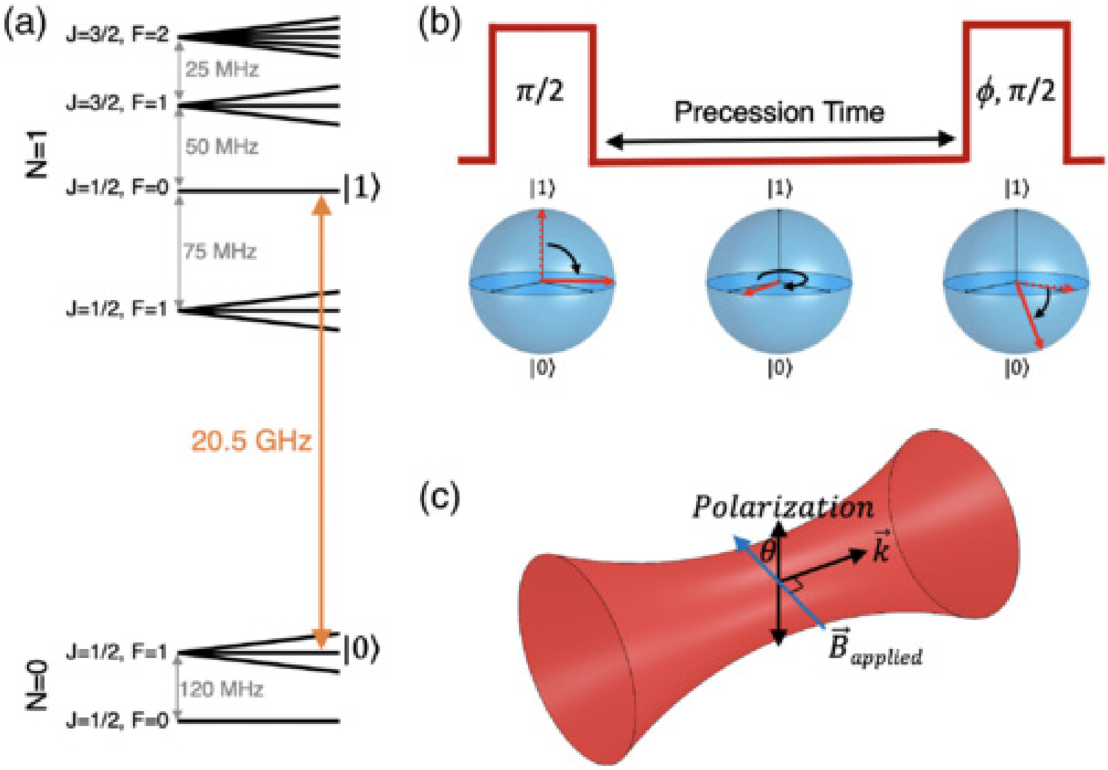

CaF structure. (a) The X-state level structure of CaF. Quantum numbers N, J, and F denote rotation, electron spin+rotation, and total angular momentum, respectively. The lower and upper qubit states are labeled $|0\rangle$ and $|1\rangle$. (b) The Ramsey pulse sequence uses a 10 μs $\pi/2$ pulse to create a coherent superposition of $|0\rangle$ and $|1\rangle$ states. The Bloch vector precesses, accumulating phase until the second $\pi/2$ pulse with a phase shift (ϕ) rotates the Bloch vector back into the measurement basis prior to imaging the N=1 population. (c) The tweezer light polarization and applied magnetic field lie in the plane perpendicular to the k vector of the tweezer light.

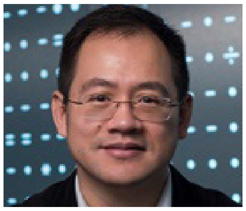

JU LI, *NSE MSE*

"Pure spin photocurrent in non-centrosymmetric crystals: bulk spin photovoltaic effect"

H-W. Xu, H. Wang, J. Zhou and J. Li
Nature Communications 12 4330. (2021)

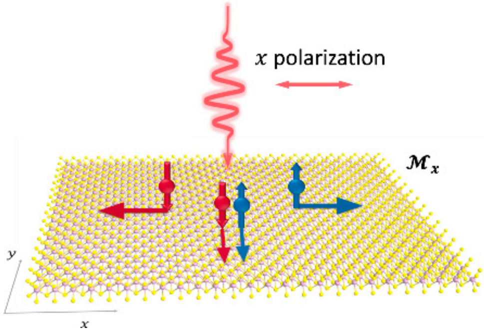

The light polarizes in the x-direction, while the system has mirror symmetry MxMx. In the x-direction, spin-up and spin-down states travel in opposite directions, so that the net charge current is vanishing, whereas the net spin current goes to the +x-direction. In the y-direction, spin-up and spin-down electrons travel in the same direction, leading to nonvanishing charge current but vanishing spin current.

"Machine learning for deep elastic strain engineering of semiconductor electronic band structure and effective mass"

E. Tsymbalov, Z. Shi, M. Dao, S. Suresh, J. Li and A. Shapeev
npj Computational Materials 7 76 (2021)

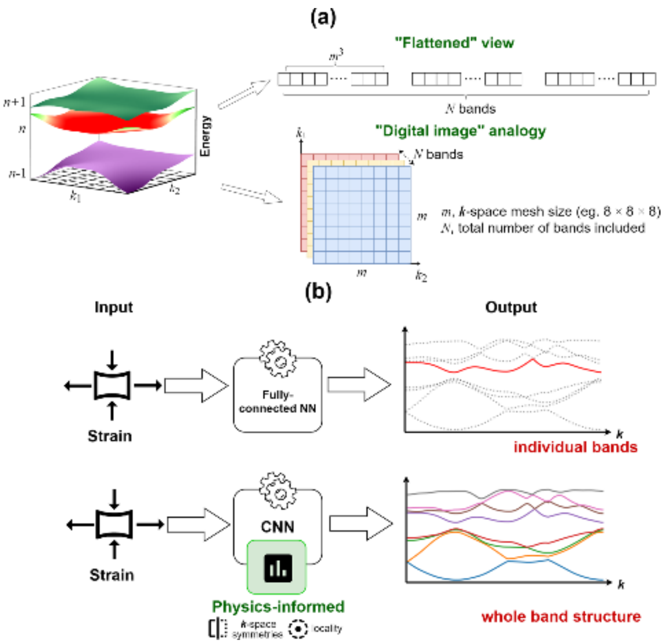

(a) Different representation of a band structure. In the "flattened" view, a band structure is represented as N stacked flattened arrays (vectors) and processed like independent values. Each array is m3 in length. In the "digital image" analogy, the band structure is envisioned as N different 3D images stacked together, each of which has a "voxel" dimension of m × m × m. The eigenvalues on an energy band can then be thought of as the "color-scale" of the voxels. (b) Comparison of the two different approaches to ML. We predict the eigenvalues for each energy band separately by utilizing the "flattened" band structure representation to obtain the entire band structure.

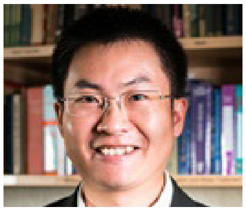

"Elucidating proximity magnetism through polarized neutron reflectometry and machine learning"
Nina Andrejevic, Zhantao Chen, Thanh Nguyen, Leon Fan,
Henry Heiberger, Valeria Lauter, Ling-Jie Zhou, Yi-Fan Zhao, Cui-Zu Chang,
Alexander Grutter, Mingda Li
arXiv:2109.08005 (2021)

"Electronic properties of correlated kagomé metals AV3Sb5 (A = K, Rb, Cs): A brief review"
Thanh Nguyen, Mingda Li
arXiv:2109.06809 (2021)

"Extended Kohler's rule of magnetoresistance"
J. Xu, F. Han, T. Wang, L.R. Thoutam, M. Li, X. Zhang, Y-L Wang, R. Fotovat,
U. Welp, W-K Kwok and Z-L Xiao
Phys. Rev. X. (2021) arXiv:2109.08089 (2021)

"Signature of Many-Body Localization of Phonons in Strongly Disordered Superlattices"
T. Nguyen, N. Andrejevic, H. C. Po, Q. Song, Y. Tsurimaki, N. C. Drucker,
A. Alatas, E. E. Alp, B. M. Leu, A. Cunsolo, Y. Cai, L. Wu, J. A. Garlow, Y. Zhu,
A. C. Gossard, A. A. Puretsky, D. B. Geohegan, S. Huang and M. Li
Nano Lett. 21, 7419-7425 (2021) Also appearing in MIT News (2021)

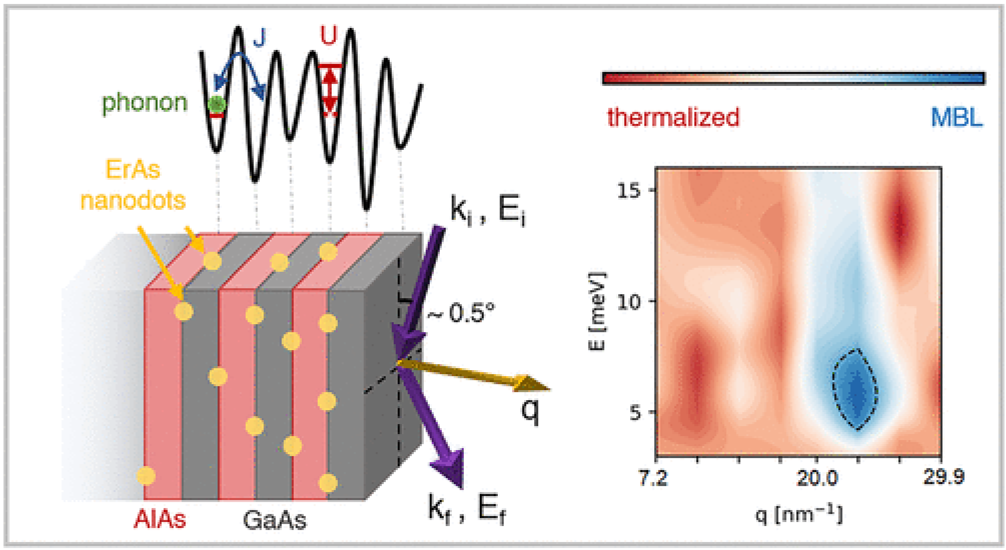

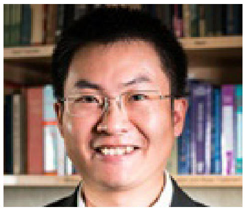

MINGDA LI, *NSE*

[“Material Learning on Neutron and X-Ray Scattering”]

Z. Chen, N. Andrejevic, N. C. Drucker, T. Nguyen, R.P. Xian, T. Smidt, Y. Wang, R. Ernstorfer, A. Tennant, M. Chan, and M. Li

[Chem. Phys. Rev. 2, 031301 (2021)]

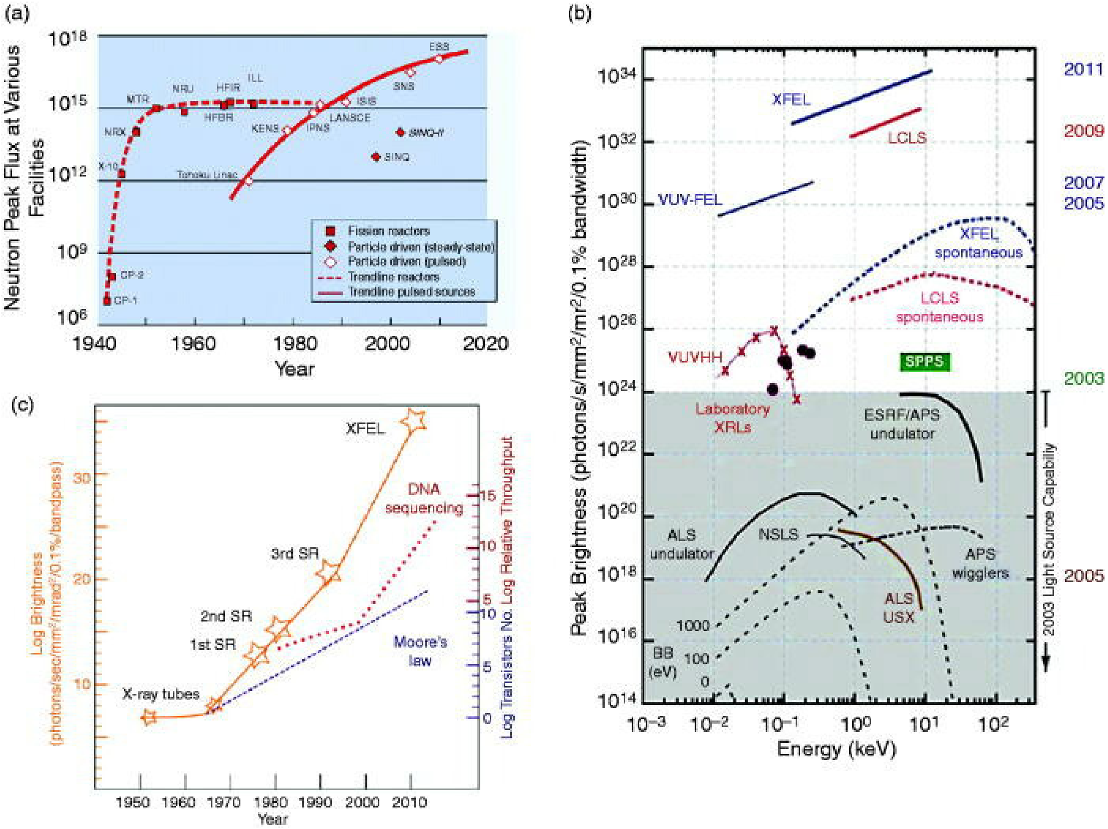

Neutron and x-ray scattering in the data era. (a) Improvement of neutron flux in reactor-based neutron generation (dashed line) and accelerator-based spallation neutron generation (solid line). Reprinted with permission from Bohn et al., ESS Project 1 (2002). Copyright 2002 European Spallation Source.3 (b) Drastic enhancement of peak brightness in x-ray scattering at various energy scales. Reprinted with permission from U.S. National Research Council, Committee on Atomic Molecular and Optical Sciences. Copyright 2007 National Academies Press.4 (c) Comparison of increasing speed of peak brightness of synchrotron x-ray scattering and the Moore›s law of microelectronics. Reprinted with permission from Su et al., Crystallogr. Rev. 21, 122–153 (2015). Copyright 2014 Taylor & Francis Group.6 BB, broadband; CP-1, Chicago Pile 1; HFBR, High Flux Beam Reactor; HFIR, High Flux Isotope Reactor; ILL, Institut Laue–Langevin; IPNS, Intense Pulsed Neutron Source; ISIS, International Science Information Service; KENS, National Laboratory for High Energy Physics Neutron Source; LANSCE, Los Alamos Neutron Science Center; Linac Coherent Light Source (LCLS), linear coherent light source; MTR, Materials Test Reactor; NRU, National Research Universal; NRX, Nuclear Rocket Experiment; SINQ, Swiss Spallation Source; SNS, Spallation Neutron Source; SPPS, solid phase peptide synthesis; VUV-FEL, vacuum ultraviolet free-electron laser; VUVHH, vacuum ultraviolet hybrid heterostructure; X-10, Nuclear Reactor Class 10; XFEL, x-ray free-electron laser.

MIT Center for Quantum Engineering · MIT · MIT Quantum Science and Engineering Consortium

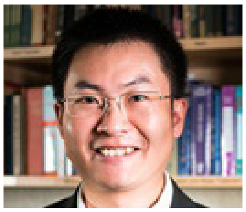

MINGDA LI, *NSE*

“Direct prediction of phonon density of states with Euclidean neural network”

Z. Chen, N. Andrejevic, T. Smidt, Z. Ding, Y-T Chi, Q. Nguyen, A. Alatas, J. Kong and M. Li

Adv. Sci. 8, 2004214 (2021) Also Appearing in MIT News (2021)

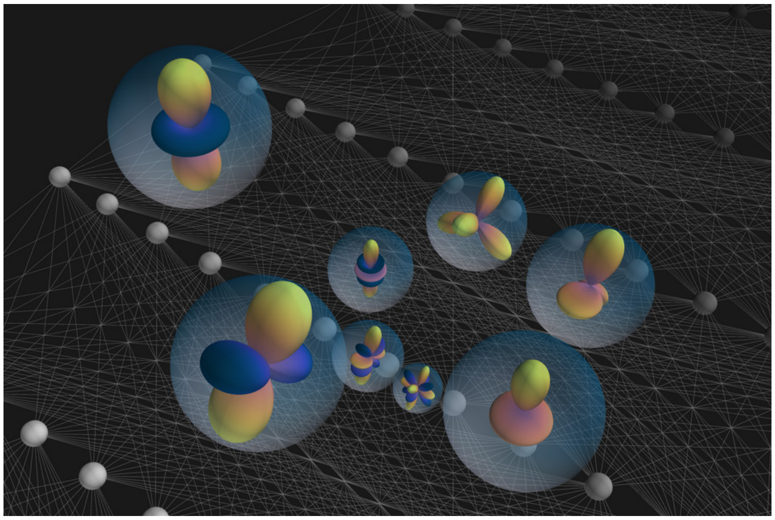

A neural network that carries the full crystal symmetry enables efficient training for crystalline solids.

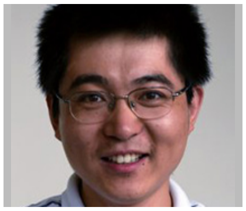

LUQIAO LIU, *EECS*

“Nonreciprocal Transmission of Incoherent Magnons with Asymmetric Diffusion Length”
Han, J., Fan, Y., McGoldrick, B. C., Finley, J., Hou, J. T., Zhang, P. & Liu, L.
Nano Letters, DOI: 10.1021/acs.nanolett.1c02575 (2021).

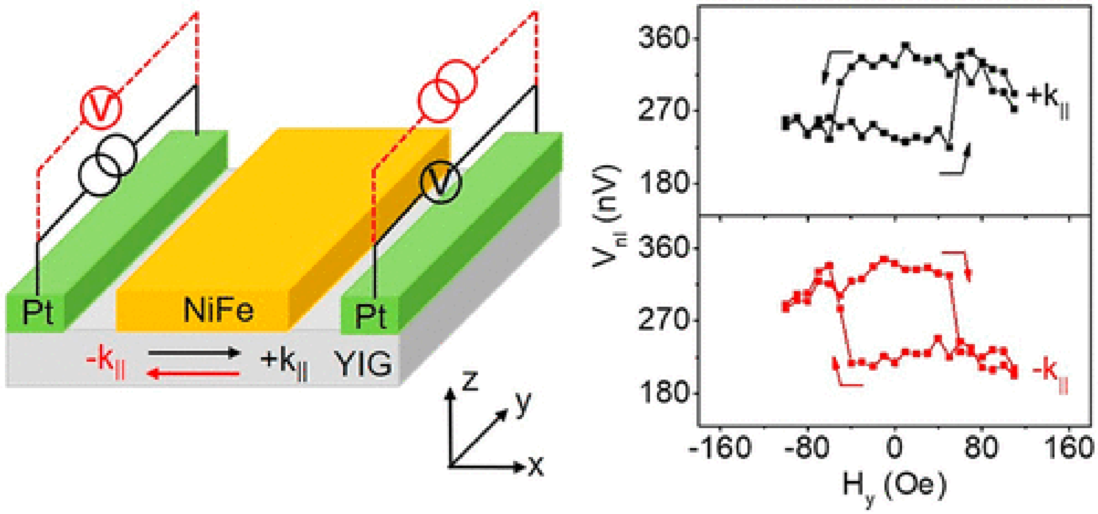

SETH LLOYD, *ME, ES, Physics*

“Non-Markovian Boost of Quantum Maxwell Demon Efficiency”
Kasper Poulsen, Marco Majland, Seth Lloyd, Morten Kjaergaard,
Nikolaj T. Zinner
arXiv:2108.08855 (2021)

“A quantum algorithm for training wide and deep classical neural networks”
Alexander Zlokapa, Hartmut Neven, Seth Lloyd
arXiv:2107.09200 (2021)

KEVIN P. O'BRIEN, *EECS*

"Engineering Purely Nonlinear Coupling Using a Quarton"

Y. Ye, K. Peng, M. Naghiloo, G. Cunningham, K. P. O'Brien
Phys. Rev. Lett. 127, 050502 (2021)

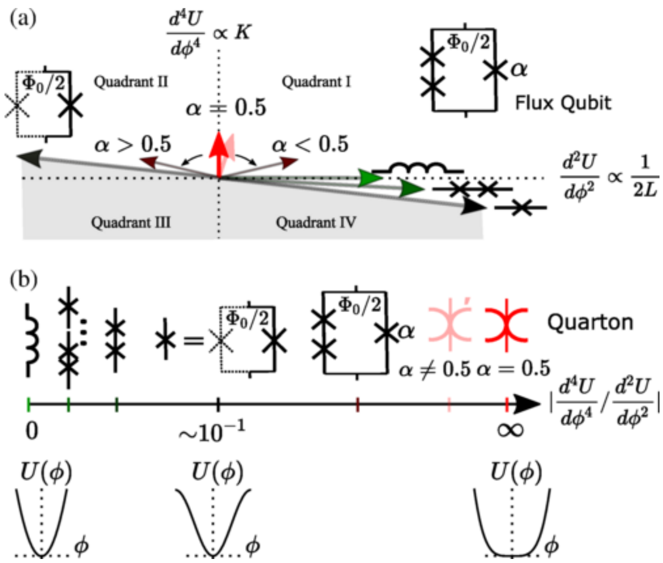

The quarton as a purely nonlinear element. (a) Schematic plot of the nonlinear (K) vs linear (1/2L) landscape of inductive superconducting elements with centrosymmetric potentials (U). The flux qubit has a negative and a positive inductance branch with strength dependent on ratio α. The quarton (red) is a special flux qubit with α=0.5 that has no linear potential. The gray region is energetically unstable (see Supplemental Material [32]). (b) Schematic line scale of the relative nonlinearity of the elements in (a). The quarton (red spider symbol) is at infinity. The respective potentials U(ϕ)'s are plotted below. The tilted quarton (light red spider symbol with apostrophe) is a quarton with small linear inductive potential.

"Qutrit Randomized Benchmarking"

Morvan, V. V. Ramasesh, M. S. Blok, J.M. Kreikebaum, K. O'Brien, L. Chen, B. K. Mitchell, R. K. Naik, D. I. Santiago, I. Siddiqi
Phys. Rev. Lett. 126, 210504 (2021)

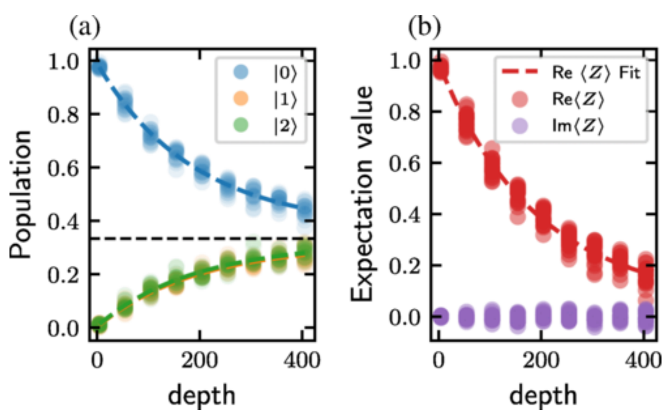

Randomized benchmarking of a single qutrit. For depths up to 400, we generate 20 Clifford-random gate sequences (with a final inversion gate) and measure (a) the resulting Z-basis state occupancies and (b) the observable ⟨Z⟩. Each measurement is repeated 1024 times. Individual points correspond to each of the 20 randomizations, with dashed lines showing fits to a single exponential decay. As qutrit Clifford twirling effectively maps gate errors into a depolarizing channel, for long sequences the populations all tend to 1/3 and the sequence-averaged qutrit state tends to the maximally mixed state ρ=1313. Panel (b) illustrates the utility of measuring the expectation value of the Pauli operator Z and taking its real part. The imaginary part of the expectation value remains at zero throughout, which means that the RB sequence is effectively depolarizing the noise.

KEVIN P. O'BRIEN, *EECS*

"Quantum Metamaterial for Broadband Detection of Single Microwave Photons"

Grimsmo, B. Royer, J. M. Kreikebaum, Y. Ye, K. O'Brien, I. Siddiqi, A. Blais
Phys. Rev. Applied 15, 034074 (2021)

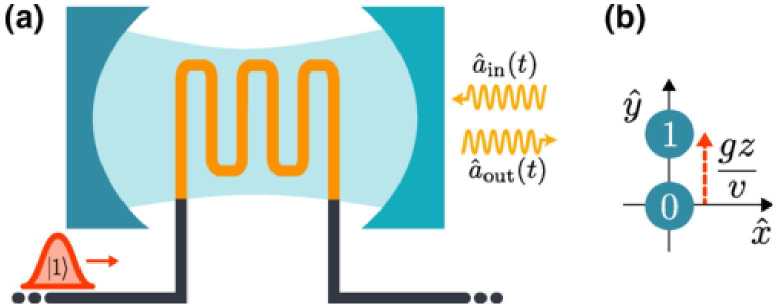

(a) Sketch of the JTWPD. Standard transmission lines (black) are coupled to both ends of a one-dimensional metamaterial (orange) of length z and linear dispersion relation, ω=vk. A cross-Kerr interaction χ between the metamaterial and the giant probe mode (blue) leads to a phase shift in the strong measurement tone (yellow) while the signal photon (red) travels through the metamaterial. (b) Phase-space picture of the probe mode. With respect to the idle coherent state |α⟩, the presence of a signal photon displaces the states by gz/v, with g=χα.

"Quantum Information Scrambling on a Superconducting Qutrit Processor"

M. S. Blok, V. V. Ramasesh, T. Schuster, K. O'Brien, J. M. Kreikebaum, D. Dahlen, A. Morvan, B. Yoshida, N. Y. Yao, and I. Siddiqi
Phys. Rev. X 11, 021010 (2021)

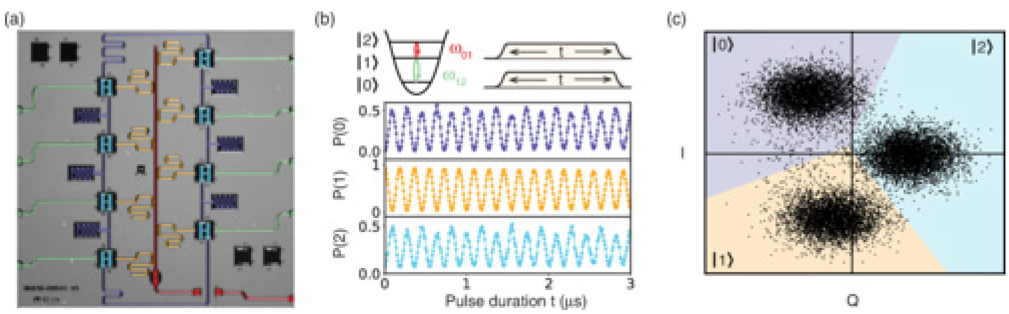

Superconducting qutrit processor. (a) Optical micrograph of the five-transmon processor used in this experiment. Transmon circuits (light blue) couple to an integrated Purcell-filter and readout bus (red) via individual linear resonators (gold), enabling multiplexed state measurement. Exchange coupling between nearest-neighbor transmons is mediated by resonators (purple), while microwave drive lines (green) enable coherent driving of individual qubits. (b) Coherent Rabi dynamics of a single qutrit induced by simultaneous microwave driving at frequencies ω_{01} and ω_{12}. Achievable Rabi frequencies are in the range of tens of megahertz, 3 orders of magnitude faster than decoherence timescales. (c) Example single-shot readout records of an individual qutrit, generally achievable with fidelities above 0.95. This qutrit is largely limited by decay during readout.

"Randomized compiling for scalable quantum computing on a noisy superconducting quantum processor"

A. Hashim, R. K. Naik, A. Morvan, J. Ville, B. Mitchell, J. M. Kreikebaum, M. Davis, E. Smith, C. Iancu, K. P. O'Brien, I. Hincks, J. J. Wallman, J. Emerson, I. Siddiqi
arXiv:2010.00215 (2021)

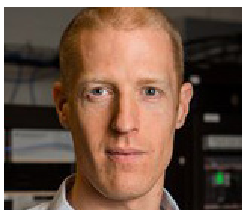

WILLIAM D. OLIVER, *EECS, Physics, Lincoln Laboratory*

with Simon Gustavsson, RLE, Terry Orlando, EECS, Mollie Schwartz, Lincoln Laboratory, Jonilyn Yoder, Lincoln Laboratory

"3D integration and measurement of a semiconductor double quantum dot with a high-impedance TiN resonator"

N. Holman, D. Rosenberg, D. Yost, J. L. Yoder, R. Das, W. D. Oliver, R. McDermott, M. A. Eriksson

npj Quantum Information 7, 137 (2021)

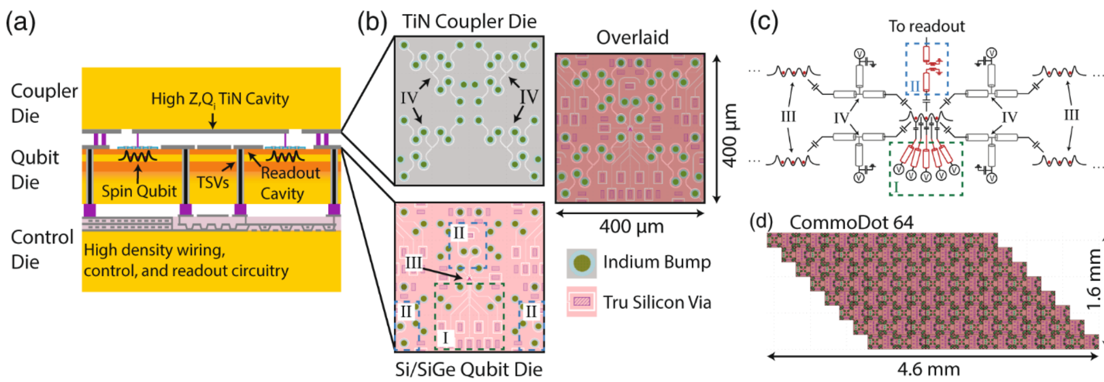

(a) Diagram of a cQED spin qubit processor utilizing a 3-tier stack. (b) Layout of an exchange only qubit cQED processor unit cell with a 0.16 mm2 footprint. Top die consists of four λ/2 high-impedance resonators with λ/4 voltage taps. Base die consists of nine control lines (I), two readout resonators (II, one centered, 1/2 in each lower corner of the unit cell), and two qubits (III, one centered and 1/4 in each corner). Control and readout lines are routed to the backplane of the die using through-silicon vias (TSVs) with a 10 × 20 μm² footprint27. (c) A simplified circuit schematic with the elements in red on the qubit die and the elements in gray on the coupler die. (d) A 64 qubit processor tiled out from the base tile design fitting in a 4.6 × 1.6 mm² area.

"Realization of high-fidelity CZ and ZZ-free iSWAP gates with a tunable coupler"

Y. Sung, L. Ding, J. Braumüller, A. Vepsäläinen, B. Kannan, M. Kjaergaard, A. Greene, G. O. Samach, C. McNally, D. Kim, A. Melville, B. M. Niedzielski, M. E. Schwartz, J. L. Yoder, T. P. Orlando, S. Gustavsson, W. D. Oliver

Phys. Rev. X 11, 021058 (2021) | arXiv:2011.01261 (2020)

See also: Press release from MIT News Office

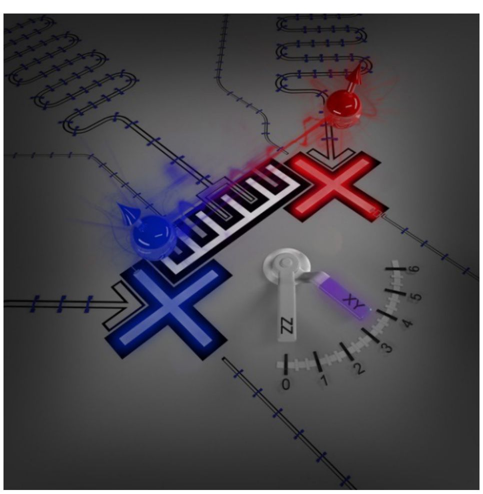

A tunable coupler can switch the qubit-qubit interaction on and off. Unwanted, residual (ZZ) interaction between the two qubits is eliminated by harnessing higher energy levels of the coupler.

Image: Krantz Nanoart

MIT Center for Quantum Engineering

MIT Quantum Science and Engineering Consortium

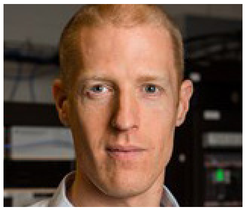

WILLIAM D. OLIVER, *EECS, Physics, Lincoln Laboratory*

with Simon Gustavsson, RLE, Terry Orlando, EECS, Mollie Schwartz, Lincoln Laboratory, Jonilyn Yoder, Lincoln Laboratory

"Hexagonal Boron Nitride (hBN) as a Low-loss Dielectric for Superconducting Quantum Circuits and Qubits"
J. I-J. Wang, M. A. Yamoah, Q. Li, A. Karamlou, T. Dinh, B. Kannan, J. Braumueller, D. Kim, A. J. Melville, S. E. Muschinske, B. M. Niedzielski, K. Serniak, Y. Sung, R. Winik, J. L. Yoder, M. Schwartz, K. Watanabe, T. Taniguchi, T. P. Orlando, S. Gustavsson, P. Jarillo-Herrero, W. D. Oliver
arXiv:2109.00015 (2021)

"Building a Quantum Engineering Undergraduate Program"
A. Asfaw, A. Blais, K. R. Brown, J. Candelaria, C. Cantwell, L. D. Carr, J. Combes, D. M. Debroy, J. M. Donohue, S. E. Economou, E. Edwards, M. F. J. Fox, S. M. Girvin, A. Ho, H. M. Hurst, Z. Jacob, B. R. Johnson, E. Johnston-Halperin, R. Joynt, E. Kapit, J. Klein-Seetharaman, M. Laforest, H. J. Lewandowski, T. W. Lynn, C. R. H. McRae, C. Merzbacher, S. Michalakis, P. Narang, W. D. Oliver, J. Palsberg, D. P. Pappas, M. G. Raymer, D. J. Reilly, M. Saffman, T. A. Searles, J. H. Shapiro, C. Singh
arXiv:2108.01311 (2021)

"Quantum transport and localization in 1d and 2d tight-binding lattices"
A. H. Karamlou, J. Braumüller, Y. Yanay, A. Di Paolo, P. Harrington, B. Kannan, D, Kim, M. Kjaergaard, A. Melville, S. Muschinske, B. Niedzielski, A. Vepsäläinen, R. Winik, J. L. Yoder, M. Schwartz, C. Tahan, T. P. Orlando, S. Gustavsson, W, D. Oliver
arXiv:2107.05035 (2021)

"CircuitQ: An open-source toolbox for superconducting circuits"
P. Aumann, T. Menke, W. D. Oliver, W. Lechner
arXiv:2106.05342 (2021)

"Lindblad Tomography of a Superconducting Quantum Processor"
G. O. Samach, A. Greene, J. Borregaard, M. Christandl, D. K. Kim, C. M. McNally, A. Melville, B. M. Niedzielski, Y. Sung, D. Rosenberg, M. E. Schwartz, J. L. Yoder, T. P. Orlando, J. I-J. Wang, S. Gustavsson, M. Kjaergaard, W. D. Oliver
arXiv:2105.02338 (2021)

"Improving qubit coherence using closed-loop feedback"
A. Vepsäläinen, R. Winik, A. H. Karamlou, J. Braumüller, A. Di Paolo, Y. Sung, B. Kannan, M. Kjaergaard, D. K. Kim, A. J. Melville, B. M. Niedzielski, J. L. Yoder, S. Gustavsson, W. D. Oliver
arXiv:2105.01107 (2021)

RAJEEV RAM, *EECS*

[Low-power swept-source Raman spectroscopy]

AH Atabaki, WF Herrington, C Burgner, V Jayaraman, RJ Ram
[Optics Express 29 (16), 24723-24734] (2021)

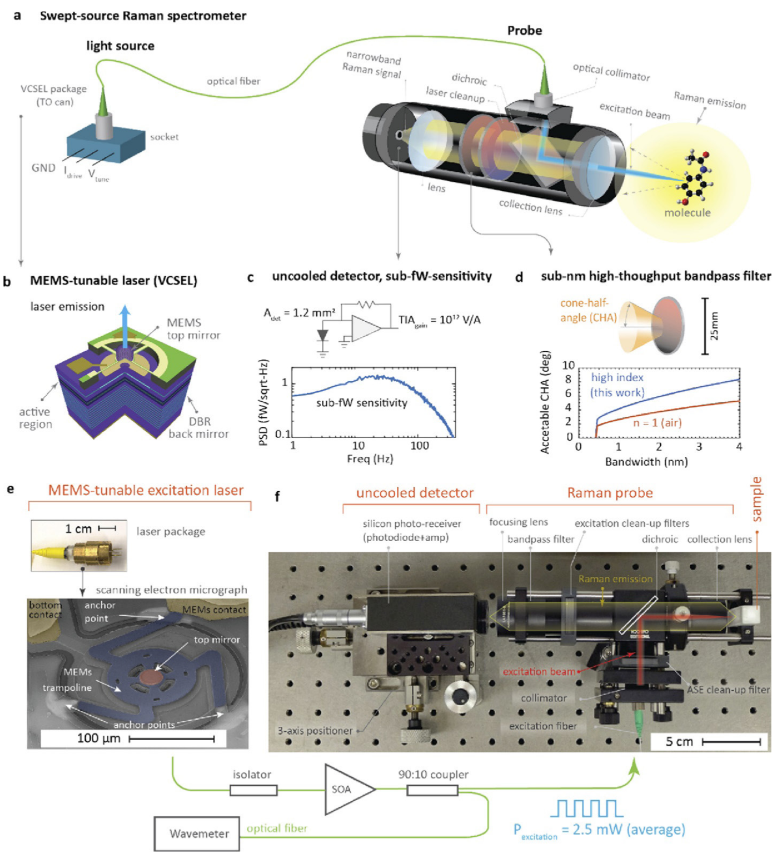

(a) Schematic of the swept-source Raman spectrometer. The excitation source (left) is a chip-scale MEMS-tunable vertical cavity surface emitting laser (VCSEL)–schematic is shown in (b). The probe is used for excitation, collection and detection of the Raman emission. The Raman probe uses a single-element photodiode (c) in conjunction with a high-throughput thin-film interference filter (d) to collect and detect a single spectral channel with high optical throughput. (b) Layout of the MEMS-tunable VCSEL used in this work [13,14]. (c) The unbiased photodiode with a high transimpedance gain of 101212 V/A. Plot shows a sub-fW/ Hz−−√Hz power spectral density for the dark noise of the detector and amplifier. (d) The Interference bandpass filter used for SSRS has high light collection power because of its large area (25-mm-diameter) and a high acceptable cone-half-angle (CHA) of 3∘∘ for a target bandwidth of 0.5 nm. Blue curve shows the simulated acceptable CHA versus bandwidth for the filter used in this work. These interference filters have a higher acceptable CHA compared to Michelson interferometers used in FT and spatial heterdoyne spectrometers [15] (red curve). (e) Photo and scanning electron micrograph of chip-scale MEMS-tunable laser used in our swept source setup. We used two such VCSELS to cover 400 cm−1−1 of spectral range in our experiments. The laser current is chopped with 50% duty-cycle for lock-in detection and the laser output is amplified to 3 mW with a semiconductor optical amplifier before entering the Raman spectroscopy setup in (a). A 90:10 coupler is used to monitor the wavelength of the tunable source with a wavemeter. (f) Experimental setup of the SSRS system. The optical assembly on the right is used for excitation, collection, and bandpass filtering of Raman emission. The silicon detector on the left is placed on a 3-axis positioner for alignment with the excitation spot on the sample (cuvette on the right). All filters and lenses have a diameter/width of 25 mm.

["Low-Voltage, High-Brightness Silicon Micro-LEDs for CMOS Photonics"]

J Xue, J Kim, A Mestre, KM Tan, ..., R. J. Ram
[IEEE Transactions on Electron Devices] (2021)

MIT Center for Quantum Engineering

MIT Quantum Science and Engineering Consortium

RAJEEV RAM, *EECS*

[“Networked Swept-Source Raman Sensors”]
Nili Persits, Jaehwan Kim, Dodd Gray, Zheng Li, Amir Atabaki, Rajeev J Ram
CLEO: Applications and Technology, ATh4Q. 6 (2021)

“Energy harvesting optical modulators with sub-attojoule per bit electrical energy consumption”
M de Cea, AH Atabaki, RJ Ram
Nature communications (2021)

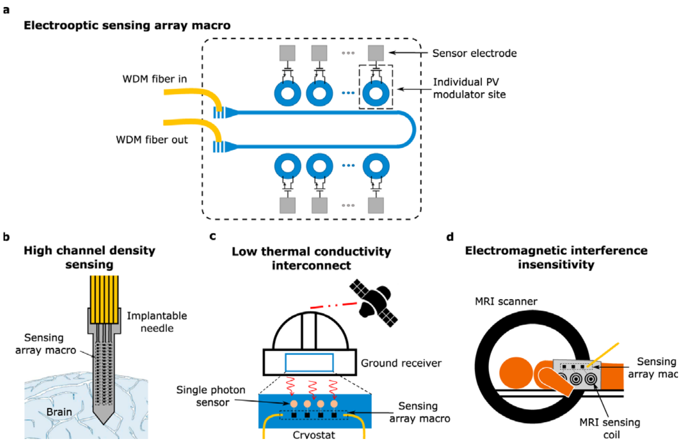

9a) Schematic of a low-power electro-optic transducer based on our photovoltaic (PV) modulator. Individual PV modulators connected to different sensing sites are addressed using different wavelengths through a wavelength division multiplexing (WDM) scheme. The development of such a compact, low-energy electro-optical transducer is essential for sensing applications where the electrical energy at the sensing site is constrained. Examples include massively parallel readout of electro-physiological signals (b), readout of single-photon sensors operating at cryogenic temperatures (c), and readout of electrical signals in environments with high electromagnetic interference, such as in magnetic resonance imaging (MRI) (d).

“High-speed, zero-biased silicon-germanium photodetector”
M de Cea, D Van Orden, J Fini, M Wade, RJ Ram
APL Photonics (2021)

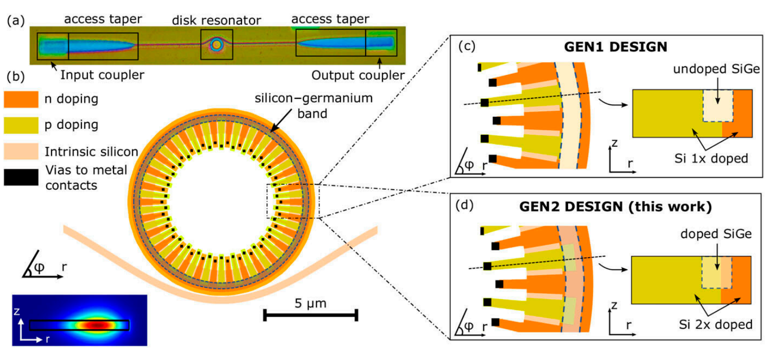

CMOS photodetector configuration and layout. (a) Optical micrograph of the device. (b) Device layout. Azimuthally interleaved p- and n-doped spokes form a ring resonator with 10 μm outer diameter. A 300 nm wide SiGe band generates photocurrent through phonon-assisted below-bandgap absorption. Electrical contact is provided through metal vias located at the inner end of the spokes. The inset shows the intensity distribution of the whispering gallery optical mode supported by the microdisk. (c) and (d) Closeup of the T-junction doping configuration optimized to minimize parasitic capacitance. In Gen1 designs,7 the SiGe band is undoped and Si is doped with 1× doping concentration (c). In this work, implants with 2× larger doping concentration are used, and SiGe is doped with the same implants as Si (d).

JEFFREY H. SHAPIRO, *EECS*

"Entanglement-Assisted Communication Surpassing the Ultimate Classical Capacity"

Shuhong Hao, Haowei Shi, Wei Li, Jeffrey H. Shapiro, Quntao Zhuang, and Zheshen Zhang
Phys.Rev.Lett (2021)

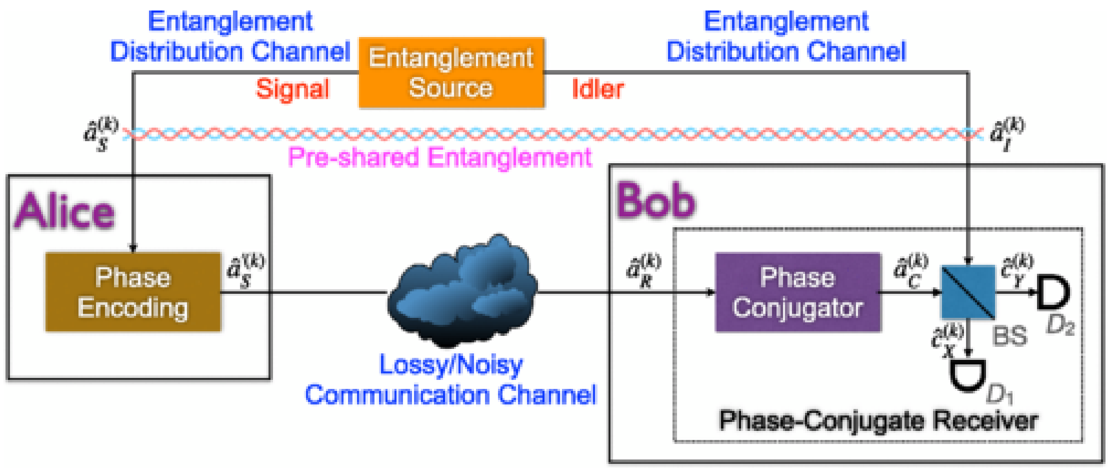

Schematic of the EACOMM protocol. An entanglement source distributes two-mode squeezed vacuum signal-idler pairs {^a(k)S,^a(k)I} to Alice and Bob. Alice phase encodes on ^a(k)S and transmits the encoded modes ^a'(k)S to Bob through a lossy and noisy channel. Bob produces ^a(k)C by phase conjugating the received modes ^a(k)R. ^a(k)C and ^a(k)I interfere on a balanced beam splitter (BS), whose outputs undergo photon counting by photodetectors D1 and D2 to derive the difference photon number, from which Alice's encoded classical bit is inferred. See text for details of the evolution of the mode operators.

"Performance analysis of free-space quantum key distribution using multiple spatial modes"

Wenhua He, Saikat Guha, Jeffrey H. Shapiro, and Boulat A. Bash
Optics Express (2021)

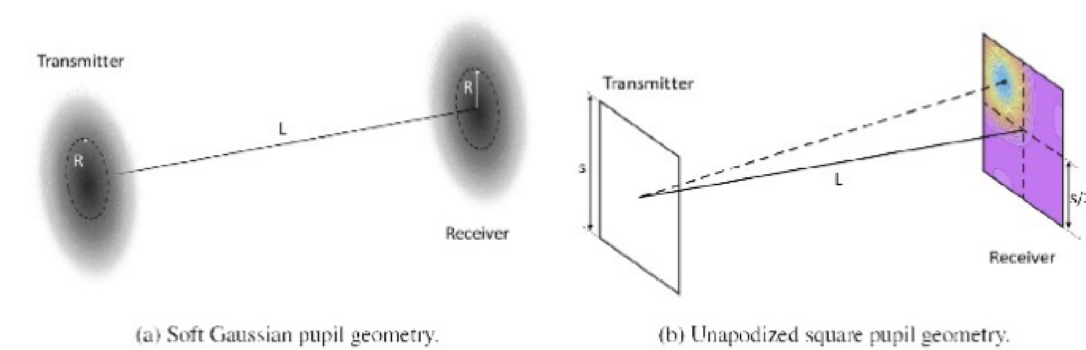

Line-of-sight system geometries. Soft Gaussian pupils in (a) support orthogonal propagation of LG modes in vacuum. An example of unapodized square pupil system in (b) uses four FBs focused on a 2 × 2-pixel receiver. The irradiance pattern from one of the FBs illustrates the cross-talk. To compare LG and FB mode sets fairly, we make their respective Fresnel number products equal.

VIVISHEK SUDHIR, *ME*

"Approaching the motional ground state of a 10 kg object"
C. Whittle, E.D. Hall, S. Dwyer, N. Mavalvala, V. Sudhir,
(LIGO Instrument Science group)
Science (2021) arXiv (2021)

"Unruh effect of detectors with quantized center of mass"
V. Sudhir, N. Stritzelberger, A. Kempf
Physical Review D arXiv Physics World, Nature India, Optics & Photonics News, Science, MIT News, The Conversation, New Scientist, Gizmodo (2021)

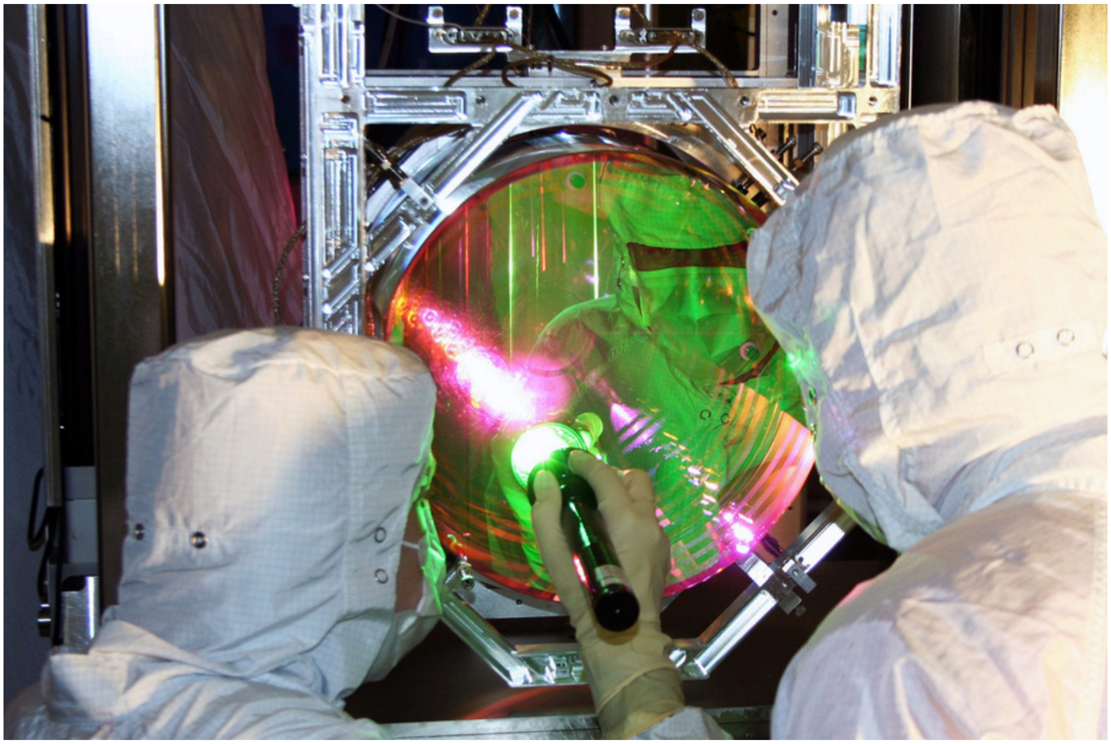

MIT scientists have cooled a 10-kilogram object to a near standstill, using LIGO's precise measurements of its 40-kilogram mirrors. Show here are LIGO optics technicians examining one of LIGO's mirrors.

Image credit: Caltech/MIT/LIGO Lab

TROY VAN VOORHIS, *Chemistry*

"Resolving the Triexciton Recombination Pathway in CdSe/CdS Nanocrystals through State-Specific Correlation Measurements"
Katherine E Shulenberger, Sophie C Coppieters 't Wallant, Megan D Klein, Alexandra R McIsaac, Tamar Goldzak, David B Berkinsky, Hendrik Utzat, Ulugbek Barotov, Troy Van Voorhis, Moungi G Bawendi
Nano Lett. 21, 18, 7457–7464 (2021)

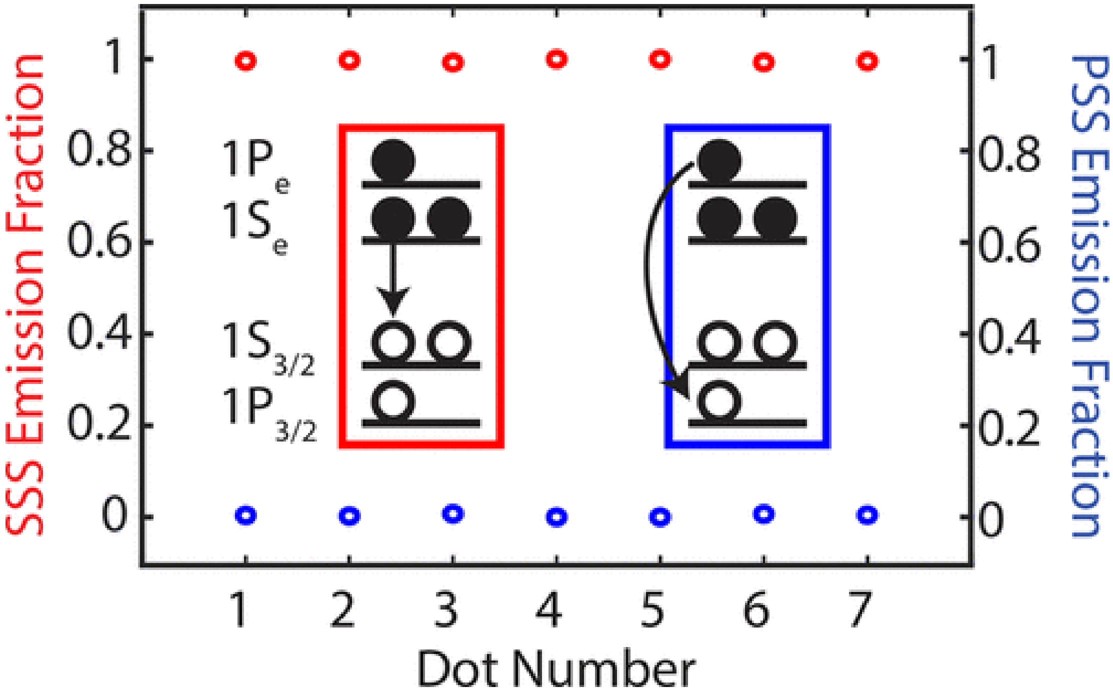

"Machine Learning Dynamic Correlation in Chemical Kinetics"
Changhae Andrew Kim, Nathan D Ricke, Troy Van Voorhis
chemrxiv (2021)

"Maximizing TADF via Conformational Optimization"
Changhae Andrew Kim, Troy Van Voorhis
Chemrxiv (2021)

TROY VAN VOORHIS, *Chemistry*

"Accurate Electronic Excitation Energies in Full-Valence Active Space via Bootstrap Embedding"
Hong-Zhou Ye, Henry K Tran, Troy Van Voorhis
Journal of Chemical Theory and Computation 17 (6), 3335-3347 (2021)

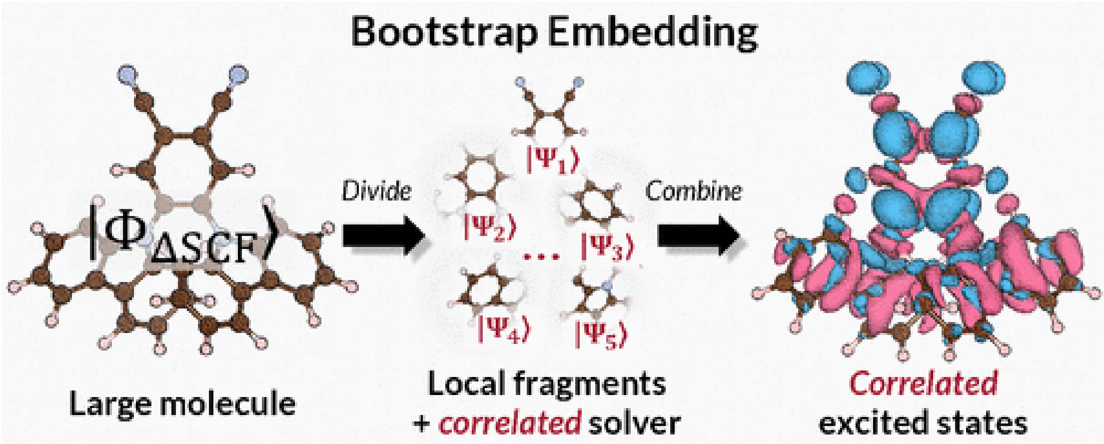

"Colloidal CdSe nanocrystals are inherently defective"
Tamar Goldzak, Alexandra R McIsaac, Troy Van Voorhis
Nat Commun 12, 890 (2021)

Spectrum and IPR for the 2 nm, methylamine-passivated Cd91Se91.

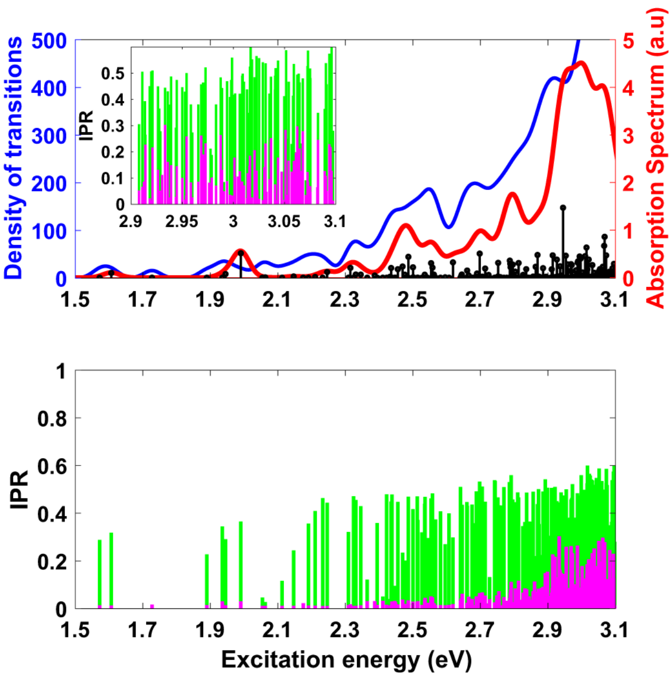

Top: Absorption spectrum in arbitrary units (red) and density of transitions (blue). Black sticks show individual excited states, whose oscillator strengths have been broadened to create the absorption spectrum. Note the high density of states with little or no oscillator strength (i.e. dark states). Bottom: Inverse participation ratio (IPR) for electrons (green) and holes (magenta) for each excitation. A larger IPR corresponds to a more delocalized wavefunction. Clearly the dark, low-energy states are associated with localized states, while the bright states are significantly delocalized. Inset: Enlarged plot of the IPR for the higher-energy part of the excitation spectrum, i.e. $E_{ex} > 2.9$ *eV.*

From the Director
CQE PI Feature
CQE Student Feature
Around the Institute
Beyond the Institute
Quantum Conferences

VLADAN VULETIC, *Physics*

“Quantum Phases of Matter on a 256-Atom Programmable Quantum Simulator”
Ebadi, T.T. Wang, Levine, A. Keesling, G. Semeghini, A. Omran, D. Bluvstein, R. Samajdar, H. Pichler, W.W. Ho, S. Choi, S. Sachdev, M. Greiner, V. Vuletić, and M.D. Lukin
Nature 595, 227-232 (2021)

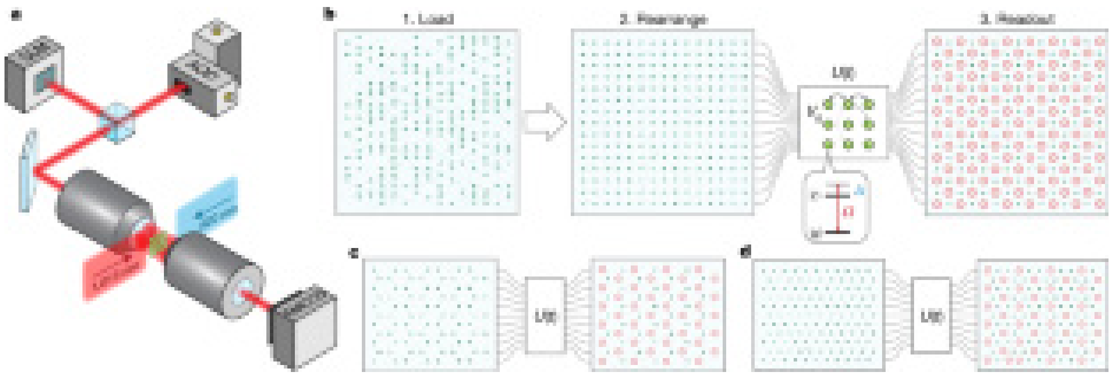

“Collective Spin-Light and Light-Mediated Spin-Spin Interactions in an Optical Cavity”
Zeyang Li, Boris Braverman, Simone Colombo, Chi Shu, Akio Kawasaki, Albert Adiyatullin, Edwin Pedrozo-Peñafiel, Enrique Mendez, Vladan Vuletić
arXiv:2106.03754 (2021)

“Time-Reversal-Based Quantum Metrology with Many-Body Entangled States
Simone Colombo, Edwin Pedrozo-Peñafiel, Albert F. Adiyatullin, Zeyang Li, Enrique Mendez, Chi Shu, Vladan Vuletic
arXiv:2105.11050 (2021)

VLADAN VULETIC, *Physics*

"Fast Preparation and Detection of a Rydberg Qubit using Atomic Ensembles"

Wenchao Xu, Aditya V. Venkatramani, Sergio H. Cantú, Tamara Šumarac, Valentin Klüsener, Mikhail D. Lukin, and Vladan Vuletić

Phys. Rev. Lett. 127, 050501 arxiv.org/abs/2105

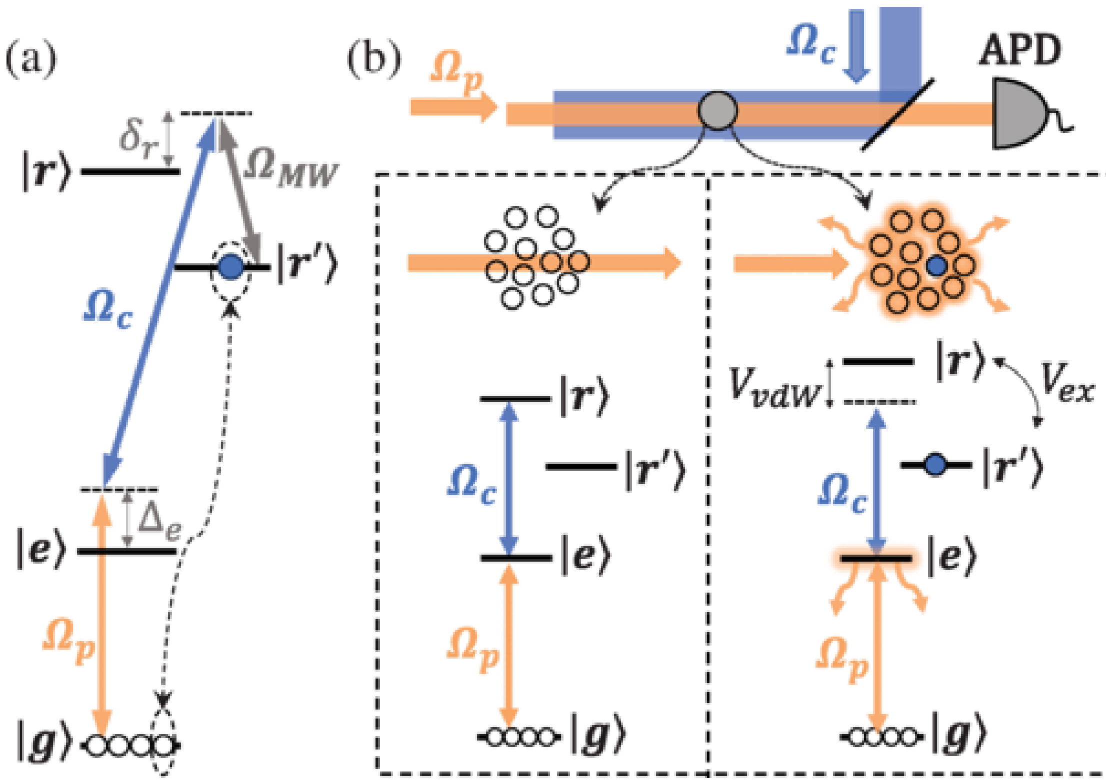

Fast collective detector of a single Rydberg atom. (a) State initialization. An atom is prepared in the Rydberg state $|r'\rangle$ through a three-photon process involving the preparation beam (Ωp, orange), the control beam (Ωc, blue), and a microwave field (ΩMW, grey). The detunings from the two intermediate states are $\Delta e=\delta r=2\pi\times100$ MHz. The preparation of a single atom in $|r'\rangle$ is ensured by the strong interaction between two atoms in $|r'\rangle$ [1]. (b) A probe field (orange, waist size $wp=4.5$ μm) in combination with the control field ($wc=12.5$ μm) couples atoms to the Rydberg state $|r\rangle$. Under conditions of EIT ($\Delta e=\delta r=0$), high transmission through the atomic medium results in a large number of detected photons (left). On the other hand, if the Rydberg state $|r'\rangle$ is populated by an atom (right), then the strong interaction between $|r\rangle$ and $|r'\rangle$ removes the EIT condition, resulting in a significant reduction of transmitted photon number due to absorption by the ensemble. The interaction Vrr' contains both dipolar-exchange (V_{ex}) and van der Waals components ($VvdW$) (see SM).

"Nanophotonic quantum interface and transportable entanglement for atom arrays"

Tamara Đorđević, Polnop Samutpraphoot, Paloma L. Ocola, Hannes Bernien, Brandon Grinkemeyer, Ivana Dimitrova, Vladan Vuletić, Mikhail D. Lukin

arXiv:2105.06485 (2021)

LINDLEY WINSLOW, *Physics*

Search for Low-Mass Axion Dark Matter with ABRACADABRA-10 cm

Chiara P. Salemi, Joshua W. Foster, Jonathan L. Ouellet, Andrew Gavin, Kaliroë M. W. Pappas, Sabrina Cheng, Kate A. Richardson, Reyco Henning, Yonatan Kahn, Rachel Nguyen, Nicholas L. Rodd, Benjamin R. Safdi, and Lindley Winslow

Phys. Rev. Lett. 127, 081801 (2021)

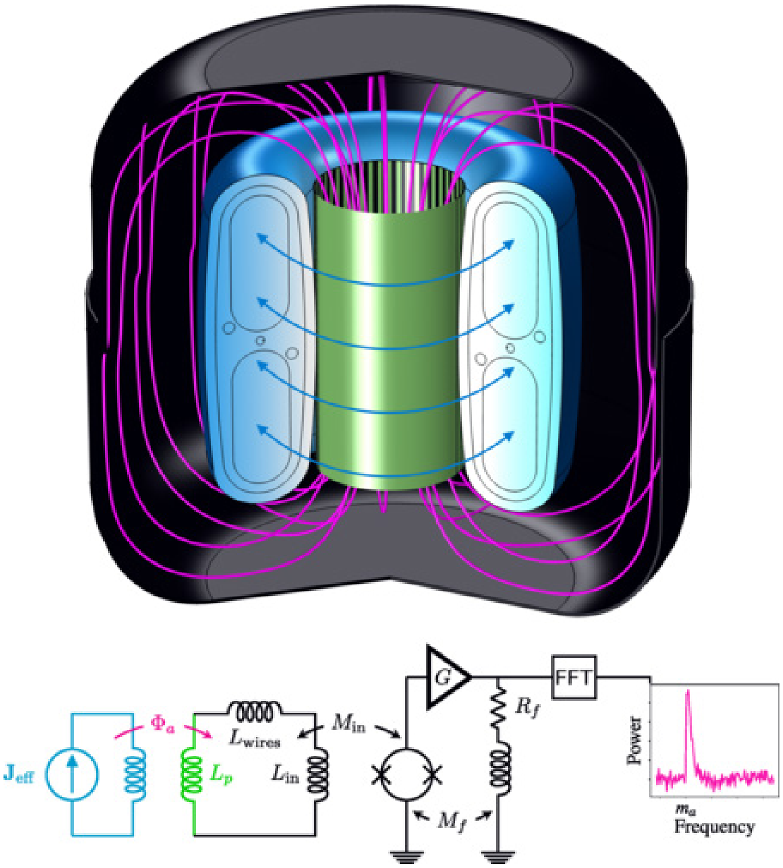

Top: schematic of ABRACADABRA-10 cm showing the effective axion-induced current (blue), sourced by the toroidal magnetic field, generating a magnetic flux (magenta) through the pickup cylinder (green) in the toroid bore. Bottom: simplified schematic of the ABRACADAB-RA-10 cm readout (full circuit diagram in Supplemental Fig. S1 [30]). The pickup cylinder Lp is inductively coupled to the axion effective current Jeff. The power spectrum of the induced current is read out through a dc SQUID inductively coupled to the circuit through Lin. An axion signal would appear as excess power above the noise floor at a frequency corresponding to the axion mass.

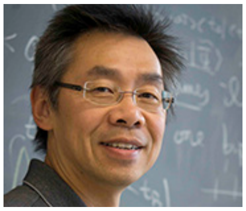

FRANCO N. C. WONG, *RLE*

"Experimental Demonstration of Conjugate-Franson Interferometry"

Changchen Chen, Jeffrey H. Shapiro, and Franco N. C. Wong
Phys. Rev. Lett. 127, 093603 (2021) arXiv:2104.15084 (2021)

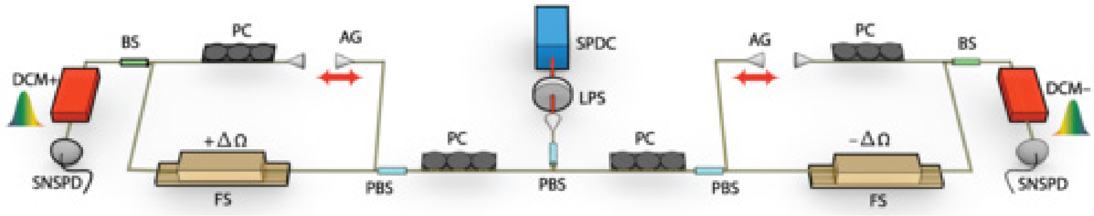

Experimental setup of our conjugate-Franson interferometer. Time-energy entangled signal-idler photon pairs generated by cw pumped SPDC were coupled into an optical fiber and routed to their respective MZIs. The signal's frequency shifter was configured to blue shift its input, whereas the idler's shifter was configured to red shift its input. The polarization and the path lengths between the two arms of each MZI were made to be the same. The fiber-based CFI was placed inside a custom-built two-stage thermal box for phase stabilization. The MZI outputs were detected with SNSPDs, and their arrival times were recorded for coincidence measurements. LPS: long-pass filter; PBS: polarizing beam splitter; PC: polarization controller; FS: frequency shifter for $\Delta\Omega$ $(-\Delta\Omega)$ *frequency shift; AG: tunable air gap; BS:* $50/50$ *beam splitter; and =: dispersion module with normal (anomalous) dispersion.*

BILGE YILDIZ, *NSE MSE*

"Antisite defects stabilized by antiphase boundaries in YFeO3 thin films"
Abinash Kumar, Konstantin Klyukin, Shuai Ning, Cigdem Ozsoy-Keskinbora, Mikhail Ovsyanko, Felix van Uden, Ruud Krijnen, Bilge Yildiz, Caroline A. Ross, James M. LeBeau
arXiv:2107.09152v1 (2021)

"Voltage control of ferrimagnetic order and voltage-assisted writing of ferrimagnetic spin textures"
Mantao Huang, Muhammad Usama Hasan, Konstantin Klyukin, Delin Zhang, Deyuan Lyu, Pierluigi Gargiani, Manuel Valvidares, Sara Sheffels, Alexandra Churikova, Felix Büttner, Jonas Zehner, Lucas Caretta, Ki-Young Lee, Joonyeon Chang, Jian-Ping Wang, Karin Leistner, Bilge Yildiz and Geoffrey S. D. Beach
Nat. Nanotechnol. 16, 981–988 (2021) Also appearing in MIT News (2021)

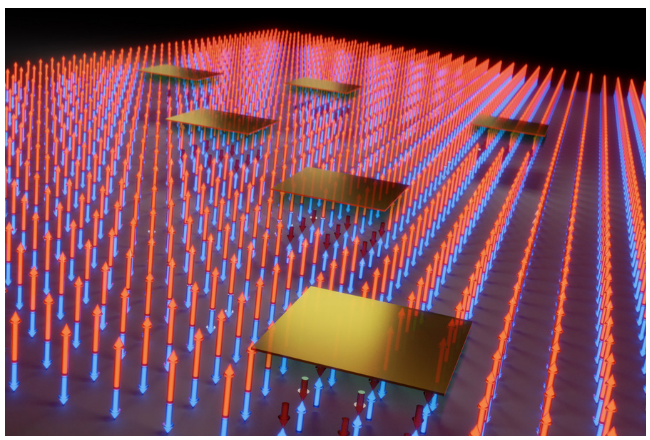

Arrows indicate the magnetizations of the arrays of gadolinium (red) and cobalt (blue) atoms in a lattice. Applying a voltage to electrodes at the top (yellow patches) loads hydrogen into the magnetic materials, which changes the relative magnitude of the magnetizations under it, flipping the direction of the overall magnetic field in that area.

Probing point and planar defects in multiferroic YFeO3 thin films
Abinash Kumar, Shuai Ning, Konstantin Klyukin, Bilge Yildiz, Caroline Ross and James LeBeau
Microscopy and Microanalysis, 27(S1), 2144-2145 (2021)

"Electronegative metal dopants improve switching consistency in Al2O3 resistive switching devices"
Zheng Jie Tan, Vrindaa Somjit, Cigdem Toparli, Bilge Yildiz, Nicholas Fang
arXiv:2104.13301 (2021)

BILGE YILDIZ, *NSE MSE*

“CMOS-compatible protonic programmable resistor based on phosphosilicate glass electrolyte for analog deep learning”
Murat Onen, Nicolas Emond, Ju Li, Bilge Yildiz, and Jesús A. del Alamo
Nano Letters, 21, 14, 6111–6116 (2021)

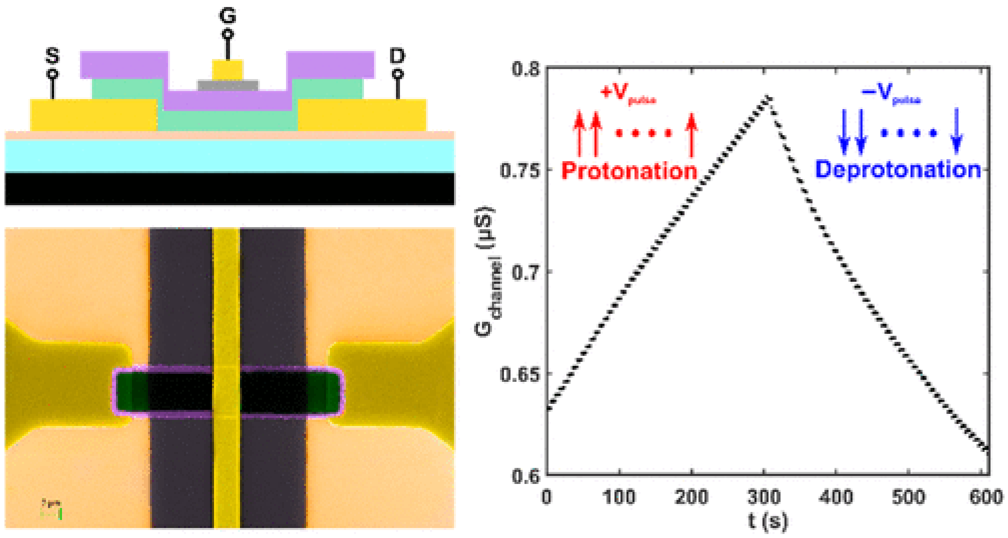

“An antisite defect mechanism for room temperature ferroelectricity in orthoferrites”
Shuai Ning, Abinash Kumar, Konstantin Klyukin, Eunsoo Cho, Jong Heon Kim, Tingyu Su, Hyun-Suk Kim, James LeBeau, Bilge Yildiz, and Caroline Ross
Nature Communications, 12, 4298 (2021)

Crystallographic origin of ferroelectricity in Y-rich YFO.

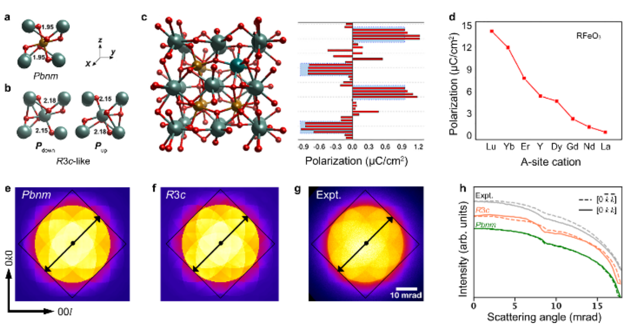

(a), (b) Schematics of centrosymmetric Pbnm (a) and non-centrosymmetric R3c-like (b) structures. (c) Crystal structure and layer-resolved polarization for Y-rich YFO. Red columns indicate the atomic contribution to the ferroelectric polarization in Y-rich YFO calculated using the Born charge approximation, while blue columns show layer-resolved contributions to the ferroelectric polarization in stoichiometric YFO. d Ferroelectric polarization for various orthoferrites $RFeO_3$ that are assumed to be epitaxially grown on $SrTiO_3$ for all calculations with R/Fe = 1.28. (e–g) PACBED patterns including the simulated patterns, using the DFT relaxed centrosymmetric Pbnm (e) and non-centrosymmetric R3c (f) and the experimental result measured from the Y-rich YFO (α = 1.19) thin film sample (g). h Intensity profiles integrated across the pattern diagonals from PACBED patterns along the black arrows shown in (e–g).

BILGE YILDIZ, *NSE MSE*

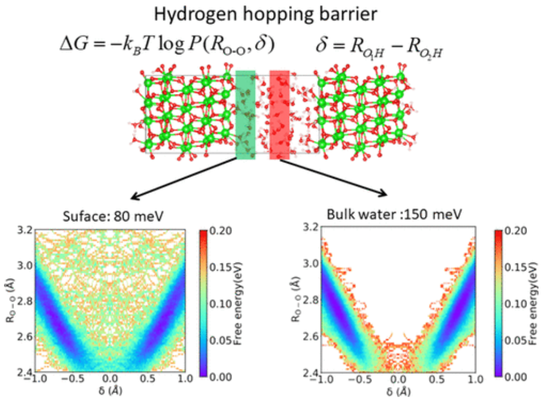

"Structure, kinetics, and thermo-dynamics of water and its ions at the interface with monoclinic ZrO2 resolved via ab initio molecular dynamics"
Jing Yang, Mostafa Youssef, and Bilge Yildiz
The Journal of Physical Chemistry C (2021)

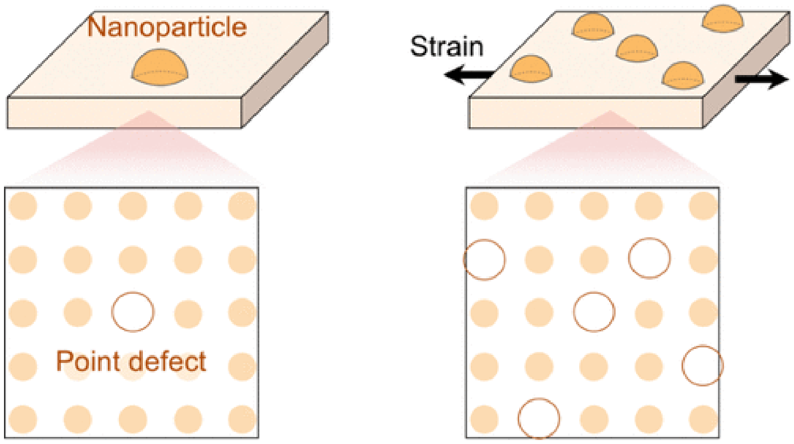

"Tuning Point Defects by Elastic Strain Modulates Nanoparticle Exsolution on Perovskite Oxides"
Jiayue Wang, Jing Yang, Alexander K. Opitz, William Bowman, Roland Bliem, Georgios Dimitrakopoulos, Andreas Nenning, Iradwikanari Waluyo, Adrian Hunt, Jean-Jacques Gallet, and Bilge Yildiz
Chemistry of Materials, 33, 13, 5021–5034 (2021)

"Highly Durable C2 Hydrocarbon Production via the Oxidative Coupling of Methane Using a BaFe0.9Zr0.1O3−δ Mixed Ionic and Electronic Conducting Membrane and La2O3 Catalyst"
Georgios Dimitrakopoulos, Bonjae Koo, Bilge Yildiz, and Ahmed F. Ghoniem
ACS Catalysis, 11, 3638–3661 (2021)

"Hf Deposition Stabilizes the Surface Chemistry of Perovskite Manganite Oxide"
Roland Bliem, Dongha Kim, Jiayue Wang, Ethan J. Crumlin, and Bilge Yildiz
The Journal of Physical Chemistry C, 125, 6, 3346–3354 (2021)

"Precipitation of dopants on acceptor-doped LaMnO3 revealed by defect chemistry from first principles"
Franziska Hess and Bilge Yildiz
The Journal of Chemical Physics, 154, 064702 (2021)

MARTIN ZWIERLEIN, *Physics*

[“Crystallization of Bosonic Quantum Hall States”]

Biswaroop Mukherjee, Airlia Shaffer, Parth B. Patel, Zhenjie Yan, Cedric C. Wilson, Valentin Crépel, Richard J. Fletcher, Martin Zwierlein
arXiv:2106.11300 (2021)

“Resonant and first-order dipolar interactions between ultracold molecules in static and microwave electric fields”

Tijs Karman, Zoe Z. Yan, Martin Zwierlein
arXiv:2106.01610 (2021)

“Pattern Formation in Quantum Ferrofluids: from Supersolids to Superglasses”

J. Hertkorn, J.-N. Schmidt, M. Guo, F. Böttcher, K. S. H. Ng, S. D. Graham, P. Uerlings, T. Langen, M. Zwierlein, and T. Pfau
Phys. Rev. Research 3, 033125 (2021) arXiv (2021)

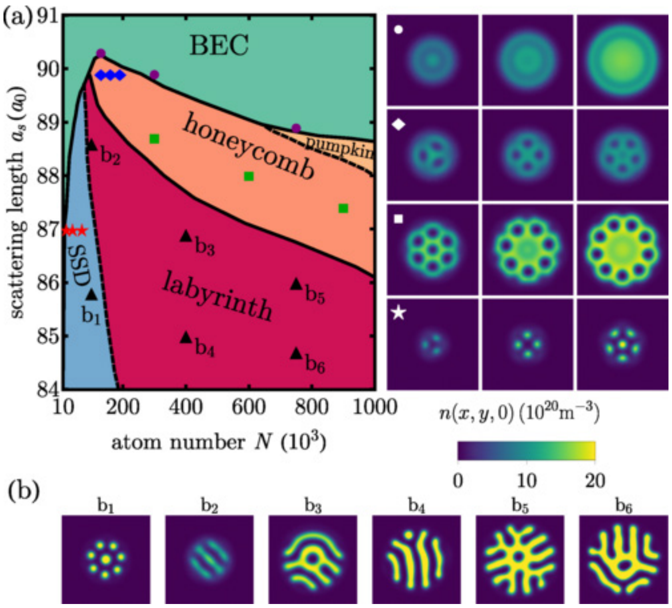

Phase diagram and morphologies beyond the supersolid droplet regime. (a) The left-hand side shows the $N-a_s$ *phase diagram for trap frequencies* $\omega/2\pi=(125,125,250)$ Hz. *The right-hand side shows 2D density cuts* $n(x,y,0)$ *at relevant points in the phase diagram, shown by the corresponding markers. The density distributions for a specific marker are ordered in atom number from left to right. The BEC at high atom numbers has a ring of depleted density near its boundary (circles) and forms honeycomb structures toward smaller scattering lengths (diamonds). The honeycomb structures persist to higher atom numbers (squares) and move outwards to the rim of the density distributions, while the core of the BEC spatially saturates in density. An example of the pumpkin state can be seen in Fig. 2. Dashed lines indicate crossovers between different regions. (b) The transition between droplets and honeycombs occurs via stripes* (b_2) *that break up into droplets at small scattering lengths* (b_1). *At high atom numbers and low scattering lengths* (b_3–b_6), *labyrinth structures form that are almost degenerate with many other morphologically different labyrinth structures. The supersolid droplets form density connections toward higher atom numbers and transition to labyrinthine structures. The field of view for the 2D densities in (a) and (b) is* $14\times14\,\mu\mathrm{m}^2$.

MARTIN ZWIERLEIN, *Physics*

“Supersolidity in Two-Dimensional Trapped Dipolar Droplet Arrays”

J. Hertkorn, J. -N. Schmidt, M. Guo, F. Böttcher, K. S. H. Ng, S. D. Graham, P. Uerlings, H. P. Büchler, T. Langen, M. Zwierlein, T. Pfau
arXiv:2103.09752 (2021)

“Roton Excitations in an Oblate Dipolar Quantum Gas”

J.-N. Schmidt, J. Hertkorn, M. Guo, F. Böttcher, M. Schmidt, K. S. H. Ng, S. D. Graham, T. Langen, M. Zwierlein, and T. Pfau
Phys. Rev. Lett. 126, 193002 (2021) arXiv:2102.01461 (2021)

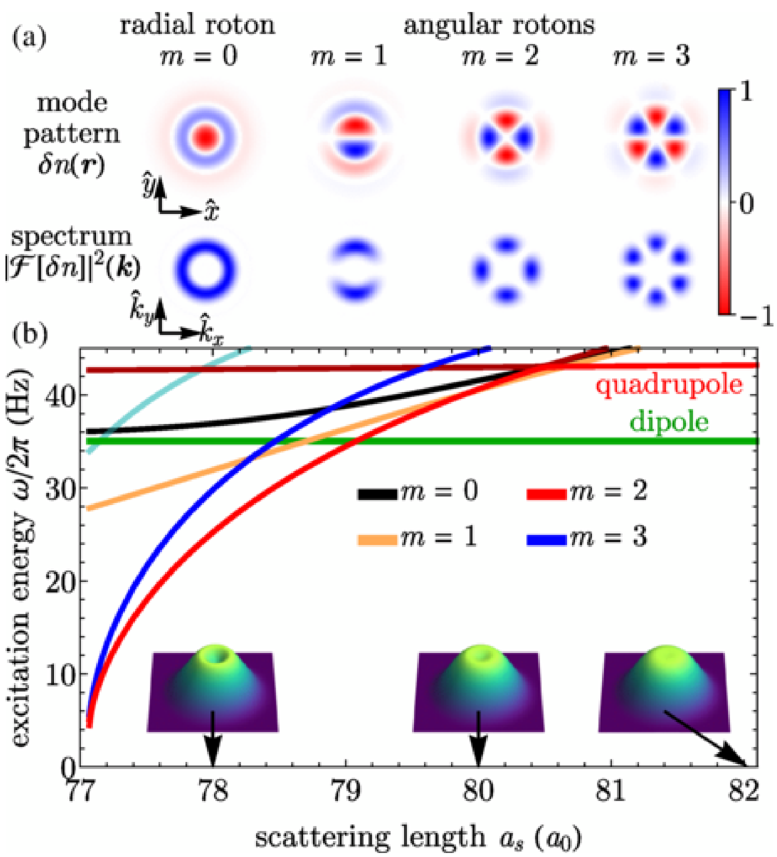

(a) Normalized mode patterns of the density fluctuations close to the transition at $as\simeq77.5a0$ *and their spatial power spectra in the* $x-y$ *plane. Shown are the lowest radial* $(m=0)$ *and angular rotons* $(m=1,2,3)$ *having* m *angular nodal lines. (b) Corresponding Bogoliubov excitation energies as a function of the scattering length as, with the insets indicating the emergence of a blood cell shape in the ground-state density close to the instability at* $as\simeq77.1a0$*. For decreasing scattering lengths, first the* $m=2$ *followed by the* $m=1$ *and* $m=3$ *angular roton modes drops below the radial dipole modes at the trap frequency and softens further toward the instability. For information on higher modes (e.g., cyan line) and details, see Refs. [27, 50].*

MARTIN ZWIERLEIN, *Physics*

[“Density Fluctuations across the Superfluid-Supersolid Phase Transition in a Dipolar Quantum Gas”]

J. Hertkorn, J.-N. Schmidt, F. Böttcher, M. Guo, M. Schmidt, K. S. H. Ng, S. D. Graham, H. P. Büchler, T. Langen, M. Zwierlein, and T. Pfau
10.1103/PhysRevX.11.011037 (2021) arXiv:2009.08910 (2020)

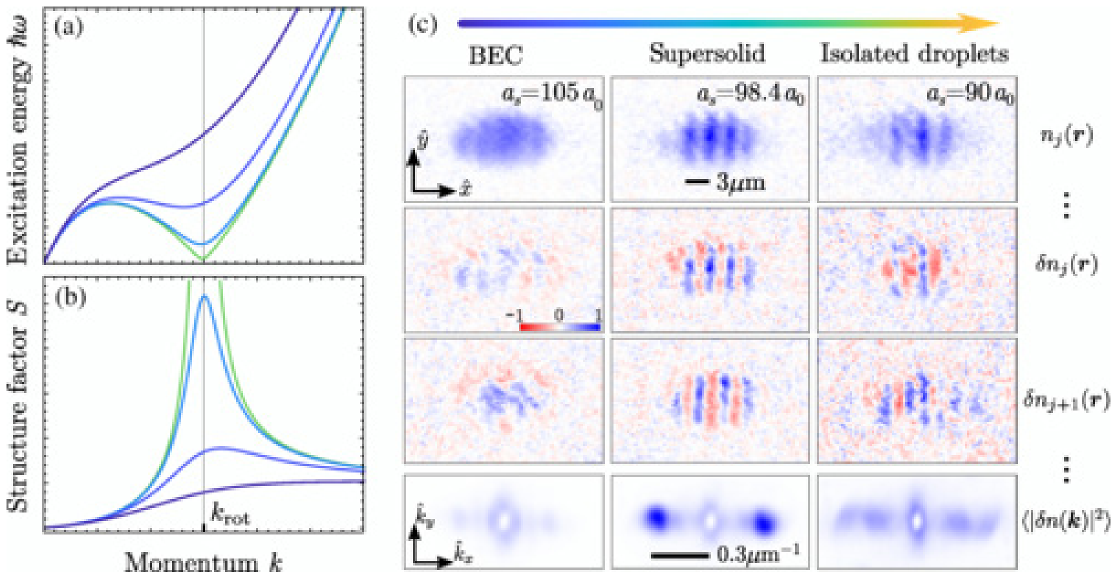

(a),(b) Schematic of the dispersion relation $\hbar\omega(k)$ and associated static structure factor $S(k)$ of an elongated and strongly dipolar BEC [22]. A decrease in scattering length a_s causes a roton minimum to emerge in the excitation spectrum, associated with a characteristic peak in the static structure factor. The roton momentum k_{rot} is indicated where the roton minimum drops near zero. (c) For a given scattering length a_s, we observe a large number of in situ densities $n_j(r)$ and calculate their mean $\langle n(r)\rangle$ and the density fluctuations $\delta n_j(r)=n_j(r)-\langle n(r)\rangle$ as the deviation of the in situ images from their mean. Investigating the mean power spectrum of the fluctuations $\langle|\delta n(k)|^2\rangle$ for different scattering lengths across the transition allows us to directly observe the static structure factor as the system passes from BEC to supersolid to isolated droplet states. The colored arrow on top indicates the direction toward lower scattering lengths, passing from BEC to supersolid to isolated droplet regimes. The color map used for the images shows the normalized amplitude of densities, density fluctuations, and mean power spectra, respectively, with the color bar referring to each row separately.

“Geometric squeezing into the lowest Landau level”

Richard J. Fletcher, Airlia Shaffer, Cedric C. Wilson, Parth B. Patel, Zhenjie Yan, Valentin Crépel, Biswaroop Mukherjee, Martin W. Zwierlein
Science, aba7202 (2021) arXiv:1911.12347 (2021)

Publications

[“Observation of Time-Crystalline Eigenstate Order on a Quantum Processor”]
Xiao Mi, et. al., including MIT-CQE member Edward H. Farhi
arXiv:2107.13571 (2021)

[“Accurately computing the electronic properties of a quantum ring”]
C Neill, et. al., including MIT-CQE member Edward H. Farhi
Nature volume 594 (2021)

[“Coherent manipulation of an Andreev spin qubit”]
M. Hays, et. al., including MIT-CQE member Kyle Serniak
10.1126/science.abf0345 (2021)

[“Observation of Time-Crystalline Eigenstate Order on a Quantum Processor”]
Xiao Mi, et. al., including MIT-CQE member Edward H. Farhi
arXiv:2107.13571 (2021)

[“Accurately computing the electronic properties of a quantum ring”]
C Neill, et. al., including MIT-CQE member Edward H. Farhi
Nature volume 594 (2021)

[“Coherent manipulation of an Andreev spin qubit”]
M. Hays, et. al., including MIT-CQE member Kyle Serniak
10.1126/science.abf0345 (2021)

Novel implementation of metrology technique amplifies it to new heights
Kwiat explains, “We realized that the discarded photons were in nearly the same quantum state that they started in. Therefore, these photons could be reused—or recycled—in multiple WVA realizations, until eventually all of them—in the absence of loss—were indeed successfully post-selected and detected.” [PhysRevLett.]

Q-CTRL, University of Sydney Devise Machine Learning Technique Used to Pinpoint Quantum Errors
In combination with Q-CTRL’s existing quantum control techniques, the researchers were also able to minimize the impact of background interference in the process. This allowed easy discrimination between “real” noise sources that could be fixed and phantom artifacts of the measurements themselves. [PhysRevLett.]

Highly programmable quantum simulator operates with up to 256 qubits
Although large numbers of atoms have already been trapped and rearranged in both two- and three-dimensional arrays, the coherent manipulation of programmable, strongly interacting systems containing over 100 qubits has remained far more challenging. [Nature]

Yale Researchers Combining 2 Approaches to Advance Quantum Computing
Two promising physical implementations for the storage and manipulation of quantum information are the electromagnetic

modes of superconducting circuits and the spins of small numbers of electrons trapped in semiconductor quantum dots. [Science]

IDB, Cambridge Quantum and Tec de Monterrey Develop Blockchain Resistant to Quantum Computing
A post-quantum cryptography layer that protects networks and offers resistance to quantum computer attacks was developed on the LACChain Besu blockchain network, based on Ethereum technology. Transactions and communications were protected with quantum-proof keys from CQ's IronBridge platform, which uses quantum computers to generate certified entropy. [arxiv]

Time Crystals in Open Systems
Hans Keßler from the University of Hamburg, Germany, and his colleagues have now reported the first observation of time-crystalline behaviors in an open quantum system. [APS Physics]

Quantum 'fingerprints' made smaller and delivered faster
"In classical protocol, the smallest 'fingerprint' required to determine whether the information is the same—to a certainty near 100%—is found by the square root of the total number of bits. So, a 1MB file would require the transmission of roughly 300 bytes. With quantum fingerprinting, the amount scales logarithmically: a 1MB file would only require around 3 bytes." [utoronto.ca] [Nature]

Magnetic Skyrmions Could Act as Qubits
Static electric and magnetic fields control the quantized energy spectra of the skyrmions, allowing the user to change the helicity between two energetically favored levels, which act as a qubit's 0 and 1 states. [APS Physics]

Superfluid Interface Mixes Classical and Quantum Behavior
In their simulations, the BECs flowed at the same speed in opposite directions. The team observed various behaviors, depending on the fluids' relative speed and on the strength of the repulsion between atoms of the two fluids. [APS Physics]

Quantum proton entanglement on a nanocrystalline silicon surface
Compared to the proton entanglement previously observed in hydrogen molecules, this entanglement is characterized by an enormous energy difference of 113 meV between the spin singlet ground state and the spin triplet excited state. [PRB]

Single-electron spin resonance in a nanoelectronic device using a global field
Here, we demonstrate a potential solution to [deliver microwave signals for large-scale qubit control] by using a three-dimensional dielectric resonator to broadcast a global microwave signal across a quantum nanoelectronic circuit. Critically, this technique uses only a single microwave source and is capable of delivering control signals to millions of qubits simultaneously. [Science]

Resonant quantum principal component analysis

Here, we develop a resonant analysis algorithm with minimal resource for ancillary qubits, in which only one frequency-scanning probe qubit is required to extract the principal components. [science]

Many-body thermodynamics on quantum computers via partition function zeros

Here, we show how to find partition function zeros on noisy intermediate-scale trapped-ion quantum computers in a scalable manner, using the XXZ spin chain model as a prototype, and observe their transition from XY-like behavior to Ising-like behavior as a function of the anisotropy. [science]

Accessing high spins in an artificial atom

By making use of the spin filtering caused by the quantum Hall effect, the researchers were able to improve upon previous methods that could only easily resolve two electrons. This work may lead to quantum computers based on the multielectron high-spin states. [phys]

Glass Chip Is Key to New Quantum Architecture

"The purpose of an ion trap is to move ions around with precision, hold them in the environment, and get out of the way of the quantum operation," explains Jason Amini, who led the evaporated glass trap team at IonQ. The 3D glass and metal structure Amini's team constructed does all three better than its previous chips could. [ieee]

Multidimensional four-wave mixing signals detected by quantum squeezed light

Here, based on a four-wave mixing process, we report an experimental study of the 2D quantum noise spectra of two-beam intensity difference squeezing. External noise erodes the resolution of classical measurements, while quantum signals remain intact. [PNAS]

A squeezed quantum microcomb on a chip

Here, we demonstrate a deterministic quantum microcomb in a silica microresonator on a silicon chip. 40 continuous-variable quantum modes, in the form of 20 simultaneously two-mode squeezed comb pairs, are observed within 1 THz optical span at telecommunication wavelengths. [Nature]

Google demonstrates vital step towards large-scale quantum computers

Google has shown that its Sycamore quantum computer can detect and fix computational errors, an essential step for large-scale quantum computing, but its current system generates more errors than it solves. [Nature]

Realization of real-time fault-tolerant quantum error correction

We use a ten qubit QCCD trapped-ion quantum computer to encode a single logical qubit using the [[7,1,3]] color code. The logical qubit is initialized into the eigenstates of three mutually unbiased bases using an encoding circuit, and we measure an average logical SPAM error of 1.7(6)×10−3, compared to the average physical SPAM error 2.4(8)×10−3 of our qubits. [arxiv]

D-Wave Quantum-Annealing Computer Enables 'Materials by Design' Research at LANL
"These results also have technological consequences particularly relevant to DOE and Los Alamos, specifically in the idea of materials-by-design, to produce future nanomagnets that might show advanced and desirable functionality for sensing and computation." [arxiv]

Phasecraft makes quantum computing breakthrough
Phasecraft's compact representation of fermions outperforms all previous representations improving memory use and algorithm size by at least 25 per cent. [PRB, QIP2021]

Classical approach extends the range of noisy quantum computers
The new algorithms divide up quantum computational resources according to which parts of the simulation require them most, making it possible to extract i nformation about a large quantum system from many smaller, more manageable calculations—in effect, running the simulation in parallel. [npj QI]

Deterministic multi-mode gates on a scalable photonic quantum computing platform
Here we propose and demonstrate the deterministic implementation of a multi-mode set of measurement-induced quantum gates in a large two-dimensional optical cluster state using phase-controlled continuous-variable quadrature measurements. [arxiv]

Aalto Researchers Unlock Radiation-Free Quantum Technology with Graphene
The exciting result in the new paper shows how a quantum state known as a "heavy fermion" can be produced by combining three twisted graphene layers. A heavy fermion is a particle —in this case an electron —that behaves like it has a lot more mass than it actually does. [PRL, arxiv]

Scientists observe a new type of topological defect in chiral magnets
Scientists used Lorentz transmission electron microscopy (LTEM) to visualize topological defects. They were able to do so by passing electrons and observing their deflections through a thin magnetic film. [Nat Comms]

Quantum simulation: Measurement of entanglement made easier
The new method for determining the quantum state in quantum simulators reduces the number of necessary measurements and makes work with quantum simulators much more efficient. [Nat Phys]

Achieving Precision in Quantum Material Simulations
the first work, we consider one-dimensional systems, like thin wires, and demonstrate how to accurately compute electronic properties, such as current and conductance. In the second work, we show how to map the Fermi-Hubbard model, which

MIT Center for Quantum Engineering   MIT   MIT Quantum Science and Engineering Consortium describes interacting electrons, to a quantum processor in order to simulate important physical properties. [Nature]

Upgrading a Hybrid Computing Algorithm
The measurements from the repeated cycles effectively give a series of snapshots of the state's energy for different input parameters. These snapshots are then used by the classical computer to map out the landscape of the energy and pinpoint the minimum. [PRL, arxiv]

Heralded entanglement distribution between two absorptive quantum memories
We build two nodes separated by 3.5 metres, each containing a polarization-entangled photon-pair source and a solid-state quantum memory with bandwidth up to 1 gigahertz. A joint Bell-state measurement in the middle station heralds the successful distribution of maximally entangled states between the two quantum memories with a fidelity of 80.4 ± 2.2 per cent. [arxiv]

Quantum walks on a programmable two-dimensional 62-qubit superconducting processor
Gong et al. used an 8-by-8 two-dimensional (2D) superconducting qubit square lattice containing 62 functional qubits to show how multiple (two) walkers traverse a 2D qubit array, interfering as they go. [arxiv]

Researchers take quantum encryption out of the lab
Researchers demonstrate an automated, easy-to-operate quantum key distribution (QKD) system using the fiber network in the city of Padua, Italy. Their simple system is stable over time and can generate quantum-secure cryptographic keys at sustained rates over a standard telecommunications infrastructure. [Phys.org]

Physicists link ‹quantum memories› in early step toward quantum internet
Two teams have now demonstrated an ensemble of technologies essential to building the backbone of such a network — devices known as quantum repeaters. The USTC and ICFO researchers have advanced a new type of "solid state" quantum hard drive: glass crystals filled, or "doped," with ions of a rare-earth metal. [livescience]

New research proves that quantum computational errors are correlated and connects them to cosmic rays
"In most cases, schemes designed to correct quantum computer errors assume that errors between qubits are uncorrelated. They are random. Correcting correlated errors is very much. It's difficult," said DuBois, co-author of LLNL's Quantum Coherent Device Physics (QCDP) group. [Nature, arxiv]

Quantum advantage for computations with limited space
We show that n-bit symmetric Boolean functions can be implemented exactly in this frame-

work through the use of quantum signal processing13 and O(n2) gates, but in the analogous classical computations some of the functions may only be evaluated with probability 1/2+O(n/2−√n). [arxiv]

Topological excitations and bound photon pairs in a superconducting quantum metamaterial
Topological states provide the crucial ingredient of such systems featuring increased robustness to disorder and imperfections. Here we use an array of superconducting qubits to engineer a one-dimensional topologically nontrivial quantum metamaterial. [arxiv]

Researchers Uncover Unique Properties of a Promising New Superconductor for Quantum Computing
Niobium diselenide ($NbSe_2$) is a superconducting metal, meaning that it can conduct electricity, or transport electrons from one atom to another, with no resistance. It is not uncommon for materials to behave differently when they are at a very small size, but $NbSe_2$ has potentially beneficial properties. [NatPhys, arxiv]

Messages scrambled by black holes stand their ground against quantum computers
Researchers at Los Alamos National Laboratory (LANL) in the US show that once a message has been scrambled by a black hole or another system with similar properties, not even a quantum computer can put it back together. [PRL, arxiv]

Biology begins to tangle with quantum computing
As Senthil says, the idea that quantum phenomena can be used to computationally solve complex problems in chemical and physical sciences “evoked curiosity in us” to explore how quantum computing might be applied in biomedicine, “especially in the light of growing challenges associated with big data and multidimensional analysis.” [Nature]

Quantum-Enhanced Data Classification with a Variational Entangled Sensor Network
Supervised learning assisted by an entangled sensor network (SLAEN) is a distinct paradigm that harnesses VQCs trained by classical machine-learning algorithms to tailor multipartite entanglement shared by sensors for solving practically useful data-processing problems. [PRX]

Exploiting a Strange State of Matter: Researchers Confront Major Hurdle in Quantum Computing
By implementing a series of electric-field pulses on electrons, the researchers were able to create a state similar to a time crystal. They found that they could then exploit this state to improve the transfer of an electron’s spin state in a chain of semiconductor quantum dots. [scitechdaily]

Experimental quantum conference key agreement
We distribute four-photon Greenberger-Horne-Zeilinger (GHZ) states, generated by high-brightness

telecom photon-pair sources, over optical fiber with combined lengths of up to 50 km and then perform multiuser error correction and privacy amplification. [scienceadvances]

Clearest picture yet of electronic particles that make up quantum spin liquid

This new study has demonstrated a way to identify spions in QSLs by imaging their distribution in the material. Scientists begin with growing single-layer samples of tantalum diselenide (1T-TaSe2) that are only three atoms thick. By using a technique called angle-resolved photoemission spectroscopy that uses X-rays, scientists characterized the thin films. [Nature]

A post-quantum chip with hardware trojans

Such chips could provide protection against future hacker attacks using quantum computers. The researchers also incorporated hardware trojans in the chip in order to study methods for detecting this type of “malware from the chip factory”. [tum.de]

Politics and Funding

Quantum Radar Offers No Benefits To The Military Say Pentagon Science Advisors

Besides the bad news for quantum radar research, the report notes applications of quantum sciences that still offer promise, include quantum sensing, quantum computers, and quantum communications.

U.S. Department of Energy Announces $61 Million to Advance Breakthroughs in Quantum Information Science

Today's new awards will pursue goals to create new quantum devices and develop a quantum internet. "Harnessing the quantum world will create new forms of computers and accelerate our ability to process information and tackle complex problems like climate change," said U.S. Secretary of Energy Jennifer M. Granholm.

Senate Panel FY2022 NDAA Markup Features Long To-Do Lists on Cyber, Tech

Requires the Secretary of Defense to establish a set of activities to accelerate the development and deployment of a large-scale, dual-use quantum computing capability.

DOE Announces $73 Million for Materials and Chemical Sciences Research to Advance Quantum Science and Technology

"Quantum science represents the next technological revolution and frontier in the Information Age, and America stands at the forefront," said Secretary of Energy Jennifer M. Granholm.

NIST maps out the migration to post-quantum cryptography

The National Institute of Standards and Technology's National Cyber-security Center of Excellence (NCCOE) has released a draft document describing migration challenges and approaches for facilitating that migration. [PDF]

Senate dilutes US Innovation and Competition Act of 2021

The directorate would define "what are the grants that are needed, how do we go after some key areas like AI and quantum," he continued. "After the Senate [Commerce] committee went through it, it all got ripped out."

Biden Administration Previews Export Control, Patent Proposals

The administration notes that in the coming months the department will advance the rulemaking process for controls related to quantum computers, semiconductors, energetic materials, and brain-computer interfaces. It also plans to publish a notice of proposed rulemaking for foundational technologies in July and a notice for emerging technologies in August.

FY22 Budget Request: Department of Defense

Among the proposed new activities this year is a $29 million program that would accelerate work on a next generation atomic clock and facilitate researcher access to quantum computing capabilities in the private sector, pursuant to a provision in the National Defense Authorization Act for Fiscal Year 2021.

Science Committee Envisions Expanded DOE Office of Science

Building on the 2018 National Quantum Initiative Act, the bill incorporates provisions from the Quantum User Expansion for Science and Technology (QUEST) Act, which proposes a program to facilitate researcher access to quantum computing resources, and the Quantum Network Infrastructure Act, which would back DOE's nascent efforts to build out a "quantum internet.

Report on Military Applications for Quantum Computing

The following is the May 24, 2021 Congressional Research Service In Focus report, Defense Primer: Quantum Technology. The Defense Science Board (DSB), an independent Department of Defense (DOD) board of scientific advisors, has concluded that three applications of quantum technology hold the most promise for DOD. [CRS PDF]

Europe loosens funding rules for non-EU quantum and space researchers

A major new round in the €95.5 billion Horizon Europe funding program announced today will allow some non-EU countries to join such projects—but the European Union will seek special "assurances" to guarantee its interests will be protected.

Governments ally for federated quantum encryption satellite network

The United States and five other countries are banding together with the United Kingdom to develop a satellite-based quantum technology encryption network. The Federated Quantum System was announced June 11 during the G7 summit.

Halftime for R&D Push as Senate Passes Endless Frontier Bill

The Senate passed a landmark competitiveness policy package this week containing the Endless Frontier Act proposal for a multi-billion-dollar technology R&D initiative. Key members of the House are now crafting a compromise proposal they regard as better-suited to existing agency strengths.

FY22 Budget Request: National Institute of Standards and Technology

NIST proposes to increase funding for its Quantum Information Science, Engineering, and Metrology program by $15 million to $62 million. The program currently supports NIST's Quantum Economic Development Consortium and a "grand challenge" initiative to develop quantum networking capabilities.

Using Advance Market Commitments for Public Purpose Technology Development

The resulting 'product'—the government-subsidized use of advanced quantum computing systems by researchers in academia and national labs to explore, understand, and enable the use of quantum computers in mission-relevant operations—provides secondary benefits to the U.S. government's ability to make best use of this revolutionary technology.

How Federal Investment in Quantum Affects State, Local Gov
A handful of states—California, Illinois, Maryland and Virginia among them—are preparing for a quantum future, doing so by trying to ensure their region can be part of the market for companies researching and ultimately selling the technology

NIST maps out the migration to post-quantum cryptography
The National Institute of Standards and Technology's National Cybersecurity Center of Excellence (NCCOE) has released a draft document describing migration challenges and approaches for facilitating that migration. [PDF]

EU Commission Welcomes Council's Support for €7B Investment in Supercomputing Infrastructure
The proposal supported by the Council today would enable an investment of €7 billion in the next generation of supercomputers, quantum computers, and their interconnection via terabit networks.

National Quantum Leaders Contemplate Current Investments and Future Innovation
"Quantum has always been global. It will continue to be global,"
Tahan said during the Inside Quantum Technology conference. "We're much better off being first together, than second or last apart."

Ireland's First Quantum Computer Engineering Centre Launched at Tyndall National Institute
A multi-million-euro investment will see 900 sq meters of research space dedicated to quantum technology at Tyndall National Institute's new facility on Cork's North Mall and will be a key part of the Institute's plans to double in size and impact by 2025.

France takes next step in quantum technology with Dutch processor
The Twente-based company Quix is supplying the processor with which France intends to take the next step in the development of quantum technology. The French quantum computer is being built by Quandela, the leading quantum technology company in France.

Japan's first commercial-use quantum computer starts operations
The next-generation system, developed by the U.S. technology company with the university holding exclusive access rights to use it, was set up at Kawasaki Business Incubation Center in Kanagawa Prefecture, southwest of Tokyo.

Federal government contributes $2.2 million to new Quantum Algorithms Institute at SFU Surrey
Funding from the federal government's Western Economic Diversification Canada program will go towards renovating an existing

campus state into a state-of-the-art physical hub.

EU to build its quantum communications infrastructure
Called EuroQCI (European Quantum Communication Infrastructure), the initiative aims to "enhance existing communication infrastructures by adding a level of security based on the principles of quantum mechanics. In particular, the infrastructure will provide services based on quantum key distribution, a highly secure form of encryption," says a European Commission statement.

China Is Pulling Ahead in Global Quantum Race, New Studies Suggest
"It's such a new problem for the U.S. to be facing," says Mitch Ambrose, a science policy analyst at the American Institute of Physics. "It was ahead for so long, and in so many areas, that it hasn't really had to do much thinking about what it means to be behind."

GAO Issues Recommendations to White House Science and Tech Wing
In September 2018, we recommended that OSTP, as co-chair of the National Science and Technology Council's Subcommittee on Quantum Information Science, take steps in coordination with the other co-chairs and participating agencies to fully implement leading practices that enhance and sustain collaboration. [PDF]

Govt launches QSim to aid quantum computing research in India
The Indian government on Thursday launched a Quantum Simulator (QSim) which will allow developers, scientists, and students to research advancements in quantum computing in the country. The platform will not require researchers to install any software on their devices. They can sign into it from any browser using qctoolkit.com.

AFRL Designated as Quantum Information Science Research Center for Air, Space Force
"This designation allows AFRL to expand its collaborations across government, industry and academia, further accelerating the research, development and deployment of quantum technologies."

NSA Updates FAQ on Post-Quantum Cybersecurity
The National Security Agency (NSA) released a frequently asked questions document on Quantum Computing and Post-Quantum Cryptography. The document answers several questions such as "What is a quantum computer?" and "What makes one cryptographically relevant?"

Ion Beams Enable Developments in Quantum Technology
"The IAEA is fully engaged with worldwide initiatives in quantum technology," said Aliz Simon, a nuclear physicist at the IAEA. "Ion beam accelerator techniques offer emerging opportunities to further explore and develop research in quantum technology."

Pronouncements and Commentary

How to Protect Quantum Computing Innovations With IP Rights
Patent filings in this space grew exponentially over the past several years to match pace with the increasing commercial prospects and private funding. To date, there are over 200 U.S. patents pertaining to quantum computing.

Defence extends funding for high-profile quantum computing project
Two international research collaborations led by Australian universities have seen their projects extended by two years with funding from Defence's Next Generation Technologies Fund (NGTF).

UK company to start sending secret quantum keys with satellites in 2023
Arqit, which recently announced collaborations with U.S. defense giant Northrop Grumman and the U.K. telecommunications behemoth BT, aims to launch two quantum key distribution satellites in 2023 from Spaceport Cornwall in the U.K. aboard Virgin Orbit's LauncherOne.

QC Ware Announces Quantum Linear Algebra APIs on Forge
Designed specifically for data scientists and quantum engineers, Forge will now offer linear algebra APIs and data loader circuits which can be used as building blocks for quantum algorithms. The latest version of Forge also includes a hardware integration with IBM.

Quantum Software Development Is Still In Its Infancy
I believe that we will start to see a VHDL-like approach applied to quantum computing. While the language constructs for quantum might be significantly different from those of electronic design, the concept for this "quantum algorithm design" is the same.

Quantum computing to reduce operational costs for oil and gas companies
"Oil majors ExxonMobil, Total, Shell and BP are among the few industry participants to venture into quantum computing. Although these companies intend to use the technology to solve diverse business problems, quantum chemistry is emerging as the common focus area of research in the initial phase."

Comstock Invests $15,000,000 in Initial Seed Round for Quantum Computing to Accelerate Material Science Discovery and Development
The Company will provide an initial $15 million in cash and stock over the next six months, and an additional $35 million upon GenMat's realization of key development milestones.

Academy of Finland Call for Research into Use of HPC, Quantum Computers Opening in August
In August 2021, the Academy of Finland will open a special funding call aimed at supporting the use of the EuroHPC supercomputing

infrastructure, the introduction of quantum computers and the application of high-performance computing.

IBM unveils new quantum computer in Germany–first outside US

The new IBM system is the company's first quantum computer outside of the United States, where it already has more than 30 such computers. It is located at a facility in Ehningen operated by Germany's Fraunhofer Society research organization.

IonQ quantum computing systems available on Google Cloud

The company said that its next-generation 32 qubit system will be available on Google Cloud later this year. IonQ is the first third-party quantum computer available on Google Cloud's marketplace.

ISC Keynote: Glimpse into Microsoft's View of the Quantum Computing Landscape

"The first is quantum is disruptive. It will change computing, and it will enable computations that are just totally unimaginable classically. But quantum computers will not be general purpose. They will not solve all problems."

SK Telecom partners with Octatco on biometric security key with quantum number generation

South Korea Telecom (SKT) has launched a keycard featuring fingerprint biometrics and quantum computing technology to provide secure logical access control for a range of sectors including financial services, defense, online administration and smart offices.

Quantum Computing Inc. Enters 3-Year Agreement with Los Alamos National Laboratory in Exascale and Petascale Simulations

QCI will collaborate with Los Alamos scientists through its administrator, Triad National Security, LLC, on a key component of large-scale simulations that are critical for a range of high-value, real-world applications, including national security.

Italian Natl Institute for Nuclear Physics, AWS to Accelerate Quantum Computing Research

As part of this collaboration, AWS is providing access to Amazon Braket quantum computing capabilities for the INFN's community, which includes associate researchers from up to 26 universities throughout Italy

Berkeley Lab Amplifies Power and Usability of Quantum Computing

The goal of AIDE-QC is to deliver a top-down open-source integrated software environment for quantum computers developed by a collaboration of scientists from national labs and academia that could democratize the power of this budding technology among researchers.

Honeywell Quantum, Cambridge Quantum Computing form joint venture

Honeywell will invest between $270 million and $300 million in the new company and have 54% of the new venture. CQC and its investors, including International Business Machines Corp will hold the rest.

Bristol quantum computing cybersecurity company raises £3.1m in latest funding round
KETS Quantum Security said it would use the investment to accelerate the development and production of its chip-based hardware, and bring it to market.

Qrypt's cloud service will distribute entropy for better cryptography
New York-based startup Qrypt on Wednesday formally publicly announced its intent to offer "entropy-as-a-service," or EaaS, to provide businesses as well as individuals with truly random number generation capabilities.

Toshiba announces breakthrough in long distance quantum communication
Toshiba has demonstrated record distances for quantum communications by introducing a novel 'dual band' stabilisation technique. This sends two optical reference signals, at different wavelengths, for minimising the phase fluctuations on long fibres.

IonQ Adds Integration with Google Cirq,
Volkswagen Group has already run the "paint shop problem" on IonQ via Cirq and found the performance to be consistent with other quantum software frameworks.

Quantum Brilliance: reimagining drug discovery with quantum computing
The company is working to revolutionise in silico approaches to drug discovery with quantum-accelerated molecular dynamics.

Paris-based C12 Quantum Electronics raises €8.2M to develop its "unique quantum computing technology"
The groundbreaking innovation of C12 Quantum Electronics uniquely uses carbon nanotubes as the fundamental building blocks of its quantum processor.

What Makes Quantum Computing So Hard to Explain?
Quantum computers, you might have heard, are magical uber-machines that will soon cure cancer and global warming by trying all possible answers in different parallel universes. The trouble is that quantum computers will not revolutionize everything.

Corporate Japan fights to keep up in quantum computing
Eleven companies, including Toshiba, NTT and Hitachi, this summer will form a council tasked with developing the technical and human resource inputs to enable Japan to compete globally in the field. More than 50 companies are expected to join.

Europe picks EuroQCI satellite quantum communications consortium
Europe has tasked an Airbus-led group to devise its own quantum communications network as startup Arqit raises $400 million for a space-based system. The 15-month agreement is worth several millions of euros.

IonQ and SoftBank Investment Advisers Team Up to Expand Quantum Computing Access Globally
The partnership expands access to IonQ's leading quantum computers globally, and the SoftBank Vision Fund 2* also joins IonQ's world-leading investor base as it approaches its public debut.

Next-gen supercomputer lays foundation for exascale
It will be used for unclassified research into advanced computing, artificial intelligence and data science as well as climate and environmental studies, semiconductor and micro-electronic research and quantum information science.

Zapata Computing Announces Launch of UK Entity
The expansion will enable Zapata to work more closely with projects restricted by export control laws or driven by the UK government, such as the Industrial Strategy Challenge Fund, the National Quantum Computing Centre and the Department of Trade and Industry.

University of Luxembourg partners with LuxTrust to study post-quantum cryptography
SnT's Quantum Lab led by Prof. Peter Ryan will work with LuxTrust on upgrading their data security systems to be resistant against quantum computers.

Keysight Technologies makes 3rd acquisition for quantum computing R&D market
Price paid for Quantum Benchmark was not disclosed. Based in Kitchener, Ontario, Canada, it is a privately held company backed by venture funds VanEdge Capital and Quantonation, according to Keysight.

Xanadu Lands $100 Million as Investments Pour Into Quantum Computing
Xanadu announced a Series B funding led by Bessemer Venture Partners, one of Silicon Valley's oldest such firms. Funding to date for the five-year-old company now totals $145 million, said Christian Weedbrook, founder and chief executive of Xanadu.

Quantum Xchange Completes Integration with Cisco to Enable Quantum-Safe Networking Equipment with No Key Delivery Limitations
Any Cisco enterprise router that supports SKIP can now use quantum-safe keys from Phio TX to protect their network traffic. Additionally, Phio TX distributes continuously rotating encryption keys to multiple nodes on the Cisco network in a quantum-safe manner over any distance or media type.

Quantum Machine Learning on QC Ware Forge built on Amazon Braket
In this post, I introduce you to QC Ware Forge, which is built on Amazon Braket. I also walk you through an example of using Forge with Amazon Braket to solve a quantum machine learning classification problem.

ColdQuanta joins IBM Working Group for Quantum Computing Startups and Research

The partnership also allows developers to create a build-to-suit program for Hilbert, the official name for ColdQuanta's first commercial product. The Hilbert is a 100 qubit quantum computer scheduled for launch in late 2021.

IBM Partners Top Indian Academic Institutions For Quantum Computing Education, Research
The collaboration will be part of the IBM Quantum Educators programme that helps faculty in the quantum field connect with one another and provides them with resources to enable quality educational experiences, it added.

Converting quantum promises into commercial realities
According to speakers at the inaugural Quantum West conference, the transition from lab-based R&D towards market-ready solutions is already under way.

NIH Releases Notice of Special Interest in Computational Approaches to Drug-Disease Research
NIDA has a particular interest in applications that include approaches in one or more of the following categories: 1) artificial intelligence, including machine learning and deep learning, 2) supercomputing/parallel computing, and/or 3) quantum computing.

Google Aims for Commercial-Grade Quantum Computer by 2029
"We are at this inflection point," said Dr. Neven, who has been researching quantum computing at Google since 2006. "We now have the important components in hand that make us confident. We know how to execute the road map."

Purdue Seeking to Boost Quantum Technology Training
David Stewart, managing director of the Purdue Quantum Science and Engineering Institute, says quantum has the potential to be revolutionary technology, but there aren't enough people to do the work.

IonQ Launches Research Credits Program to Support Pioneering Quantum Research
Now, in support of this mission, graduate students, PhD candidates, post-docs, and faculty can submit proposals for up to $10,000 in credit per project for use on IonQ's hardware.

Dutch startup QphoX raises €2M to enable quantum computers "to talk to one another"; here's how
Simon Gröblacher, CEO & co-founder of QphoX, says, "Thanks to this investment, we will be able to create and provide the missing link between quantum computers and the quantum internet, and further help scaling quantum processors to realise their computing power."

Rigetti Computing introduces world's first scalable multi-chip quantum processor
The processor incorporates a proprietary modular architecture. Rigetti expects to make an 80-qubit system powered by the breakthrough

multi-chip technology available on its Quantum Cloud Services platform later this year.

NVIDIA Platform Accelerates Quantum Circuit Simulation Ecosystem
Researchers at the Jülich Supercomputing Centre have harnessed the state vector method to simulate physical realizations of quantum computers on GPUs. Their benchmark tests, discussed at GTC, showed a 25x speedup on GPU clusters compared with CPU-based systems

IBM to install a quantum computer in Japan
IBM is expanding its quantum computing program to Japan and will be working with companies such as Toyota, Sony and other tech firms, according to a report in the Nikkei news service.

Nippon Steel tested quantum computing to help improve plant scheduling
The company said it collaborated with Cambridge Quantum Computing and Honeywell to develop an optimal schedule for enhancing efficiencies in the products it uses during the steel manufacturing process. The companies developed an algorithm and tested it on Honeywell's quantum System Model H1.

USPTO asks: Is patent eligibility jurisprudence affecting business?
The notice requests comment on how the "current state of patent eligibility jurisprudence" affects specific fields including quantum computing, artificial intelligence and pharmaceutical treatments, as well as the U.S. economy as a whole. Inventions covering abstract ideas, natural phenomena and laws of nature can't be patented under Section 101 of the Patent Act. [PDF]

US visa restrictions 'necessary but don't affect many Chinese students'
Key technologies being targeted under MCF include quantum computing, big data, semiconductors, biotechnology, 5G, advanced nuclear technology, aerospace technology and AI, the spokesman said, as these have both military and civilian applications.

China Claims To Have World's Most Powerful Quantum Computer, Tops Google
According to a preprint uploaded to arXiv, the quantum computer was able to solve a problem with 56 of its 66 qubits (the quantum equivalent of bits in a conventional computer); breaking the previous record by Google.

Oxford Quantum Circuits Claims UK's First Quantum Computing as-a-Service
OQC said its core innovation, the Coaxmon, addresses these challenges using a three-dimensional architecture that moves the control and measurement wiring out of plane and into a 3D configuration, simplifying fabrication, improving coherence and boosting scalability.

IU Bloomington, IUPUI part of coalition to develop quantum technologies

The new Center for Quantum Technologies, led by Purdue University, will be established through the National Science Foundation's Industry-University Cooperative Research program. Industry partners would provide research funding to the center's scientists and gain early access to findings applicable to their businesses.

Strangeworks Launches Early Access to Qiskit Runtime from IBM Quantum

Users of the Strangeworks ecosystem can take advantage of this technology for free starting today via a dedicated IBM 7-qubit quantum computer. By registering at quantumcomputing.com, users can utilize Qiskit Runtime programs and additional programs as they become available.

PsiQuantum Closes $450M Funding Round to Build Commercially Viable Quantum Computer

The funding round was led by funds and accounts managed by BlackRock, along with participation from insiders including Baillie Gifford and M12—Microsoft's venture fund—and new investors including Blackbird Ventures and Temasek.

New RIKEN Center to Focus on Quantum Computing

The center is focusing on superconducting qubits, based on the work of Director Nakamura and Team Leader Tsai, and is also looking at the development of optical quantum computers led by Deputy Director Akira Furusawa.

QUEST for quantum computing in the energy sector

The Quantum Upgraded Electric System of Tomorrow (QUEST) initiative, which has been launched at the University of Denver, is aimed to build a university-industry consortium to bring the power of quantum information and quantum computing to the challenges of building the grid of the future.

Quantum Computing Inc. Lists on Nasdaq Capital Market

With the opening bell, QCI will become one of the few pure-play quantum software companies to list on the Nasdaq exchange. Its common stock commenced trading at market opening on July 15, 2021, under the same symbol, QUBT.

Algorithm Solves Combinatorial Optimisation Problems Faster

Using the Honeywell System Model H1 quantum computer, the new approach outperformed existing "gold standard" algorithms such as the Quantum Approximate Optimisation Algorithm (QAOA) and the original VQE, reaching a good solution 10 to 100 times faster.

IBM's Quantum Computing Compromise—a Road to Scale?

After this week, all of the more than 20 processors available on the IBM Cloud will rely on the design. And Nation says heavy hex will be used in all devices outlined in its quantum roadmap, at least up until the 1,121-qubit Condor processor planned for 2023.

Volkswagen breaks new ground in automotive quantum computing
The German company has real substance behind its investment into applications of quantum computing. “We’re not interested in doing research for research’s sake. We want to bring this technology into the real world,” Neukart stressed.

Quantum computers: China has ambitious plans
As part of this document, by the end of the 14th Five-Year Plan, it is planned to develop quantum computers with more than a few hundred qubits.

Buyer Beware! Wall Street Discovers Quantum Computing
I do believe this is a real technology with a demonstrated, scientific foundation and I am excited that the technology is very achievable. However, from an investment perspective it’s a disaster waiting to happen.

Xanadu and imec Partner to Develop Photonic Chips for Fault Tolerant } Quantum Computing
“Imec is one of the few semiconductor R&D centers that does advanced technology R&D on advanced 200mm and 300mm lines, as well as volume manufacturing on their 200mm line, capable of delivering up to a thousand wafers per year per customer on a few platforms including ultralow-loss photonic platforms.”

German group achieves quantum-secured video conference by Federal agencies
On August 10th, two German Federal agencies communicated via video over an optical link for the first time in a quantum-secure manner. The QuNET project, an initiative funded by the German Federal Ministry of Education and Research (BMBF) to develop highly secure communication systems, is demonstrating how data sovereignty can be guaranteed in the future.

2021:

8–19 Nov: Scientific Quantum Computing Simulations on Near-term Devices

8–12 Nov: Quantum Techniques in Machine Learning

15 Nov: International Workshop on Quantum Computing Software

29 Nov–2 Dec: European Quantum Technology Conference, Dublin, Ireland

30 Nov–2 Dec: International Conference on Rebooting Computing

7-9 Dec: Q2B: Practical Quantum Computing

2022:

3 Jan–25 Feb: Towards Classically Intractable Quantum Simulations of Physics and Chemistry, Santa Barbara, California

16–18 Feb: Energy Consequences of Information Workshop, Santa Fe, New Mexico

7–11 Mar: QIP, Pasadena, CA

14–18 Mar: APS March Meeting, Chicago, Illinois

18–22 Mar: International Symposium on Multiple-Valued Logic, Dallas, Texas

1–3 Apr: Quantum Computing Applications in Chemical and Biochemical Engineering Workshop, Copenhagen, Denmark

3–7 Apr: Security, Robustness, and Trust in Artificial Intelligence and Distributed Architectures, Orlando, Florida

3–7 Oct: Quantum Information Science, Sensing, and Computation XIV, Orlando, Florida

3–7 Oct: Advanced Photon Counting Techniques XVI, Orlando, Florida

3–7 Oct: Sensors and Systems for Space Applications XV, Orlando, Florida

11–15 Jul: International Conference on Quantum Communication, Measurement and Computing, Lisbon, Portugal